IDENTIFICATION OF QTLS ASSOCIATED WITH NUT SHAPE CHARACTERISTICS IN PECAN (*CARYA ILLINOINENSIS)*

AND

EVALUATING TEXTURE AND STORABILITY IN MUSCADINE GRAPE (*VITIS ROTUNIDOLIA)*

by

ANNE MARIE GAHAGAN

(Under the Direction of Patrick J. Conner)

ABSTRACT

Pecan and muscadine are important agricultural commodities in Georgia, contributing to both economic and cultural value. Pecan cultivars display wide morphological diversity, with nut shape influencing shelling efficiency and kernel yield. This study identified QTLs associated with nut shape traits in a biparental (‘Pawnee’ × ‘Elliott’) population using R/qtl, revealing consistent regions on ‘Pawnee’ chromosome 11 and ‘Elliott’ chromosome 8 linked to key morphometric traits. These findings support marker-assisted selection to develop cultivars with uniform nut shape and improved processing efficiency. Muscadine, valued for its rich flavor and health benefits, faces limitations in fresh-market expansion due to thick skins and soft pulp. To improve consumer acceptance, diverse genotypes were evaluated for texture traits and storability, identifying variation that can guide breeding for enhanced firmness and shelf life. Together, these studies advance

breeding efforts to strengthen Georgia's specialty crop industries through improved quality and marketability.

INDEX WORDS: *Carya illinoinensis*, pecan nut shape, Tomato Analyzer, QTL analysis, plant breeding, horticulture, muscadine grape, *Vitis rotundifolia*, postharvest, fruit firmness, fruit texture

IDENTIFICATION OF QTLS ASSOCIATED WITH NUT SHAPE CHARACTERISTICS IN PECAN (*CARYA ILLINOINENSIS)* AND EVALUATING TEXTURE AND STORABILITY IN MUSCADINE GRAPE (*VITIS ROTUNIDOLIA)*

by

ANNE MARIE GAHAGAN

B.S., Louisiana State University, 2023

A Thesis Submitted to the Graduate Faculty of The University of Georgia in Partial Fulfillment of the Requirements for the Degree

MASTER OF SCIENCE

TIFTON, GEORGIA

2025

IDENTIFICATION OF QTLS ASSOCIATED WITH NUT SHAPE CHARACTERISTICS IN PECAN

(*CARYA ILLINOINENSIS)*

AND

EVALUATING TEXTURE AND STORABILITY IN MUSCADINE GRAPE (*VITIS ROTUNIDOLIA)*

by

ANNE MARIE GAHAGAN

Major Professor:	Patrick Conner
Committee:	Dario Chavez
	Juliet Chu

Electronic Version Approved:

Ron Walcott
Vice Provost for Graduate Education and Dean of the Graduate School
The University of Georgia
December 2025

DEDICATION

My work reflects all that my grandparents have instilled in me. To my grandmothers, who nurtured my appreciation for southern crops: Grandmama with her holiday pecan pies and chocolate turtles, and Grandmother with her signature mayhaw and muscadine jellies. To my grandfathers, who encouraged my love of cultivation: Daddy Bart through the resurrection ferns and rose bushes gifted for birthdays, and Grandfather through his passion for the pecan trees and garden in his backyard. I dedicate this thesis, with love and gratitude, to them. Thank you for planting the seeds that led me here.

ACKNOWLEDGEMENTS

I would like to express my deepest gratitude to all those who have supported me throughout my academic journey. My sincerest thanks go to Dr. Conner, for your unwavering support, patience, and commitment to helping me grow as both a scientist and a person. Your mentorship has provided a foundation that will guide me throughout my career. I am also grateful to my committee members, Dr. Chu and Dr. Chavez, for your invaluable guidance, thoughtful feedback, and for challenging me throughout this project. Finally, I want to thank my lab mates, Achyut and Khyathi, who I'm grateful to also call friends. Your encouragement, collaboration, and willingness to help made this experience so rewarding. To everyone who offered support along the way, thank you, endlessly.

TABLE OF CONTENTS

CHAPTER 1

PECAN: AMERICA'S NATIVE NUT TREE

BACKGROUND AND INTRODUCTION

Pecan's Ancient Roots

The walnut family, Juglandaceae, has ancient origins, with evidence of its pollen first appearing 135 million years ago (McWilliams 2013). Over millennia, climatic shifts and biotic interactions drove diversification within the family. Animal-mediate seed dispersal by birds and rodents promoted geographic spread and lineage splitting, contributing to the emergence of new genera and species (Frei 2021). Reconciling archaeological, morphological, and genetic evidence has proved challenging, and earlier hypotheses that divided Juglandaceae into two sister genera, the hickories (Carya*)* and the walnuts (Juglans), have been refined by recent phylogenomic work (Frei 2021; Zhang et al. 2013). Current evidence supports that there are five genera within the family: Juglans, Pterocarya, Cyclocarya, Platycarya, and Carya. The genus Carya diverged earliest in history, followed by Platycarya and Cyclocarya, then Pterocarya which is sister to Juglans (Zhou et al. 2021; Ding et al. 2023). Carya likely emerged 58 million years ago, with subsequent dispersal across North America, Europe and Asia (Frei 2021; Zhou et al. 2021). Geographic barriers in Europe and climatic change contributed to local extinction there, but the North American populations were able to migrate with Earth's cooling and warming periods and persist (Frei

2021; McWilliams 2013). It was within North America that the pecan, *Carya illinoinensis,* became established.

The History of Pecan in America

Pecan is one of thirteen *Carya* species native to the United States. Its name comes from the northern limits of its native range, which follows the Mississippi river from northern Illinois to the Gulf Coast in Louisiana, extending west toward central Texas and south into Mexico (Thompson and Conner 2012). Occupying rich alluvial soils along the river basins, pecan thrived in the moist, well-draining substrates enriched by periodic flooding. The species developed a deep taproot that reached the groundwater along with an extensive lateral root system that exploited surface moisture and the fertile humus layers. This allowed the trees to outcompete other native plants by reaching heights of up to 50-55 meters, eventually dominating bottomland canopies (McWilliams 2013). Animal dispersers, including squirrels, foxes, and wild turkeys, preferentially transported larger, thinner-shelled nuts because they were easier to consume, contributing to seed dispersal and early selection for those traits (McWilliams 2013). All factors seemed aligned for the species to thrive, and as McWilliams suggests, these trees "should have been nowhere else except exactly where they were." This perfect storm of attributes allowed dense groves of pecan to develop.

With centuries establishing themselves across this landscape, pecans became a pervasive part of lower Mississippi river valley flora. When the first humans entered the region, Indigenous communities incorporated pecans into subsistence, culture, and trade. As populations transitioned from a highly nomadic to semi-nomadic lifestyle, pecans

became a reliable and transportable food source that could be collected, stored, and eaten raw. The nuts provided substantial caloric energy, vitamins, minerals, healthy lipids, and antioxidants, making them vital when other food resources were scarce (McWilliams 2013). Indigenous peoples also used pecans and related hickories for cultural and medicinal purposes. Powcohiccora, a fermented beverage prepared from several hickory species including pecan, had ritual significance in some groups; leaves and bark were employed for dermatological and respiratory illnesses like tuberculosis (Wells 2017). Evidence also suggests pecans circulated as trade goods or forms of currency. Some tribes became specialized traders, strengthening intergroup ties, and transporting pecans far beyond their wild range in the process (McWilliams 2013).

The relationship between people and pecans turned out to be mutually influential. Traveling along the Mississippi and its tributaries, people dispersed nuts deliberately or inadvertently at campsites and trade nodes, expanding the species' range and promoting the persistence of desirable traits. Human selection likely favored larger, thinner-shelled nuts because they were easier to crack and provided the greatest volume of edible kernel (Wells 2017). This choice mirrors the selection process by animals, who were the first dispersers of pecan (McWilliams 2013). However, because of their roles in propagation and trade, Indigenous peoples were the primary agents in taking pecans farther than animals alone could have accomplished. This long history of cultural association explains why pecans "have cultural importance that far predate their scientific documentation" (Frei 2021). Centuries ago, the pecan provided life-giving sustenance, courage, and community to Indigenous communities, who, in return, helped shape the modern pecan.

Pecans of Modern America

The transition from the wild use of pecans to large-scale commercialization unfolded over the 19th and 20th centuries. At first, Texan landowners exploited existing wild pecan stands simply by collecting nuts as they fell. These pre-existing groves soon evolved into a business through "passive cultivation." Amongst the trees already on their property, landowners removed less desirable trees and allowed superior trees to flourish with minimal management (McWilliams 2013). The species' capacity to produce abundantly with limited human input encouraged rapid expansion of pecan cultivation. People living in the states to the east of the native region soon realized this fact, and pecan trees became prevalent across the whole southern landscape. Primarily, families planted them to provide shade, sustenance, and supplemental income (Wells 2017). Before long, these trees were viewed as more than a simple backyard perk, and commercial orchards later developed.

The pecan boom in Georgia exemplifies the crop's rapid rise in commercialization. An interesting trifecta of favorable environment, speculation, and cheap land drove the boom. Many enterprises failed when profitability claims proved to be over-exaggerated, and orchard management more intensive than expected (Wells 2017). But the growing pecan economy in Georgia found ways to thrive.

Organized grower efforts helped stabilize and professionalize the industry, eventually contributing to Georgia's prominence in world pecan production. The Southeastern Pecan Growers Association was a key group of stakeholders responsible for safeguarding the industry during these early times. This group also hoped to standardize the debate of how to

pronounce “pecan,” suggesting “pee-CAN” as the proper pronunciation (Wells 2017). While many southeasterners retained this pronunciation, regional pronunciation still varies widely, reflecting the crop’s deep cultural ties across communities. For example, I prefer “puh-KAHN” as a nod to my Louisiana roots.

Commercialization of pecan brought a need for intensified orchard management. Practices such as selective thinning, soil and canopy management, and attention to pollination became necessary to sustain productivity and reduce disease susceptibility (Wells 2017). The overarching lesson is that successful commercialization required integrating tree biology into orchard design and management, often by taking inspiration from the ecological patterns of ancient natural groves.

Pecan Reproductive Strategy

Firstly, it was important to note natural reproductive strategies of pecan. Pecans are wind-pollinated, monoecious, and dichogamous. Therefore, the female flowers will not be receptive at the time the male flowers are producing pollen. Trees may be protandrous (male flowers releasing pollen before female flowers are receptive) or protogynous (females flowers receptive before male pollen releases) (Fronza et al. 2018). This temporal separation of male and female function promotes outcrossing which produced a wide base of genetic diversity in wild populations, contributing to the species’ ecological success (McWilliams 2013). During early production years, orchards of mother trees exhibiting favorable characteristics were allowed to open-pollinate. This approach facilitated the creation of substantial and diverse germplasm that contributed to genetic improvement prior to formal breeding programs (Thompson and Conner 2012).

Despite this biological propensity to out-cross, many historical orchards did not prioritize pollination. Early 20th-century planting recommendations often placed complementary cultivars in large blocks rather than interplanting them. This left many trees too distant from compatible pollen sources for optimal wind pollination. At this time, grafting techniques were not perfected, often leading to off-types generated from the seedling rootstock which provided random sources of pollen, vital for the success of such orchards (Wood 2000). The pollen from off-types enhanced early orchard productivity but likely masked true pollination requirements. Research indicates that pollination quality critically affects yield and nut quality. In fact, cross-pollinated orchards produce 75% more crop yield than self-pollinated orchards (Rhola 2016). Decreased yield can occur due to an abortion of nuts that either did not get fertilized, or that were self-fertilized. In addition, even if a self-fertilized nut does not abort, it will have greatly diminished kernel quality (Wood 2000). Ensuring proper proximity and compatibility of pollinator varieties is essential in maximizing nut yield and quality.

Traditional block planting (e.g., four rows of a pollinator cultivar followed by ~20 rows of a main cultivar) creates yield gradients across the orchard. Highest yields occur on rows immediately adjacent to pollinizer rows and decline with distance (Wood 2000). Furthermore, weather extremes can exacerbate these problems by disrupting pollen movement or altering the synchrony of pollen release and stigma receptivity (Wells 2016). The arrangement of cultivars is not the only issues at stake, however. While many orchards are planted with only two complementary cultivars, including at least four cultivars would

be optimal for best pollination (Carroll and Smith 2017). Again, this underscores the vital need of providing an abundance of available pollen.

Interspersing pollinizers among rows would also improve proximity and pollen availability. However, this strategy introduces operational complications during post-harvest cracking and shelling. Therefore, it is only feasible in cases where the complementary trees share similar nut shape characteristics (Wells and Conner 2015).

Scab epidemiology

Another major problem which arose during the development of modern pecan orchards is scab epidemics. Pecan scab, a disease caused by the fungus *Venturia effusa,* is the most economically damaging disease of pecan, affecting both leaves and shucks. The fungus is managed with the application of various fungicides, but spray regiments are costly and increase the risk of selecting fungicide-resistant populations (Standish et al. 2021).

The pecan scab pathogen occurs in multiple races, each exhibiting varying degrees of compatibility with different pecan cultivars. Some races are incapable of infecting all genotypes, while others affect many but demonstrate heightened aggressiveness toward particular cultivars (Conner and Stevenson 2004). Planting several cultivars with different resistance profiles lowers the probability that a single race will devastate an entire orchard. Cultivar diversity therefore acts as a risk-management strategy. If one cultivar is highly susceptible to a particular race, another less susceptible cultivar can maintain yield, making outbreaks more manageable under moderate fungicide regimes.

Apple scab, caused by *Venturia inequalis,* similarly devastates apple crops worldwide by reducing fruit quality and yield. One method for limiting the spread of scab in

apples was to develop orchards with mixtures of cultivars possessing varying degrees of susceptibility to apple scab. Such an orchard showed reduction in both incidence and severity of scab, especially when the cultivars were mixed within a row (Didelot et al. 2007). Although concerns exist that cultivar mixtures might favor the emergence of a more virulent "super-race," field observations of *V. inequalis* in apple monoculture and mixed orchards indicate that cultivar mixtures contribute to sustainable scab management rather than accelerating virulence evolution (Stewart et al. 2023). By analogy, increasing cultivar diversity in pecan plantings could reduce the epidemic potential of pecan scab.

Nut Cracking and Processing

Human selection for thinner shells began with Indigenous peoples who preferred nuts that were easier to crack by hand (McWilliams 2013). Such varieties remained in favor as the industry commercialized, and new cracking methods were developed. When the industry was first commercialized, it was fiscally advantageous to transport shelled nuts to reduce space and weight. In response, immigrant laborers were employed in San Antonio, one of the first pecan selling and shipping hot spots, to crack the nuts manually using railroad spikes. Another early cracking method initiated at a facility in Saint Louis utilized a hammer and a lead base to complete the task. It wasn't until the early 1900s that the first power-driven cracker was invented. The machinery increased throughput but requires greater uniformity among nuts to avoid kernel damage (Wells 2017). Variability in nut size and shape from wild or unimproved stands resulted in frequent kernel shattering, a challenge that persists in modern processing.

Post-harvest processing is a critical component of the pecan industry, with approximately 90% of pecans shelled before reaching the consumer (Thompson and Grauke 2003). Post-harvest shelling is a multistage pipeline designed to separate the kernel from the shell through cleaning, size grading, cold storage, nut conditioning, cracking, shelling, sorting (by size, moisture, and color), and packaging (Sims 1994). Given the scale of the shelled nut market, shelling efficiency plays a central role in determining quality. While nut quality is inherently multifaceted, harvest quality describes how readily nuts can be shelled with minimal kernel loss. Orchards with similar in-shell yields may differ substantially in shelled kernel recovery due to differences in kernel fill, shell characteristics, and susceptibility to breakage (Charles R. Santerre 1994b). Thus, shelling efficiency and the production of complete kernel halves are essential metrics of orchard productivity.

Modern processing minimizes breakage by size grading prior to cracking and calibrating equipment for each grade (Charles R. Santerre 1994a). Cracking involves applying force to both ends of the nut to shatter the shell. Although modern equipment performs this task efficiently, each nut is still cracked individually, and shell thickness and size directly influence the required pressure. Following cracking, nuts proceed along a conveyor system where kernels are separated from shells and other debris. This step employs various cleaning methods, including water flotation, vibrating tables, suction fans, and electronic sorters (Sims 1994). Whole kernels are easier to sort out since their size distinguishes them from unwanted material, emphasizing the importance of minimizing kernel shattering.

While smaller kernel pieces retain some value, they may be difficult to separate from shell fragments, insects, and other debris, leading to losses. To mitigate loss, processors aim to maximize whole kernel production during cracking through equipment adjustments (Charles R. Santerre 1994a). Equipment calibration cannot manage all kernel shattering, however. Beyond size, nut shape also plays a role in harvest quality and shelling efficiency, as certain shapes are more compatible with mechanical cracking and tend to produce a higher proportion of intact kernels.

Nut Shape

While shelling machinery can be adjusted to specific size grades, it cannot accommodate the individual pressure requirements needed for each nut, which is affected by nut shape (Thompson and Grauke 2003). Although pecans generally exhibit an ovoid-ellipsoid shape reminiscent of an American football, their shape is more nuanced and can be described from multiple morphological perspectives.

When viewed from the suture side, pecans are categorized with six basic shapes: round, oval, oblong, ovate, obovate, and elliptic. Additional shape descriptors are derived from the cross-sectional view, with the nut observed from the apex. A complete shape profile also includes descriptions of basal and apical morphology. The base, or proximal end, may range from round to obtuse to acuminate and may be asymmetrical in some cases. The apex, or distal end, follows similar classifications but tends to be more angular or pointed (Sparks 1992).

In general, nuts displaying moderate elongation and minimal angularity at both ends are best suited for mechanical cracking (Sparks 1992). Overly elongated nuts will often

cause the kernel to be broken in half during cracking, but the same is not true for a blockier nut of similar size. Conversely, overly rounded nuts are more likely to fall crosswise into the cracker, leading to more kernel casualties (Bhattarai et al. 2022). This shape-related effect on shelling efficiency is supported by Thompson and Grauke (2003), who found that nuts with higher length-to-width ratios produced a greater percentage of whole kernel halves. This indicates slightly elongated nuts are better producers of intact kernels during processing.

Nut shape varies by cultivar and serves as a primary characteristic for cultivar identification. For growers, selecting cultivars with favorable nut shape for superior cracking ability can provide a financial benefit due to a higher percentage of whole kernel halves, even when yield (pounds of nuts per acre) is less competitive (Sparks 1992). In this way, nut shape plays a critical role in both processing efficiency and economic return. To link nut morphology with genetics and breeding, I next describe the phenotyping and genetic tools used to quantify shape and map its underlying loci.

Tomato Analyzer

High-throughput, objective phenotyping is the first step in mapping nut shape, and Tomato Analyzer (TA) provides a practical platform for extracting precise two-dimensional shape descriptors from nut images (Brewer et al. 2006). TA traces object contours using adjustable boundary points and computes a suite of shape descriptors that are difficult or laborious to measure manually. The program extracts up to 37 quantitative attributes, including basic dimensions (maximum height and width), derived indices (external shape index, rectangularity, circularity), and angular or blockiness measures at distal and proximal

ends (Rodríguez et al. 2010). Bhattarai et al. (2022) applied TA to pecan nuts, measuring ten descriptors: maximum height, maximum width, external fruit shape index, distal fruit blockiness, proximal fruit blockiness, circularity, ovoidity, rectangularity, distal angle (macro), and proximal angle (macro). TA precision provides the capacity to produce the phenotypic resolution required for QTL discovery.

Quantitative Trait Loci (QTL)

QTL mapping can link TA-derived shape phenotypes to genomic regions that influence those traits. Quantitative traits are controlled by many genes showing continuous phenotypic distributions. A single trait may be influenced by tens to thousands of loci, each with a small to moderate effect (Boopathi 2020). For example, many agronomically important traits like yield, quality, and stress responses are often quantitative.

QTL analysis links phenotype and genotype by testing whether genetic markers co-segregate with trait variation across a mapping population. Common mapping approaches include single-marker tests, interval mapping, composite interval mapping, and multiple-QTL models; each method balances detection power, false-positive control, and computational complexity (Boopathi 2020). Accurate QTL detection requires reliable heritable phenotype measures across environments, dense and high-quality genotypic markers, and a mapping population with sufficient size to localize effects.

These methodological requirements guided the implementation of QTL analysis in this study. To account for environmental variability and gene × environment interactions, phenotyping was conducted on a population of 119 individuals replicated three times across four locations over multiple years. Traits previously reported to be heritable were

selected and measured using precision phenotyping software to ensure consistency and accuracy. Genotyping-by-sequencing (GBS) was employed to generate SNP markers with adequate density and quality, providing a robust genomic framework for QTL analysis.

Mapping Population

Developing a suitable mapping population is a foundational step in QTL analysis. Mapping populations are composed of individuals derived from controlled crosses between defined parents and can take several forms (F_2, backcross, recombinant inbred lines, double haploids, and multi-parent populations). Certain population structures are better suited to certain crops (Boopathi 2020).

Pecan is a highly heterozygous species because of preferential outcrossing due to heterodichogamy. Severe inbreeding depression and long generation times preclude development of large, inbred populations in pecan and many other tree fruit species like apple and pear. In these crops, F_1 mapping populations are constructed from crossing heterozygous parental trees, resulting in a highly heterozygous population (Thompson and Conner 2012). In such cases, an individual genetic map is often constructed for each parent using a two-way pseudo-testcross mapping strategy. Markers used to create the maps may be segregating in one parent (1:1 ratio) or in both of the parents (1:2:1 ratio) (Grattapaglia and Sederoff 1994). With a suitable population in place, the next consideration is the heritability of the shape traits we measure.

Heritability and Marker Assisted Selection

Estimating heritability determines whether nut shape traits have sufficient genetic control to warrant mapping and early selection. Heritability quantifies the proportion of

phenotypic variance attributable to genetic variance in a given population and environment. Narrow-sense heritability (h^2) estimates the additive genetic component relevant to selection response. Bhattarai et al. (2022) used TA descriptors on biparental pecan populations to estimate narrow-sense heritability for multiple shape traits. Size-related traits (maximum height and width) showed the highest h^2, while other shape descriptors exhibited moderate to high narrow-sense heritability (Bhattarai et al. 2022). When heritability is moderate to high, QTL analysis and marker-based selection become feasible strategies.

Marker-assisted selection (MAS) translates QTL discoveries into actionable breeding decisions, enabling early selection for favorable nut shape in pecan breeding programs. MAS can improve tree breeding by allowing early, resource-efficient selection of individuals carrying favorable alleles at QTLs of interest.

Because many nut shape traits exhibit moderate to high heritability and clear processing relevance, MAS offers a practical route to reconcile cultivar diversity with processing compatibility, enabling breeders to select parents and progeny that support both orchard resilience and downstream efficiency.

RESEARCH PURPOSE AND OBJECTIVE

Nut shape strongly influences mechanical cracking, shelling efficiency, and processor profitability, yet its genetic basis in pecan remains poorly characterized. Because roughly 90% of pecans are shelled before sale, small improvements in the proportion of whole kernels translate directly into substantial economic gains for growers and processors

(Thompson and Grauke 2003). Simultaneously, the long lifespan of pecan orchards makes mixed-cultivar plantings an attractive strategy to sustain productivity and resilience over generations.

Mixed-cultivar orchards offer clear agronomic benefits: increased pollination improves both yield and nut quality, and cultivar diversity can reduce the epidemic potential of pecan scab, lowering reliance on intensive fungicide programs. However, diversity introduces a practical trade-off for processors. Greater variation in nut shape increases grading time and cost, and certain shapes are intrinsically less compatible with mechanical cracking, reducing profit through decreased proportion of intact kernels.

This study addresses this tradeoff by mapping the genetic architecture of nut shape in pecan. Using high-resolution phenotyping coupled with quantitative trait loci (QTL) mapping, I aim to identify genomic regions associated with nut shape traits. The resulting markers and trait insights will help breeders and growers select cultivars that reconcile the benefits of mixed-cultivar plantings with the operational constraints of modern shelling systems, improving both orchard resilience and downstream profitability.

Literature Cited

Bhattarai, Gaurab, Vincent Bonhomme, and Patrick Conner. 2022. “Image-Based Morphometric Analysis Reveals Moderate to Highly Heritable Nut Shape Traits in Pecan.” *Euphytica* 218 (7): 102. https://doi.org/10.1007/s10681-022-03049-1.

Boopathi, Manikanda. 2020. *Genetic Mapping and Marker Assisted Selection: Basics, Practice and Benefits*. Springer Singapore. https://doi.org/10.1007/978-981-15-2949-8.

Brewer, Marin Talbot, Lixin Lang, Kikuo Fujimura, Nancy Dujmovic, Simon Gray, and Esther van der Knaap. 2006. “Development of a Controlled Vocabulary and Software Application to Analyze Fruit Shape Variation in Tomato and Other Plant Species.” *Plant Physiology* 141 (1): 15–25. https://doi.org/10.1104/pp.106.077867.

Carroll, Becky, and Michael Smith. 2017. “Establishing a Pecan Orchard.” Oklahoma State Extension, February 1. https://extension.okstate.edu/fact-sheets/establishing-a-pecan-orchard.html.

Conner, Patrick J., and Katherine L. Stevenson. 2004. *Pathogenic Variation of Cladosporium Caryigenum Isolates and Corresponding Differential Resistance in Pecan*. HortScience. June 1. https://doi.org/10.21273/HORTSCI.39.3.553.

Didelot, Frederique, Laurent Brun, and Luciana Parisi. 2007. “Effects of Cultivar Mixtures on Scab Control in Apple Orchards.” *Plant Pathology* 56 (6): 1014–22. https://doi.org/10.1111/j.1365-3059.2007.01695.x.

Ding, Ya-Mei, Xiao-Xu Pang, Yu Cao, et al. 2023. “Genome Structure-Based Juglandaceae Phylogenies Contradict Alignment-Based Phylogenies and Substitution Rates Vary with DNA Repair Genes.” *Nature Communications* 14 (1): 617. https://doi.org/10.1038/s41467-023-36247-z.

Frei, Jonas. 2021. “A Brief History of Juglandaceae.” *Arnoldia* 78 (3): 10–17.

Fronza, Diniz, Jonas Janner Hamann, Vanderlei Both, Rogério de Oliveira Anese, and Evandro Alcir Meyer. 2018. “Pecan Cultivation: General Aspects.” *Ciência Rural* 48 (February): e20170179. https://doi.org/10.1590/0103-8478cr20170179.

Grattapaglia, Dario, and R. Sederoff. 1994. “Genetic Linkage Maps of Eucalyptus Grandis and Eucalyptus Urophylla Using a Pseudo-Testcross: Mapping Strategy and RAPD Markers.” *Genetics* 137 (4): 1121–37. https://doi.org/10.1093/genetics/137.4.1121.

McWilliams, James. 2013. *The Pecan: A History of America’s Native Nut*. University of Texas Press. http://ebookcentral.proquest.com/lib/ugalib/detail.action?docID=3571814.

Rhola, Charles. 2016. “Cross Pollination Is Essential for Pecan Production.” *Noble Research Institute*, June 14. https://www.noble.org/regenerative-agriculture/silvopasture/cross-pollination-is-essential-for-pecan-production/.

Rodríguez, Gustavo, Jennifer Moyseenko, Matthew Robbins, Nancy Huarachi Morejón, David Francis, and Esther van der Knaap. 2010. “Tomato Analyzer: A Useful Software Application to Collect Accurate and Detailed Morphological and Colorimetric Data from Two-Dimensional Objects.” *Journal of Visualized Experiments : JoVE*, no. 37 (March): 1856. https://doi.org/10.3791/1856.

Santerre, Charles. 1994a. “Pecan Processing.” In *Pecan Technology*, by Charles Santerre. Springer. http://ebookcentral.proquest.com/lib/ugalib/detail.action?docID=6488987.

Santerre, Charles. 1994b. *Pecan Technology*. Springer. http://ebookcentral.proquest.com/lib/ugalib/detail.action?docID=6488987.

Sims, Kevin. 1994. “Mechanization of Post-Harvest Pecan Processing.” In *Pecan Technology*, by Charles Santerre. Springer. http://ebookcentral.proquest.com/lib/ugalib/detail.action?docID=6488987.

Sparks, Darrell. 1992. *Pecan Cultivars: The Orchard’s Foundation*. Pecan Production Innovations.

Standish, Jeffrey, Timothy Brenneman, Clive Bock, and Katherine Stevenson. 2021. “Fungicide Resistance in Venturia Effusa, Cause of Pecan Scab: Current Status and Practical Implications.” *Phytopathology®* 111 (2): 244–52. https://doi.org/10.1094/PHYTO-06-20-0221-RVW.

Stewart, Katherine, Thomas Passey, Carol Verheecke-Vaessen, et al. 2023. “Is It Feasible to Use Mixed Orchards to Manage Apple Scab?” *Fruit Research* 3 (1). https://doi.org/10.48130/FruRes-2023-0028.

Thompson, Tommy, and Patrick Conner. 2012. “Pecan.” In *Fruit Breeding*, edited by Marisa Luisa Badenes and David H. Byrne. Springer US. https://doi.org/10.1007/978-1-4419-0763-9_20.

Thompson, Tommy, and Larry Grauke. 2003. “Pecan Nut and Kernel Traits Are Related to Shelling Efficiency.” *HortScience: A Publication of the American Society for Horticultural Science* 38 (July). https://doi.org/10.21273/HORTSCI.38.4.586.

Wells, Lenny. 2016. *Planting Time Is The Time To Think About Pollination | UGA Pecan Extension*. January 21. https://site.extension.uga.edu/pecan/2016/01/planting-time-is-the-time-to-think-about-pollination/.

Wells, Lenny. 2017. *Pecan: America's Native Nut Tree*. University of Alabama Press. http://ebookcentral.proquest.com/lib/ugalib/detail.action?docID=4805182.

Wells, Lenny, and Patrick Conner. 2015. "Pecan Varieties for Georgia Orchards." University of Georgia Extenstion, February 24. https://extension.uga.edu/publications/detail.html?number=C898&title=pecan-varieties-for-georgia-orchards.

Wood, Bruce. 2000. *Pollination Characteristics of Pecan Trees and Orchards*. HortTechnology. January 1. https://doi.org/10.21273/HORTTECH.10.1.120.

Zhang, Jing-Bo, Rui-Qi Li, Xiao-Guo Xiang, et al. 2013. "Integrated Fossil and Molecular Data Reveal the Biogeographic Diversification of the Eastern Asian-Eastern North American Disjunct Hickory Genus (Carya Nutt.)." *PLOS ONE* 8 (7): e70449. https://doi.org/10.1371/journal.pone.0070449.

Zhou, Huijuan, Yiheng Hu, Aziz Ebrahimi, et al. 2021. "Whole Genome Based Insights into the Phylogeny and Evolution of the Juglandaceae." *BMC Ecology and Evolution* 21 (October): 191. https://doi.org/10.1186/s12862-021-01917-3.

CHAPTER 2

IDENTIFICATION OF QTLS ASSOCIATED WITH NUT SHAPE CHARACTERISTICS IN PECAN (*CARYA ILLINOINENSIS)*

Anne Marie Gahagan, Gaurab Bhattarai, Nolan Bentley, Patricia Klein, Clive H. Bock, Cristina Pisani, and Patrick J. Conner. To be submitted to *The Journal of the American Society for Horticultural Science*.

Abstract

Pecan nuts exhibit vast morphological diversity, with cultivars producing characteristically unique nut shapes. Pecan cracking and shelling machinery requires uniform nut size and shape to minimize kernel shattering and maximize the production of complete kernel halves. Mixed cultivar orchards, which could enhance pollination, mitigate pecan scab, and increase yields, are impractical due to cultivar variation in nut shape. Identification of QTLs associated with nut shape characteristics would support the development of cultivars with similar nut shape in the breeding program. Nuts from 119 individuals of a biparental ('Pawnee' × 'Elliott') mapping population were harvested over multiple years and analyzed using Tomato Analyzer (TA) software to assess 10 morphometric traits related to nut shape. QTL analysis of these traits as well as nut weight was conducted using R/qtl with parental maps created via a pseudo-testcross mapping strategy. Phenotypic data were analyzed separately for each parental map across two near-complete yearly datasets (2023, 2024), as well as a combined dataset spanning multiple years. Analysis revealed a QTL region on 'Pawnee' chromosome 11 that was consistently associated with nut shape index, circularity, distal angle, and height across all datasets. Likewise, a consistent QTL region on the 'Elliott' map was revealed on chromosome 8 associated with the same traits in addition to width rather than height. Additional potential QTLs were detected for each trait in single datasets. These regions were searched for potential candidate genes based on relevance of protein function. Overall, this analysis represents a first step towards the development of marker-assisted-selection of pecan nut shape traits and improves our understanding of the inheritance of these important traits.

Introduction

Carya illinoensis, known commonly as pecan, is the most valuable nut crop native to North America and is grown commercially throughout northern Mexico and the southern United States (Thompson and Conner 2012). The pecan nut consists of a hard outer shell that protects the edible portion, the kernel, which is valued for its flavor, nutritional content and diversity of uses. Before reaching consumers, roughly 90% of nuts will have the kernels extracted in a two-step mechanical process (Thompson and Grauke 2003). The goal of cracking is to break the outer shell by simultaneously applying force to both ends of the nut such that it shatters. However, this process can also shatter the kernel, resulting in kernel pieces. After cracking, all nut fragments will move along a conveyor system for the shelling process where electric sorters, fans, and flotation systems separate kernels from shell debris (Santerre 1994). Kernel shattering should be minimized since broken pieces are more difficult to sort from shell material and may be lost during shelling – reducing total production volume of kernels. Furthermore, pieces of kernel must be size-graded, increasing processing time and costs. In contrast, whole kernels are easier to sort from shell fragments and are more valuable in the consumer market (Sparks 1992). The production of complete kernels can be improved, in part, by properly grading nuts by size and adjusting equipment accordingly prior to cracking (C. R. Santerre 1994). However, nut shape also plays a role, as certain shapes are more compatible with mechanical cracking and tend to produce a higher proportion of intact kernels.

Nuts can be categorized into six basic shapes– round, oval, oblong, ovate, obovate, and elliptic – as viewed from the nut's suture side, and further described by their cross-

sectional, basal, and apical morphology. In general, nuts displaying moderate elongation, producing a football-like shape with less angular ends are best suited for mechanical cracking (Sparks 1992). Shattered kernels are more common in overly elongated nuts, which are more likely to break in half during processing, and rounded nuts, which are prone to fall crosswise in the machinery (Bhattarai et al. 2022). Nut shape also varies by cultivar and serves as a primary characteristic for cultivar identification. For growers, selecting cultivars with favorable nut shape for superior cracking ability can provide a financial benefit due to a higher percentage of whole kernel halves, even when yield (pounds of nuts per acre) is less competitive (Sparks 1992). In this way, nut shape plays a critical role in both processing efficiency and economic return.

However, cultivar selection is not based solely on nut shape. Pecan orchard design must also consider pollination dynamics, which introduces additional complexity. Many commercial orchards are planted with a primary cultivar alongside one or more pollinator cultivars. Pecan is a monoecious, hetero-dichogamous species in which individuals can be either protandrous or protogynous. This promotes outcrossing and genetic diversity in wild populations. Commercially, self-pollination may occur but leads to a reduction in fruit set and poor kernel quality (Wood 2000). To prevent this, growers establish orchards with pollinator varieties that complement the flowering type of the main cultivar. Traditionally, these pollinators are planted in blocks or interspersed among rows when they share similar nut characteristics (Wells and Conner 2015). Although many orchards use only two cultivars, some research suggests including at least four complementary varieties to optimize pollination (Carroll and Smith 2017; Wood 2000). While this strategy improves yield

and kernel quality, it also increases variability in nut shape within the orchard. This necessitates either harvesting individual rows or trees separately or complicates mechanical shelling by introducing a mixed shape product, potentially reducing the proportion of intact kernels or increasing production time and costs for additional grading and sorting.

In addition to improving pollination, mixed-cultivar orchards may help limit the spread of pecan scab caused by the fungus *Venturia effusa*. *V. effusa* exists as numerous races which may be more compatible with specific cultivars (Conner and Stevenson 2004). Integration of multiple cultivars within orchard rows proved to be effective at reducing both severity and incidence of apple scab, *Venturia inequalis*, which is similarity detrimental to apple production worldwide (Didelot et al. 2007; Stewart et al. 2023). Integrating multiple cultivars may reduce the risk of a single race infecting the entire orchard by slowing disease spread and making scab outbreaks more manageable under moderate fungicide regimes. Moreover, having multiple cultivars can stabilize yield output if one cultivar is severely impacted by an aggressive scab race. The development of cultivars with similar nut shape would support processing efficiency in mixed-cultivar orchards.

Quantification of fruit shape can be achieved by a variety of precise measurements obtained either manually or through specialized software. Tools like Tomato Analyzer (TA) enable accurate, high-throughput measurement of shape-related traits. Initially developed for tomatoes, this software has been widely applied to study diversity in shape, size, and color across a wide range of crops (Brewer et al. 2006). Numeric data extracted from the program has a broad range of uses including QTL or GWAS analysis as seen in eggplant

(Mangino et al. 2021), pepper (Khokhar et al. 2022; Nankar et al. 2020), grape (Zhang et al. 2022), and apple (Keller et al. 2024), among others. The applications of these programs are now extending to nut crops as well. A 2024 study utilized similar software to investigate the shape of almond nuts in search of QTLs (Pérez de los Cobos et al. 2024). Furthermore, Bhattarai et al (2022), effectively used Tomato Analyzer to evaluate ten morphological traits related to pecan nut shape despite the software being originally designed for fleshy fruits. Trait values were analyzed using mid-parent-offspring regression and revealed moderate to high heritability (Bhattarai et al. 2022). Given these heritability estimates, the traits were considered strong candidates for QTL analysis. Therefore, this study aims to examine nut-shape QTLs as a first step in the potential development of marker assisted selection for shape traits in pecan.

Methods

Plant Materials

This study aimed to identify QTLs associated with pecan nut shape characteristics using a bi-parental mapping population of 119 F_1 individuals. The population was derived from a cross between seed parent 'Pawnee', which produces relatively large, oblong-shaped nuts, and pollen parent 'Elliott', which produces small, round nuts (Fig. 1.1). An initial cross in 1986, produced 55 offspring that were planted at the USDA station in Byron, Georgia, (32°40'8.55"N, 83°43'34.26"W), forming the Byron Mother Tree (BMT) orchard. In 1999, a second iteration of the same cross produced 64 offspring which were planted at the University of Georgia's Ponder farm, establishing the Tifton Mother Tree (TMT) orchard (31°30'34.88"N, 83°38'55.26"W). Scion wood from the mother trees, grown from seed on

their own roots, was topworked onto seedling rootstocks in 2017-2019 to generate two clonal replicates of all 119 individuals. These trees were located on UGA land in Tift County, Georgia, forming the Tifton Replicate 1 (TR1) and Tifton Replicate 2 (TR2) orchards. TR1 trees are located on the same farm as the TMT population, while the TR2 trees are located on a separate farm also in Tift Co., GA approximately 12.3 km distant (31°30'30.65"N, 83°31'13.95"W). In total, the plant material for this study is grown across four orchards for three replicates of the progeny population.

Trees were planted at a spacing of 3.0 m between trees and 4.6 m between rows. Trees were pruned every other year to maintain tree spacing and maximize fruiting canopy. Trees were irrigated either by sprinkler (TMT) or drip tubing (all others). Nitrogen was applied annually at 112 kg•ha^{-1}, while other nutrients and lime were applied according to leaf or soil analysis. Fungicides and insecticides were applied following Georgia Extension Service recommendations as needed to ensure enough crop for analysis (Hudson et al., 2006).

Sample Collection

Nut samples were collected from fruiting trees over six years: 2017, 2019, 2020, 2022, 2023, and 2024. However, the TR1 and TR2 trees did not begin fruiting enough to warrant sampling until 2023, and variability in annual nut production meant that not all genotypes yielded samples every season. Figure 2 illustrates the number of genotypes sampled per year in each orchard throughout the study period.

Imaging and Phenotyping

For each sampled tree, at most ten nuts were harvested for imaging and phenotyping. If there were three or fewer nuts, however, the tree was not sampled that year. First, the nuts

were weighed to find the average mass per nut. Then, they were arranged on a flat, white surface with the suture side facing up alongside an American quarter for size reference. To maintain consistent position, the nuts were placed within indentations on a felt sheet while photographs were taken. Images were converted to black and white, then inverted so that the background appeared black and the nuts white, optimizing processing in TA version 4.0. Within the software, each nut's vertical orientation (proximal end at top of image), perimeter boundary, and proximal and distal markers were carefully inspected and adjusted as necessary. Using this approach, ten morphometric traits were quantified (Fig. 1.3). An average for each trait was calculated across the total number of nuts (4-10) for each sample, and the values for maximum height and width were converted from pixels, as recorded by TA, to centimeters using a U.S. quarter dollar coin reference in each photo (diameter = 2.426 cm).

BLUE Calculation

To account for environmental variation across locations and years, genotypic values were calculated using best linear unbiased estimator (BLUEs) derived from a one-step mixed model approach. This method was chosen to minimize confounding effects and enhance the accuracy of trait estimates in a design where individual trees were evaluated across multiple years and genotypes were present in multiple orchards.

Each tree was assigned a unique identifier (Tree_Code) to distinguish it as a replicate of a specific genotype within a given orchard. Additionally, each sample was labeled with an environmental code (Envi_Code), a combination of orchard and year, thereby controlling variation attributable to temporal and spatial factors. BLUEs were calculated using the

"lmer" function from the lme4 package in R. Genotype was modeled as a fixed effect to estimate genetic contribution to trait variation, while tree identity and environment were treated as random effects to account for replication and environmental noise.

lmer(Trait ~ Genotype + (1|Tree_Code) + (1|Envi_Code))

Due to differences in the number of genotypes represented across years (Fig. 1.2), this procedure was applied to three distinct datasets:

1. Combined dataset of all years and locations (Combined Dataset)
2. Single-year dataset for 2023 all locations (2023 Dataset)
3. Single-year dataset for 2024 all locations (2024 Dataset)

For each dataset, one BLUE value per genotype per trait was calculated using the *lmer*() model above and used as input for subsequent QTL analysis. This ensured consistency in trait estimation and reduced the influence of environmental noise, including variation in year, location, and individual tree performance.

Analysis of Data

Pairwise correlation coefficients (*r*) were calculated for the combined dataset to quantify the strength and direction of linear associations between all nut shape characteristics. For each trait pair, Pearson correlation coefficients were computed with the *cor.test*() function in R, which estimates *r* as the covariance between two variables divided by the product of their standard deviations. At the same time, the function performs a two-tailed t-test to assess statistical significance, with null hypothesis $r = 0$.

Descriptive statistics were calculated for each dataset to assess the extent of variation present within the measured phenotypic traits. For each trait, the mean, standard

deviation (SD), and coefficient of variation (CV) were computed. The CV was expressed as a percentage, calculated as the ratio of the SD to the mean multiplied by 100. In addition, the minimum and maximum values were determined to define the range of observed phenotypic variation. All calculations were performed in R using standard base R functions.

Broad Sense Heritability

Broad-sense heritability (H^2) was estimated for each nut shape trait using linear mixed models in R with the package "lme4". Genotype and genotype-by-environment (G×E) interaction were treated as random effects, with environment defined as the combination of orchard and year as used in the BLUE calculation. Heritability was calculated across environments to account for environmental heterogeneity, with the harmonic mean of replicates per genotype used to adjust for unbalanced replication across environments.

Sequencing and Linkage Map Construction

The genotyping and linkage map construction methods for this population are detailed in Bhattarai et al. 2025. In short, genomic DNA was extracted from young leaf tissue of both parents and all F_1 progeny. DNA was isolated using a CTAB protocol, quantified using a DeNovix DS-11 spectrophotometer, and genotyped using a modified genotyping-by-sequencing (GBS) protocol. DNA fragments were ligated to unique 12-bp barcodes, pooled into two libraries, and sequenced on an Illumina HiSeq 2500 (150-bp single-end reads).

Following a quality check in FastQC, sequence reads were demultiplexed and aligned to the 'Elliott' reference genome. Initial variant discovery with GATK yielded 171,356 putative SNP and indel sites. After removing indels, 162,838 raw SNPs were retained. Variant filtering in VCFtools applied thresholds retaining only biallelic SNPs with a minor allele

frequency of 0.1, a mean read depth between 8 and 60, less than 10% missing data, and the proportion of reference and alternative allele read depth of 0.25. This process reduced the dataset to 5904 high-confidence SNPs.

Because pecan is a highly heterozygous outcrossing species, linkage maps were constructed for each parent using a two-way pseudo-testcross strategy (Grattapaglia and Sederoff 1994). Filtered SNPs were converted to JoinMap format, and 2274 markers for 'Pawnee' and 1861 markers for 'Elliott' were selected for initial map construction. Cosegregating markers and markers showing significant segregation distortion from the expected 1:1 ratio were removed. Linkage group assignment using independent LOD scores produced 16 linkage groups for each parent, consistent with the haploid chromosome number of pecan. Marker order was generated using the regression mapping algorithm with a maximum recombination frequency of 0.4 and the Kosambi mapping function.

To refine marker order and resolve linkage phase uncertainty, preliminary JoinMap results were reanalyzed in MAPMAKER using its multipoint maximum-likelihood framework. Overlapping marker subsets were ordered and merged using the order, try, and ripple functions, and final distances were recalculated using the Kosambi function with error detection enabled. The finalized genetic maps contained 1347 markers spanning 4493 cM for 'Pawnee' and 1050 markers spanning 3758 cM for 'Elliott', covering 92.7% and 89.5% of the physical reference genome, respectively. Synteny between the parental genetic maps and the 'Elliott' genome was evaluated to reveal that all 16 linkage groups from both parents displayed strong collinearity with the physical genome, confirming consistent chromosomal structure and the accuracy of marker assignment in both parental maps.

Transformation Investigation

Before conducting quantitative trait locus (QTL) analyses, BLUE values were assessed for normality within each of the three datasets via the Shapiro-Wilk test, alongside skewness and kurtosis statistics calculated with the *e1071* package in R. To examine the effect of non-normality on subsequent QTL analysis, a subset of data was transformed. Traits exhibiting significant deviation from normality ($p < 0.05$ in Shapiro-Wilk Test), substantial skewness ($|skewness| > 1$), or excessive kurtosis ($kurtosis > 5$) were flagged for transformation. For these traits, a Box-Cox transformation was applied using the MASS package to stabilize variance and approximate normal distributions. Optimal transformation parameters were determined by maximum likelihood estimation.

To evaluate whether data transformation affected QTL detection results, paired t-tests were conducted to compare QTL peak positions (cM) and LOD scores between analyses performed on transformed and untransformed trait datasets. Because the same QTLs were detected using either set of values, they were matched based on their order of detection, and comparisons were made using R's *t.test*() function with the argument paired = TRUE. The mean difference in QTL position between datasets was 0, and the mean difference in LOD scores was –0.02, with a non-significant p-value (0.3364). Because no statistical differences were observed between transformed and untransformed analyses, subsequent QTL detection and interpretation were based on non-transformed BLUE values.

QTL Analysis

To begin QTL mapping, outliers exceeding three standard deviations from the trait mean were removed. Analyses were conducted in RStudio using the R/qtl package (version

1.7), mapping BLUE values to both the ‘Pawnee’ and ‘Elliott’ genetic maps (Bhattarai et al. 2025). Marker positions were refined with the *jittermap*() function, followed by calculation of genotype probabilities using *calc.genoprob*() with a step size of 2 cM and an assumed genotyping error rate of 0.001.

To determine the significance threshold for QTL detection, permutation tests were conducted by randomly shuffling phenotypes relative to genotypes, thereby generating a null distribution of genome-wide maximum logarithm of odds (LOD) scores expected under the assumption that there is no true QTL (Browman and Sen 2009). The 95th percentile of this distribution represents the genome-wide LOD threshold corresponding to a 5% experiment-wise error rate. Using the permutation approach accounts for features specific to the dataset, including genome size, marker density, and missing genotype patterns, which influence the null distribution of maximum LOD scores. The permutation analysis was integrated into the *scanone*() function via the n.perm argument, using 1,000 permutations and the Haley–Knott regression method (method = "hk").

However, no significant QTL were detected under the permutation-derived thresholds, likely due to limitations in sample size (n = 119), the heterozygosity of the cross used, and the nature of a pseudo-testcross mapping strategy (Grattapaglia and Sederoff 1994; Browman and Sen 2009). Because the mapping strategy uses only a subset of genome-wide markers informative for each parent, the resulting reduction in effective marker coverage and genotypic completeness may reduce statistical power to detect true QTLs (Wu et al. 2010). Consequently, subsequent analyses employed the Haley–Knott regression method (method = "hk") with a fixed LOD threshold of 2.5 to identify putative

QTLs. A QTL was considered of biological and practical significance if detected in all three datasets on either parental map.

To identify QTL peaks, the *scanone*() function was iteratively applied to each phenotypic trait, producing genome-wide LOD profiles. For each trait, the output was parsed to extract peak positions exceeding the fixed LOD threshold. The chromosome, peak position (cM), and corresponding LOD value for each significant region were recorded. To further refine these results, a 95% Bayesian credible interval (CI) was calculated for each detected QTL using the *bayesint*() function, providing an estimate of the most probable genomic region surrounding the peak that contains the causal locus. These intervals are less sensitive to local fluctuations in the LOD curve and offer a more biologically meaningful confidence range than simple 1-LOD drop intervals (Manichaikul et al. 2006).

Candidate Gene Investigation

QTLs were considered stable when detected across all three datasets on either parental map. The genomic region surrounding each stable QTL peak, as defined by the Bayesian CI, were examined in the Phytozome database using the JBrowse genome browser (https://phytozome-next.jgi.doe.gov/). The corresponding linkage groups for each parental map (LG 11 in 'Pawnee' or LG 8 in 'Elliott') were explored to identify genes within the CI boundaries. All annotated genes with potential protein-coding functions were examined for relevance to nut shape or size. Protein sequences of candidate genes were then evaluated using BLAST (Altschul et al. 1997) against the NCBI database. Sequences were further investigated through UniProtKB for functional annotation. Top accession hits were selected from UniProt based on species similarity (primarily Juglans) and the lowest E-values.

Results and Discussion

Building of Datasets

From all phenotypic data collected, three datasets were generated based on the years in which nuts were harvested. The mapping population originated from crosses between ‘Pawnee’ and ‘Elliott’ established in 1986 and 1999, with additional replications produced after topworking scion wood in 2017–2019. During the early harvest years (2017–2022), fruit production from topworked trees was limited, preventing sufficient sampling. The 2023 and 2024 datasets were selected for separate analysis primarily because they contained the most complete phenotypic records and the fewest missing genotype–phenotype combinations, thereby maximizing the number of individuals available for mapping and increasing power for QTL detection. In addition to these year-specific analyses, a combined dataset (all years and locations) was analyzed to evaluate QTL reproducibility across environments and utilize the full scope of data collected. Having three datasets for analysis gives the opportunity for consistent QTL detection across multiple conditions.

Characterization of Nut Shape

This study’s population was produced from a cross between seed parent ‘Pawnee’, producing somewhat large and elongated nuts, and pollen parent ‘Elliott’, producing small and round nuts. Variation in shape was visually apparent among the 119 offspring, with nuts ranging from round and blocky to elongated and from small to large (Fig. 1.1). Variation in nut shape was examined through the evaluation of eleven traits: weight, width, height, nut

shape index, proximal blockiness, distal blockiness, circularity, rectangularity, proximal angle, distal angle, and ovoid (Fig. 1.2).

Weight is the average mass (g) per nut, width is the maximum distance (cm) across the horizontal plane, and height is the maximum distance (cm) across the vertical plane. These three characteristics give a basic representation of the size of a nut since higher values, in general, represent larger nuts. Nut shape index (NSI), the ratio between height and width, will describe if the nut is more elongated (higher NSI), as in the case of 'Pawnee' or more round (lower NSI), like 'Elliott' (Fig. 1.1).

Both blockiness and angle give a smaller-scale description of nut shape on either end of the nut. The proximal end is that which connects to the branch of the tree. The distal end is furthest from the branch and will be the first part of the nut exposed as the shuck opens. In general, the distal end of the nut is more pointed, thus having smaller blockiness and angle values. Circularity and rectangularity measure if the nuts are more similar to a circle or a rectangle. Small circularity measures show that a nut is rounder, while higher rectangularity values show that a nut is more rectangular. Ovoid quantifies the asymmetry of nut shape along the vertical plane, describing how much fuller the nut appears above the midpoint (proximal end) versus below the midpoint (distal end). Higher values indicate that nuts are fuller/rounder above mid-height.

Mean, range, standard deviation, and coefficient of variation were calculated to describe within trait variation across each dataset (Table 1.1). These values quantify the variation visually apparent when examining the progeny nuts (Fig. 1.1). Variation was present for every trait in each dataset, with coefficients of variation ranging from ~3% for

rectangularity and ~28-31% for circularity. Means and ranges of shape traits were remarkably similar between years highlighting the relative stability of shape measures across environments. However, the range of nut weight was 1.5 to 2.0 grams lower in 2024 compared to 2023. Rainfall in the nut sizing period (May 1 to Aug. 15) was lower in 2024 (41.2 cm) compared to 2023 (49.6 cm). Additionally, the month of June 2024 was very dry which may have reduced nut size in 2024 despite the application of irrigated water (Fig. 1.4).

Correlations Among Traits

Pairwise correlations of each of these traits revealed that many traits were significantly associated with each other, indicating the interdependence of pecan nut shape traits (Fig. 1.5). Strong positive correlations were observed between fundamental size traits like weight and height (r = 0.597) and width (r = 0.675) as nuts that are larger (wider and longer) are likely to weigh more. Interestingly, width and height were not strongly correlated with each other, suggesting that when nuts increased in size it was either through an increase in width or height, but not normally both. Width and height were also strongly correlated to nut shape index (NSI) because these values are used in its calculation (NSI = height/width). It was surprising, however, that weight was not correlated to NSI (r = 0.003). This suggests that nuts can be small (have less mass) but still have an elongated shape. Therefore, nut shape and size should be measured separately with different metrics to fully describe these characteristics.

The strongest correlation between traits was observed between nut shape index and circularity (r = 0.987), indicating the traits measure a very similar characteristic in pecan, that being how round the nut appears. A larger NSI indicates the nut is more elongated,

whereas a larger circularity value indicates the nut is less round. Circularity is also highly correlated to proximal angle (r = -0.855) and distal angle (r = -0.733). Again, these traits are working together to describe the roundness of a nut. With larger proximal and distal angles, the nut is more round which produces a smaller circularity value. In the same vein, ovoid is highly correlated to both proximal blockiness (r = 0.755) and distal blockiness (r = -0.578). Because ovoid is used to measure if the nut is wider above the midpoint (near the proximal end), it is expected that as the proximal blockiness is greater, so too is the nut more ovoid. Conversely, the opposite must be true for distal blockiness as the area below the midpoint will be smaller as the ovoid value increases. In this way, ovoid is able to describe the general shape of the nut while the proximal and distal blockiness are more specifically descriptive. There were also some unexpected correlations. For example, rectangularity and circularity were only slightly negatively correlated (r = -0.233) even though they measure seemingly opposite characteristics.

These patterns indicate that many traits tend to covary in expected directions, but multiple traits are necessary to fully describe nut shape in pecan. Collectively, these correlations support the use of multiple, complementary metrics to comprehensively characterize nut morphology from a specific or general perspective.

BLUE Utilization and Data Normality

Because there were differences in the number and locations of fruitful trees each year, data was split into three data sets for further analysis. A combined dataset included all data collected across all years and locations. A second dataset included all data from samples harvested in the year 2023 across all locations, and a final dataset included all data

from samples harvested in the year 2024 across all locations. For every dataset, BLUE values were calculated to obtain a single best fit average for each trait for every genotype, to account for variation in the number and locations of fruiting trees across the study period. Normality of BLUEs was examined visually (Figs. 1.6-1.8) and mathematically via the Shapiro-Wilk test, alongside skewness and kurtosis statistics (Table 1.1).

Normality of trait distributions was first assessed on the raw phenotypic data. In the combined dataset of raw values, proximal blockiness, distal blockiness, circularity, proximal angle, and ovoid deviated from normality due to moderate skew or heavier tails. Distal blockiness was consistently right skewed with elevated kurtosis across datasets, while circularity and ovoid tended toward slight negative skew and flatter tails. Year-specific assessments of raw data revealed that most traits in 2023 were normally distributed with the exception of distal blockiness. In 2024, width, nut shape index, distal blockiness, circularity, and proximal angle showed significant departures from normality.

When the same tests were applied to BLUE values, distributions more closely approximated normality (Table 1.1). In the combined BLUE dataset, all traits were normally distributed (Shapiro-Wilk p-value > 0.05), although width, distal blockiness, and proximal angle showed moderate skewness. Year-specific BLUE data largely reflected these trends: in 2023, all traits were consistent with normality, with minor skewness in weight, width, height, and distal blockiness. For 2024 data, weight ($p = 0.0535$, kurtosis = 4.06), circularity ($p = 0.0463$), and proximal angle ($p = 0.0296$) exhibited modest non-normality, while all other traits were normally distributed ($p > 0.05$).

BLUEs were calculated to account for environmental variation; however, they also helped reduce non-normality by stabilizing trait distributions. Standard transformations were examined, but yielded no meaningful change to subsequent analysis. For clarity and interpretability, non-transformed values were retained in all downstream analyses.

Broad Sense Heritability

Broad sense heritability (H^2) was estimated to assess the genetic contribution to phenotypic variation in nut shape traits. Using a mixed model with genotype-by-environment interaction as random effects, all traits exhibited high heritability, with H^2 values ranging from 0.874 to 0.987 (Table 1.2), indicating that most observed variation is genetically determined and thus suitable for QTL analysis. In a previous study of similar traits in a different pecan population, heritability estimates ranged from 0.41 to 0.83 using mid-parent–offspring regression and from 0.26 to 0.78 using a variance component approach (Bhattarai et al. 2022). The comparatively higher estimates in the present study may reflect differences in population structure, experimental design, or the number of environments sampled, underscoring the strong genetic control of nut shape traits in this mapping population.

QTL Analysis

Broad-sense heritability estimates (Table 1.2) indicated a strong genetic contribution to nut shape traits, and descriptive statistics (Table 1.1) showed sufficient variation within traits for QTL analysis. However, permutation tests within the R/qtl *scanone*() function yielded no significant associations. This may be the results of the relatively small mapping population limiting statistical power to detect loci above stringent, permutation-based

thresholds and truly quantitative gene function having relatively small effects on phenotype. To ensure biologically meaningful signal detection, genome-wide LOD profiles were instead evaluated using a fixed threshold of 2.5, allowing identification of local maxima corresponding to putative QTL regions. For each detected peak, Bayesian credible intervals were calculated to estimate the region likely containing the causal locus. QTLs consistently identified across all three datasets were interpreted as robust and biologically relevant, representing strong candidates for loci influencing nut shape traits.

Genome-wide QTL analyses conducted for each parental map using the BLUE values from the combined dataset, the 2023 dataset, and the 2024 dataset revealed between eight and ten putative QTLs detected in both 'Pawnee' and 'Elliott' for different traits across multiple chromosomes (Tables 1.3, 1.4).

A whole genome scan of the combined dataset aligned to the 'Pawnee' genome identified QTLs for 7 of the 11 nut shape traits: width, height, nut shape index, circularity, rectangularity, distal angle, and ovoid (Table 1.3). Peak LOD scores for these loci ranged from 2.5 to 3.98, with an average of 3.25. The QTLs were distributed across chromosomes 3, 6, 9, 10, 11, and 13. A parallel analysis of the combined dataset aligned to the 'Elliott' genome showed similar outcomes. Putative QTLs were detected for width, nut shape index, proximal blockiness, circularity, proximal angle, and distal angle with peak LOD scores ranging from 2.55 to 3.51, with an average score of 2.96 (Table 1.4). These regions were located on chromosomes 4, 7, and 8.

Whole genome scans were also conducted using the 2023 and 2024 independent datasets. When the 2023 phenotypic data was mapped to 'Pawnee', a total of eight QTLs

were detected for weight, width, height, nut shape index, distal blockiness, circularity, distal angle, and ovoid across chromosomes 1, 6, 7, 8, and 11 (Table 1.3). LOD peaks ranged from 2.51 to 3.24 with an average of 2.76. When the 2024 phenotypic data was mapped to 'Pawnee', ten QTLs were detected, correlating to traits height, nut shape index, proximal blockiness, distal blockiness, circularity, rectangularity, proximal angle, distal angle, and ovoid across chromosomes 3, 9, 10, 11, and 12 (Table 1.3). LOD peaks for this dataset ranged from 2.6 to 4.11 with an average score of 3.29.

When mapping to the 'Elliott' map, the 2023 phenotypic data revealed nine total QTLs correlating to width, height, nut shape index, circularity, proximal angle, and distal angle (Table 1.4). LOD score ranged from 2.63 to 3.77 with an average of 3.15. The 2024 dataset revealed eight QTL when mapped to 'Elliott' (Table 1.4). QTL for width, nut shape index, proximal blockiness, circularity, proximal angle, distal angle, and ovoid had LOD peaks ranging from 2.57 to 3.15 with an average score of 2.97.

Several QTLs were consistent across all three datasets and were therefore considered stable. In the 'Pawnee' genome, four traits (circularity, nut shape index, height, and distal angle) mapped to two distinct regions on chromosome 11. This linkage group had 82 total markers across a map length of 217.8 cM for an average intermarker distance of 2.7 cM. Nut shape index and circularity consistently peaked near 62-64 cM, while height and distal angle peaked around 108 cM (Fig. 1.9). Similarly, in the 'Elliott' genome, four traits had valid QTLs, all on chromosome 8. 'Elliott' linkage group 8 had 68 total markers across the 206.8 cM map length resulting in an average intermarker distance of 3 cM. Nut shape index, circularity, and distal angle peaked near the beginning of the chromosome, while width

peaked at 78 cM (Fig. 1.9). Additional QTLs were detected in the combined and single-year analyses but were considered putative due to lack of consistency across datasets (Tables 1.3, 1.4).

Notably, many of the traits with co-locating significant QTLs are highly correlated. For example, nut shape index and circularity show an extremely strong correlation of r = 0.987 (Fig. 1.5). This increases the likelihood that these QTLs represent a single underlying genetic factor influencing both traits because the two metrics are essentially capturing the same aspect of nut morphology. Additionally, distal angle is moderately to strongly correlated with height (r = –0.514), nut shape index (r = –0.732), circularity (r = –0.733), and width (r = 0.485). However, these correlations do not always translate into co-localizing QTLs. For instance, distal angle does not map to the same region as nut shape index and circularity in the 'Pawnee' genome near 64 cM, nor does it overlap with width in the 'Elliott' genome. Thus, while the QTLs identified here are treated as distinct, they may represent broader genomic regions affecting nut shape or more complex gene interactions not captured by this analysis.

There are also features within the parental maps that may reflect biological differences or mapping limitations. For example, nut shape index and distal angle are strongly correlated (r = –0.732) but map to different regions in the 'Pawnee' genome while co-localizing in the 'Elliott' genome. Similarly, height correlates strongly with nut shape index (r = 0.728) but does not consistently map to the same positions, and in the 'Elliott' genome no significant QTL was detected for height despite the presence of QTLs for nut shape index. These inconsistencies highlight the complexity of nut shape genetics.

A more detailed examination of the regions of interest on chromosome 11 of 'Pawnee' and chromosome 8 of 'Elliott' through fine mapping could more precisely pinpoint QTL peaks associated with nut shape traits. Expanding the mapping population would also increase statistical power, improving QTL detection under permutation testing and likely shortening the Bayesian credible intervals around each peak.

Candidate genes

The genomic regions of the stable QTLs (Fig. 1.9) were examined for candidate genes using the JBrowse feature in Phytozome. Genes located within the Bayesian credible intervals of stable QTLs were screened for functional annotations related to fruit or organ morphology. While many genes within these intervals were unrelated to fruit shape or size, those associated with cell proliferation, cell elongation, or cell wall modification were prioritized for further investigation.

In the 'Pawnee' genome, four stable QTLs were located on chromosome 11, with peaks occurring at approximately 62-64 cM and 106-108 cM (Table 1.3). As the confidence intervals of these QTLs overlapped, the region spanning from 24–128 cM (2,041,454 – 34,030,840 bp; ~31.99 Mb) was examined to encompass all associated loci. Within this region, four candidate genes were identified with potential roles in nut morphology (Table 1.5). First, a cytochrome P450 was found, a family of genes which has been shown to regulate organ size in tomato (Chakrabarti et al. 2013). A UDP-arabinopyranose mutase was also identified. Members of this gene family are implicated in polysaccharide biosynthesis and cell wall organization (Honta et al. 2018). Given that pecan nut shells are rich in cellulose, hemicellulose, and lignin, this gene may influence nut size and shape (Agustin-

Salazar et al. 2018; de Souza et al. 2023). An expansin-like gene was also detected, which facilitates growth by expanding cells through loosening plant cell walls (Cosgrove 2015). Expansin proteins have specifically been correlated with fruit enlargement in peach (Cao et al. 2016). Finally, a JMJ zinc-finger gene was identified, which are expressed in the flowers, ovaries, and developing fruits of melon, suggesting a function in fruit development (Jin et al. 2023).

In the 'Elliott' genome, four stable QTLs were detected on chromosome 8, with peaks occurring near 0-2 cM and at 78.1 cM (Table 1.4). Because the confidence intervals of these QTLs overlapped, the region spanning from 0 to 88 cM (1,596,408–11,651,264 bp; ~10.05 Mb) was examined to capture the full span of associated loci. Within this region, four candidate genes were identified (Table 1.5). The first was a YUCCA2-related gene, part of a family known to regulate fruit growth via auxin biosynthesis (Cao et al. 2019). An auxin-responsive SAUR-like gene was also found. SAUR proteins are often associated with cell expansion, implying that nut size may be influenced by cell size (Peng et al. 2022). An ADP-ribosylation factor 1 (ARF1) protein was discovered; ARF1 proteins mediate protein trafficking and are essential for plant growth and development (Min et al. 2013). Lastly, an agenet domain-containing gene with a DUF724 domain was detected. These proteins have been associated with cell division and polar cell growth, with DUF724 domains in Arabidopsis showing high expression in pollen (Brasil et al. 2015; Cao et al. 2010).

Together, these findings suggest that pecan nut growth is influenced by both cell proliferation and elongation processes, with genes involved in cell wall modification and hormone-mediated growth regulation emerging as key contributors to nut shape variation.

Studies in other fruit crops have provided important insights such as the SUN gene in tomato (Wang et al. 2019; Yu et al. 2022) and CIFS1 in watermelon (Dou et al. 2018). The limited number of candidate genes identified here underscores the need for further investigation into the genetic mechanisms underlying nut development.

Conclusions

This study represents a foundational step toward understanding nut shape in pecan. By integrating high-throughput morphometric analysis with robust QTL mapping across a multi-year, multi-location dataset, we identified stable genomic regions associated with key shape traits and uncovered candidate genes with plausible roles nut shape development. These findings validate the heritability of nut morphology and provide tangible targets for future marker-assisted selection of uniform nut shape in pecan.

Uniform nut shape is critical for optimizing shelling efficiency and increasing the production of whole kernels when cracking. Moreover, the ability to breed cultivars with compatible shape traits could enable the adoption of mixed-cultivar orchards which have potential to enhance pollination, mitigate disease pressure, and stabilize yield without compromising processing efficiency. Despite the limited number of candidate genes identified, the consistency of QTLs across datasets and the biological relevance of associated genes underscore the need for deeper functional exploration. Ultimately, this research lays the groundwork for a more integrated approach to pecan breeding which balances genetic diversity, orchard resilience, and processing performance through the establishment of mixed-cultivar orchards.

Tables and Figures

Figure 1.1: Variation in pecan nut shape ranged from very round (left) to elongated (right) in between the shapes observed by the pollen parent 'Elliott' (top left) and seed parent 'Pawnee' (top right) as well as overall size from small (second row) to large (bottom row).

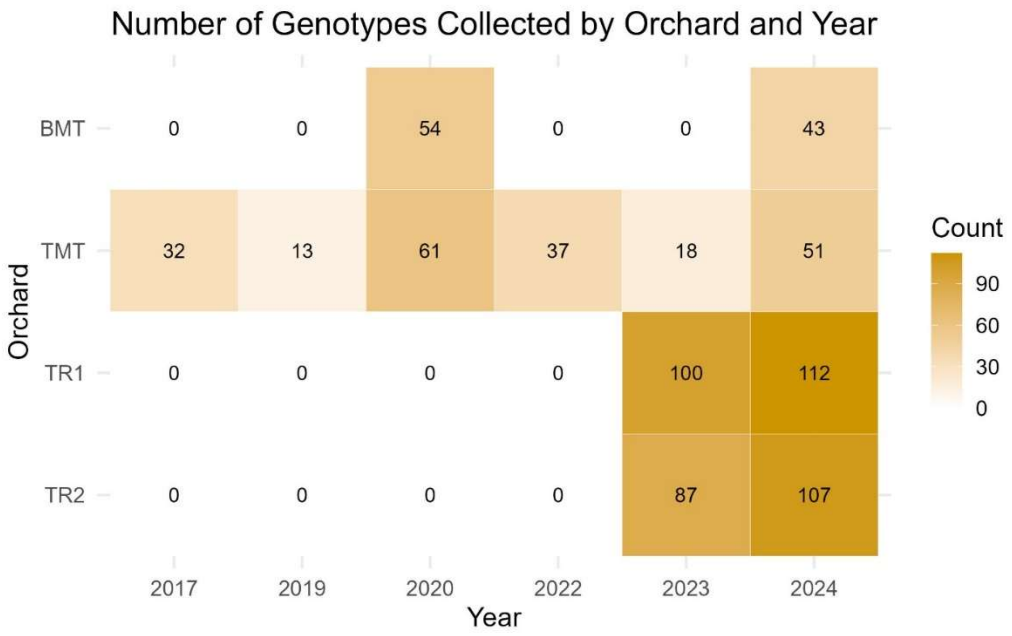

Figure 1.2: The number of pecan genotypes from which samples were taken at each orchard during the study period. Total number of samples possible were BMT = 55, TMT = 64, TR1 = 119, TR2 = 119.

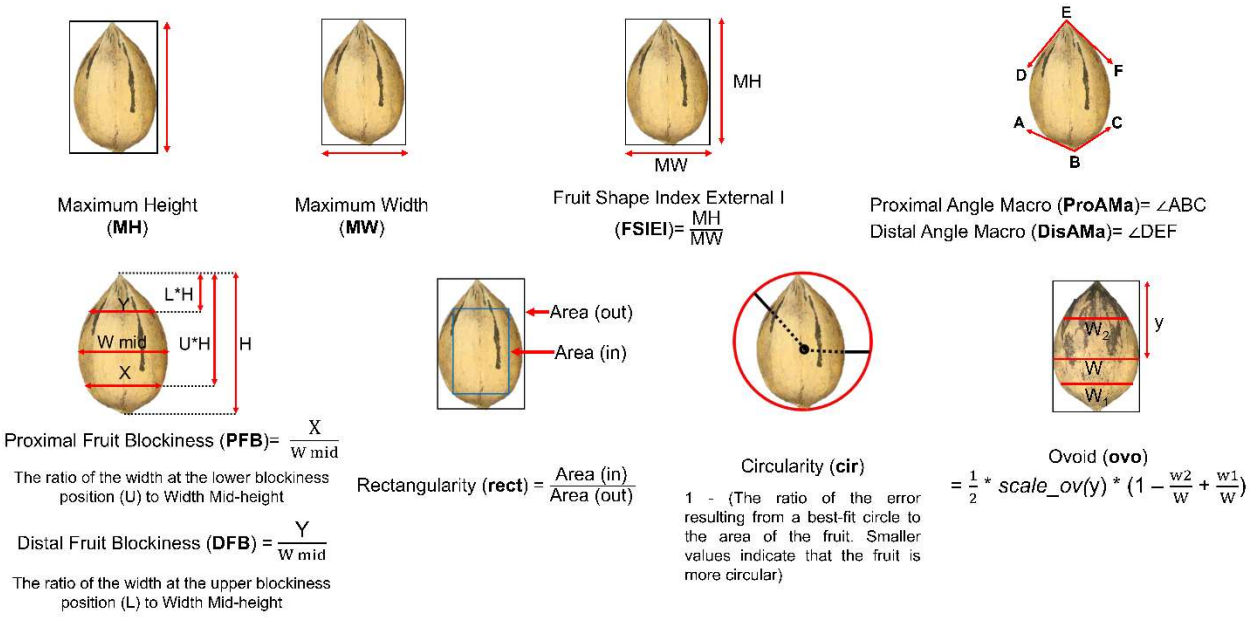

Figure 1.3: Depiction of the ten morphometric traits measured for each sampled pecan nut using Tomato Analyzer software (from Bhattarai et al. 2022).

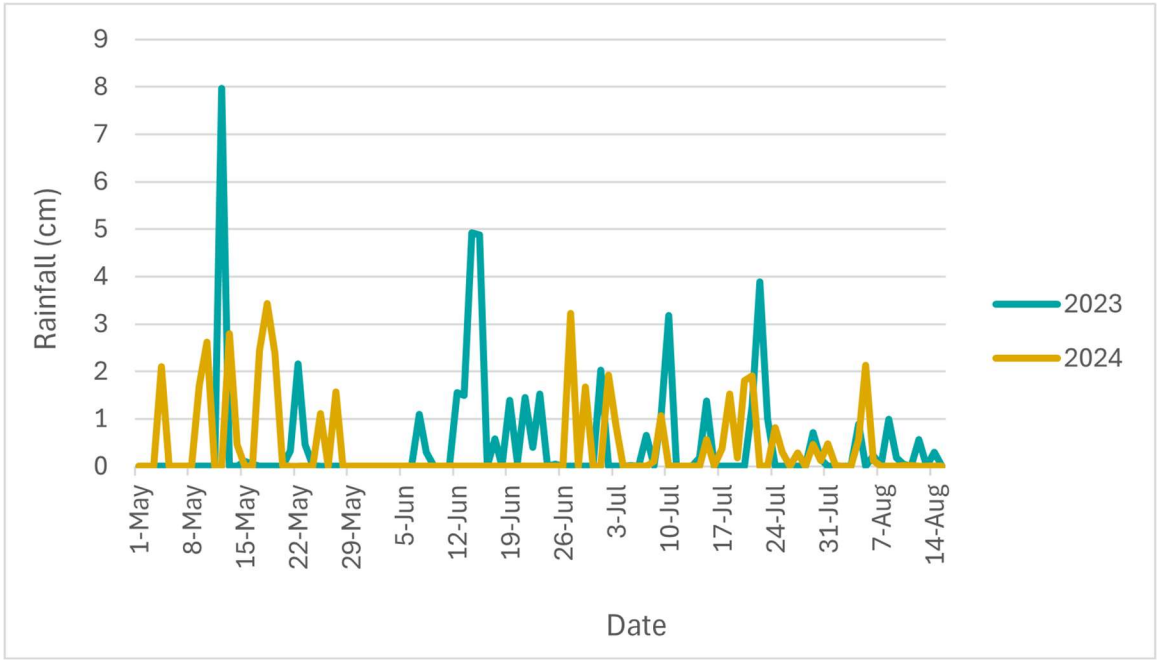

Figure 1.4: Rainfall at the University of Georgia Ponder Farm in 2023 and 2024 during the pecan nut sizing period of May 1 through August 15.

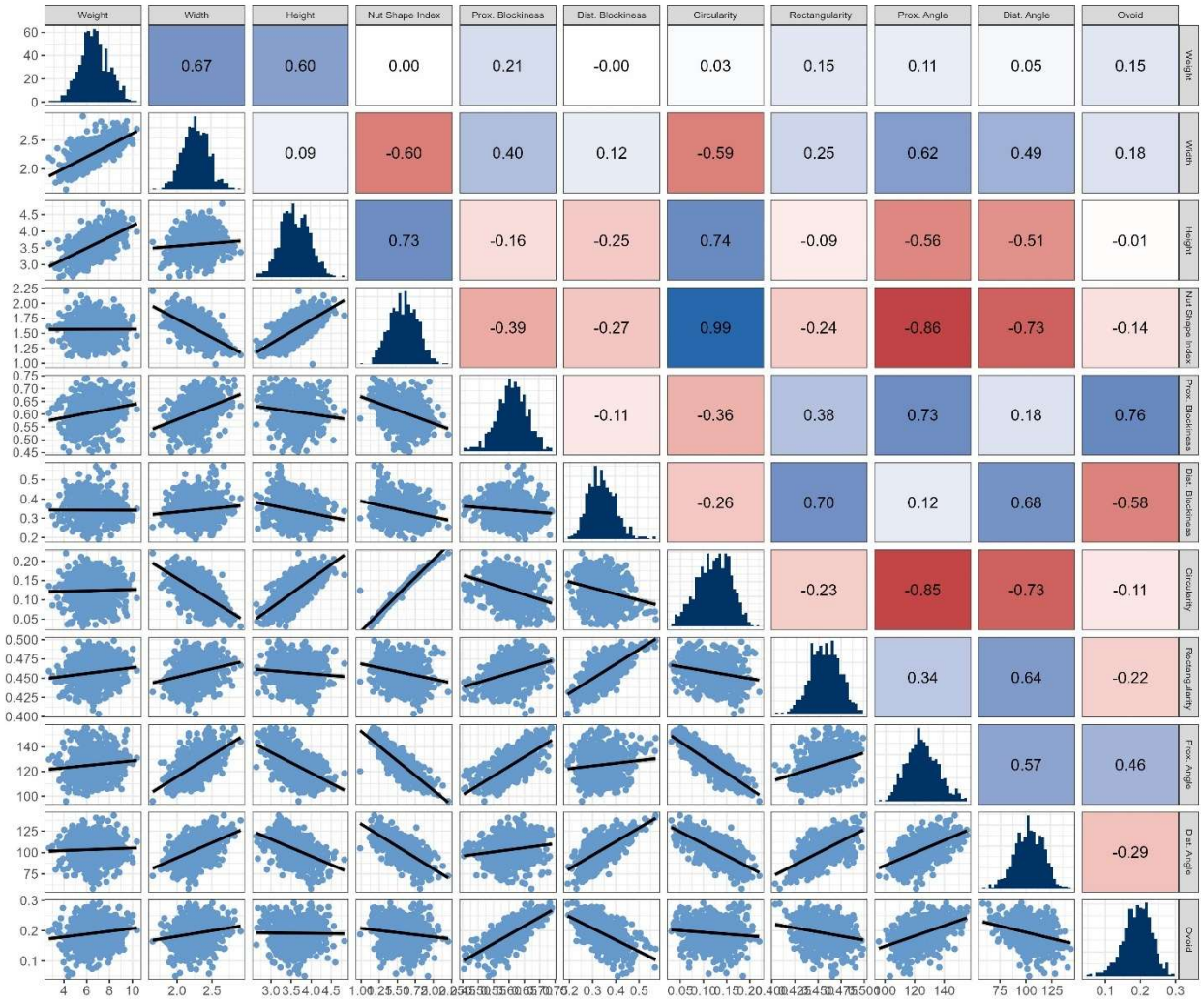

Figure 1.5: Pearson correlation matrix describing the relationship between pecan nut shape and size characteristics across all years, genotypes, and orchards.

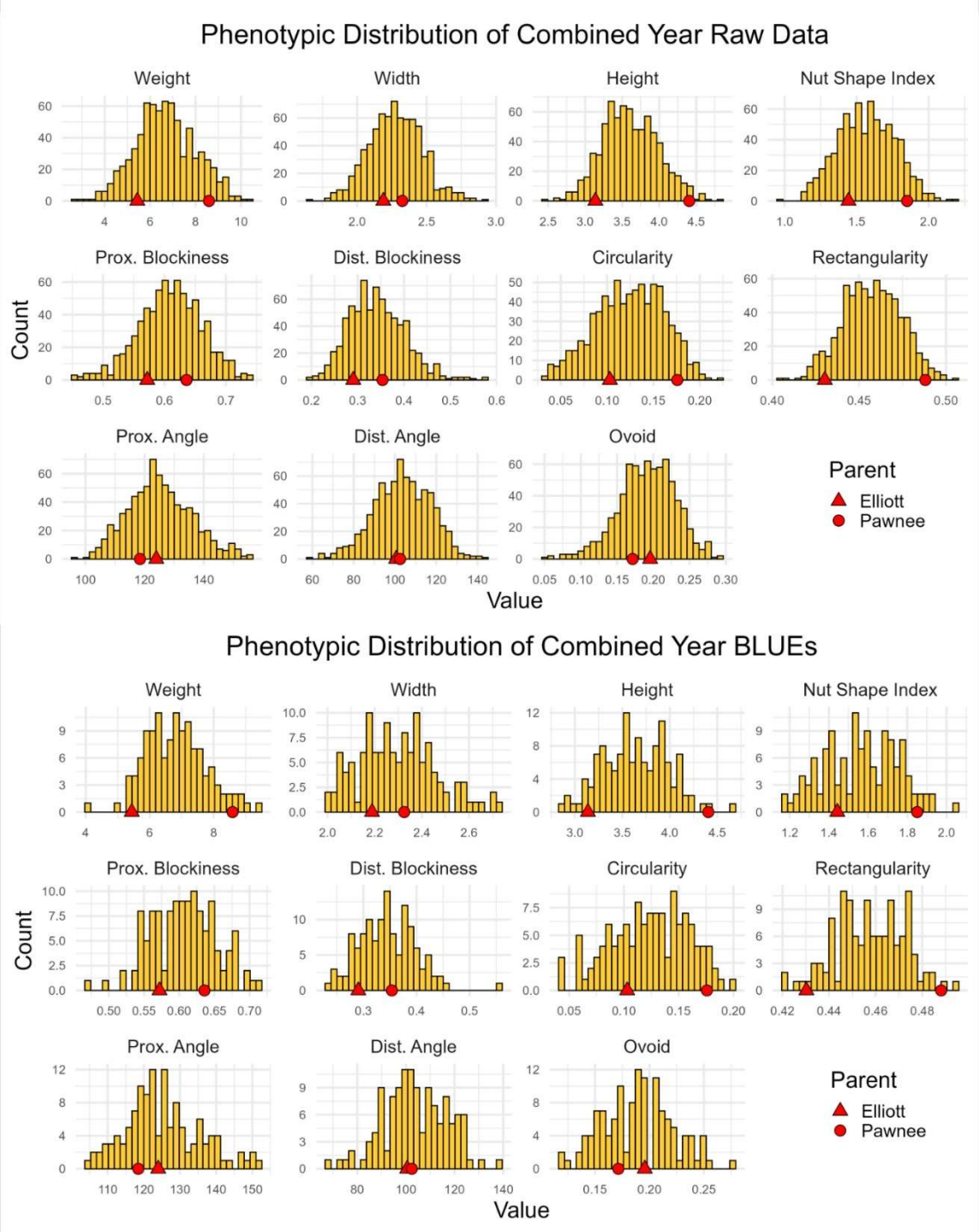

Figure 1.6: Phenotypic distribution of pecan nut shape traits in the F1 pecan mapping population. Distributions represent phenotypic values for raw data (top) and BLUEs (bottom) for a combined years dataset.

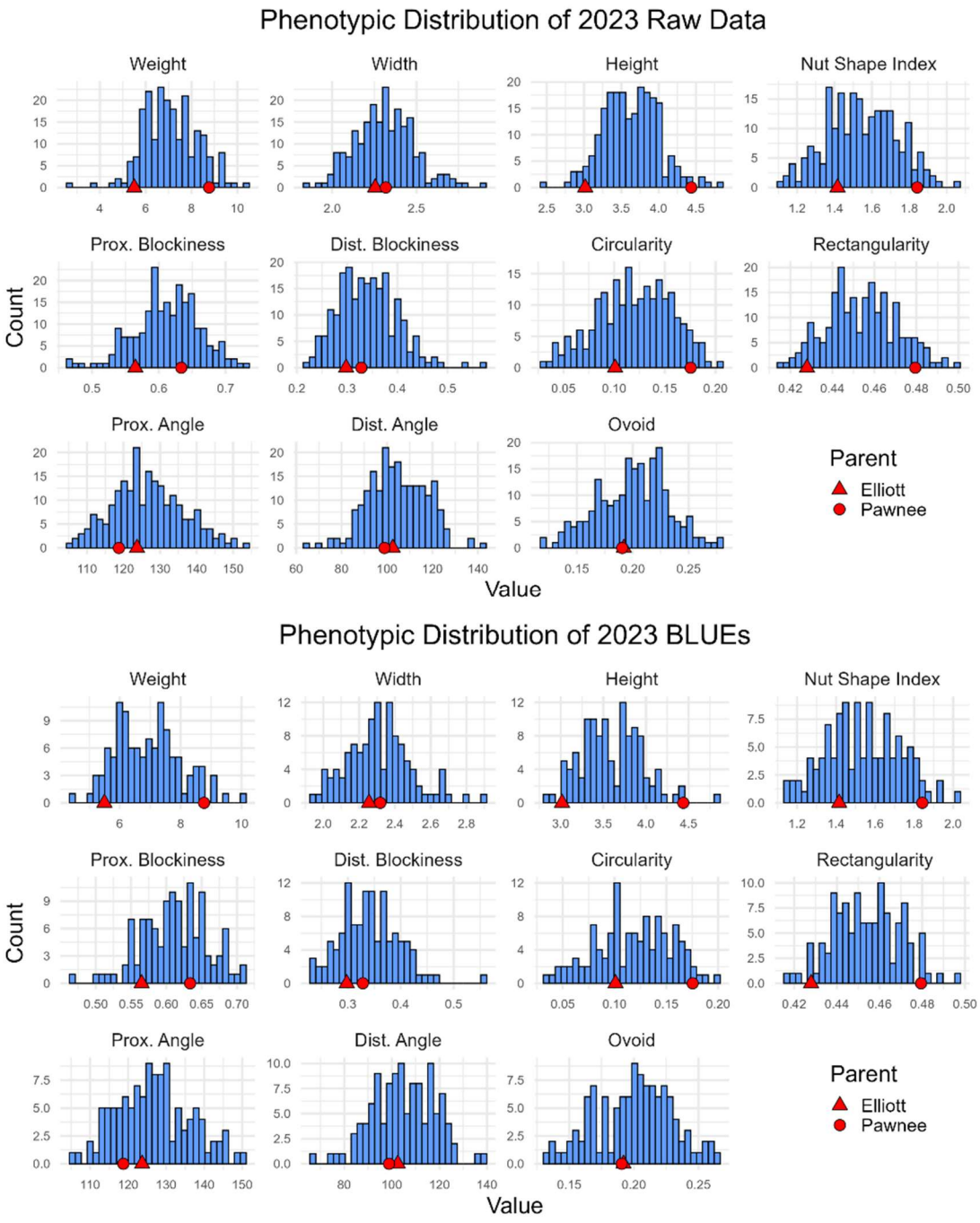

Figure 1.7: Phenotypic distribution of pecan nut shape traits in the F1 pecan mapping population. Distributions represent phenotypic values for raw data (top) and BLUEs (bottom) for a dataset including data from samples harvested in 2023.

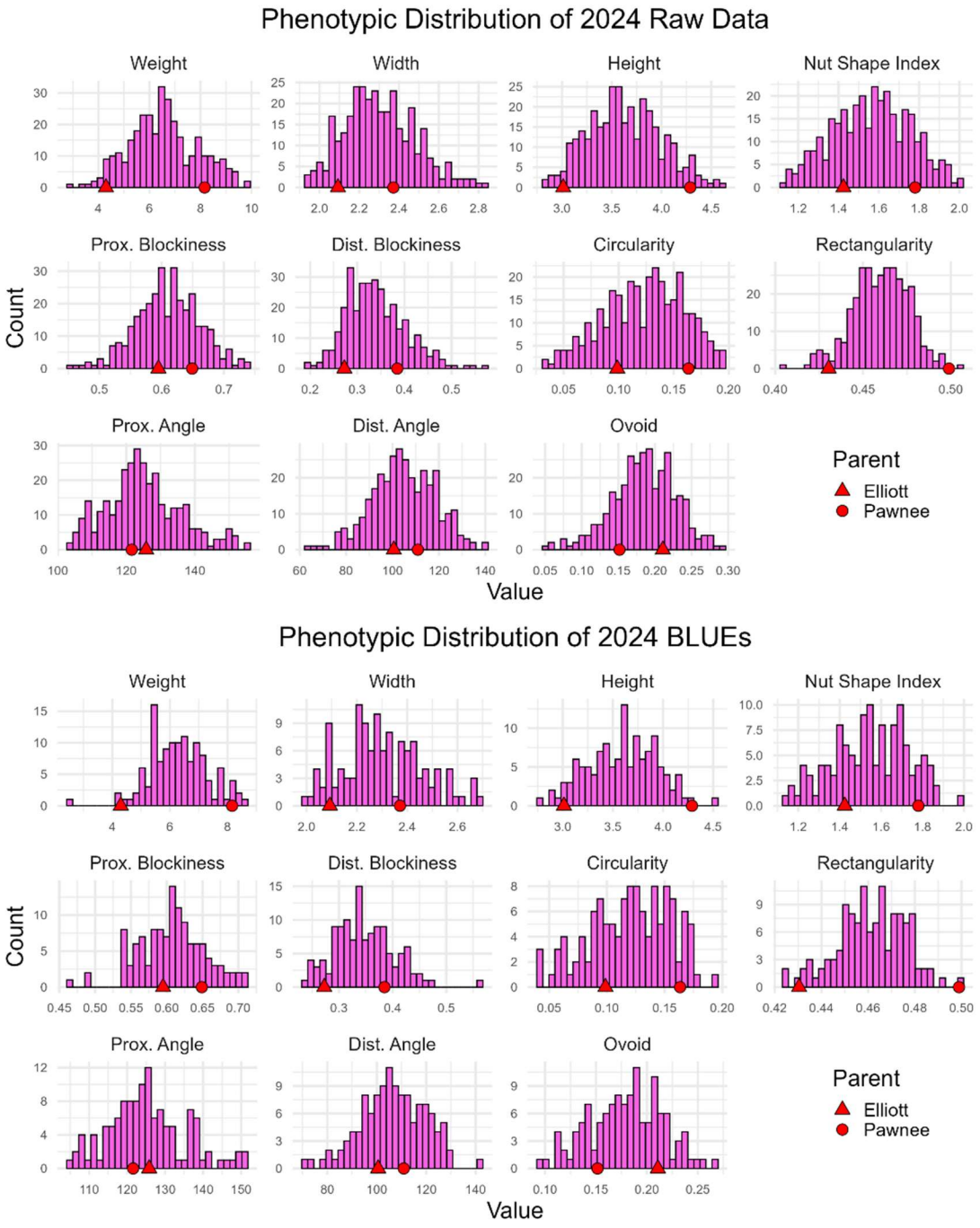

Figure 1.8: Phenotypic distribution of pecan nut shape traits in the F1 pecan mapping population. Distributions represent phenotypic values for raw data (top) and BLUEs (bottom) for a dataset including data from samples harvested in 2024.

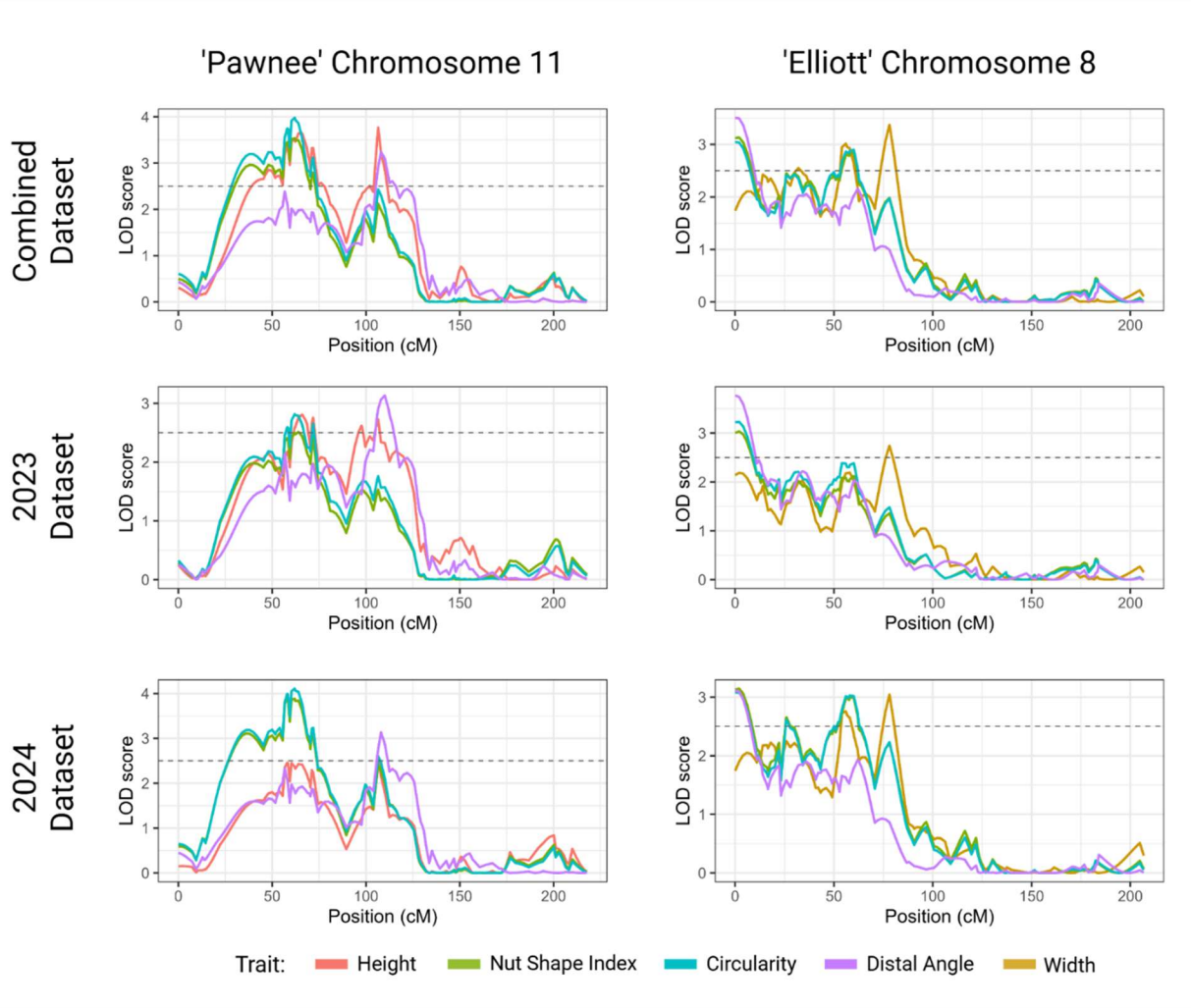

Figure 1.9: Chromosomal LOD scores of QTLs identified consistently across all three datasets. Height, nut shape index, circularity, and distal angle have significant QTLs on chromosome 11 of the 'Pawnee' pecan genome (left) while nut shape index, circularity, distal angle, and width have significant QTLs on chromosome 8 of the 'Elliott' pecan genome (right).

Table 1.1: Normality test results and descriptive statistics of nut shape traits for each dataset as assessed on the BLUE values used for QTL analysis.

Trait	Data Set	Shapiro-Wilk p-Value	Skewness	Kurtosis	Mean	Range	SD	CV(%)
Weight	Combined	0.51	0.24	3.06	6.83	4.06 - 9.41	0.92	13.49
Width	Combined	0.08	0.37	2.75	2.30	1.99 - 2.72	0.16	7.09
Height	Combined	0.62	0.12	2.71	3.64	2.88 - 4.68	0.34	9.24
Nut Shape Index	Combined	0.33	-0.05	2.33	1.57	1.17 - 2.04	0.19	11.95
Proximal Blockiness	Combined	0.77	-0.08	2.87	0.61	0.47 - 0.71	0.05	7.58
Distal Blockiness	Combined	0.08	0.45	3.84	0.35	0.23 - 0.55	0.05	15.36
Circularity	Combined	0.10	-0.24	2.33	0.12	0.04 - 0.2	0.04	28.46
Rectangularity	Combined	0.63	-0.16	2.62	0.46	0.42 - 0.49	0.01	3.06
Proximal Angle	Combined	0.06	0.42	2.88	125.30	104.93 - 152.28	10.31	8.23
Distal Angle	Combined	0.74	-0.15	2.84	104.07	67.46 - 137.86	12.93	12.42
Ovoid	Combined	0.70	0.11	2.56	0.19	0.12 - 0.27	0.03	16.93
Weight	2023	0.16	0.42	2.86	6.93	4.52 - 10.14	1.07	15.36
Width	2023	0.07	0.50	3.40	2.31	1.95 - 2.91	0.18	7.83
Height	2023	0.16	0.37	3.38	3.60	2.85 - 4.84	0.35	9.66
Nut Shape Index	2023	0.71	0.07	2.47	1.53	1.14 - 2.01	0.19	12.26
Proximal Blockiness	2023	0.75	-0.24	3.02	0.61	0.47 - 0.71	0.05	7.52
Distal Blockiness	2023	0.11	0.46	3.84	0.34	0.23 - 0.55	0.06	16.08
Circularity	2023	0.32	-0.16	2.33	0.12	0.03 - 0.2	0.04	31.36
Rectangularity	2023	0.93	0.06	2.71	0.45	0.42 - 0.5	0.02	3.3
Proximal Angle	2023	0.54	0.21	2.57	126.79	105.34 - 150.24	9.72	7.67
Distal Angle	2023	0.77	-0.11	2.95	104.94	67.91 - 139.7	13.08	12.47
Ovoid	2023	0.30	-0.15	2.51	0.20	0.133 - 0.27	0.03	15
Weight	2024	0.05	-0.21	4.06	6.29	2.45 - 8.53	0.97	15.46
Width	2024	0.10	0.31	2.59	2.30	1.99 - 2.69	0.16	6.86

Height	2024	0.70	-0.07	2.54	3.59	2.77 - 4.52	0.34	9.41
Nut Shape Index	2024	0.27	-0.16	2.35	1.55	1.14 - 1.98	0.18	11.75
Proximal Blockiness	2024	0.45	-0.16	3.24	0.61	0.47 - 0.71	0.05	7.58
Distal Blockiness	2024	0.07	0.52	3.71	0.35	0.23 - 0.56	0.06	16.09
Circularity	2024	0.05	-0.32	2.40	0.12	0.04 - 0.19	0.04	29.17
Rectangularity	2024	0.19	-0.34	2.72	0.46	0.42 - 0.49	0.01	3.04
Proximal Angle	2024	0.03	0.44	3.00	125.34	105.55 - 151.64	10.20	8.14
Distal Angle	2024	0.84	-0.21	2.96	106.69	69.96 - 140.84	12.98	12.17
Ovoid	2024	0.82	-0.07	2.58	0.18	0.1 - 0. 27	0.04	19.44

Table 1.2: Broad sense heritability of nut shape characteristics.

Trait	Heritability (H^2)
Weight	0.874
Width	0.951
Height	0.974
Nut Shape Index	0.985
Proximal Blockiness	0.970
Distal Blockiness	0.972
Circularity	0.987
Rectangularity	0.967
Proximal Angle	0.981
Distal Angle	0.982
Ovoid	0.941

Table 1.3: QTLs detected in 'Pawnee' for the combined dataset (top), 2023 dataset (middle) and 2024 dataset (bottom) when a genome-wide QTL analysis was conducted using BLUE values. Peak positions (cM) and corresponding LOD values within the QTL region are reported. Interval start and end were calculated with a 95% Bayesian credible interval. QTLs detected within all three datasets are listed in bold.

Trait	LG	QTL peak (cM)	LOD	Interval start (cM)	Interval end (cM)
'Pawnee' Combine Dataset QTLs					
Rectangularity	3	156.0	3.12	108.5	208.1
Width	6	178.2	2.67	19.7	196.2
Rectangularity	9	56.4	3.54	0	126
Ovoid	10	55.6	2.89	2	90
Circularity	11	62.0	3.98	30	72
Nut Shape Index	11	62.0	3.54	28	74
Height	11	106.5	3.76	36	112
Distal Angle	11	108.0	3.24	36	126
Distal Angle	13	114.5	2.50	0	224
'Pawnee' 2023 Dataset QTLs					
Weight	1	2.0	2.54	0	308.9
Width	6	178.2	3.24	147.9	196.2
Distal Blockiness	7	281.5	2.51	136	404
Ovoid	8	96.0	2.64	0	130
Circularity	11	62.0	2.82	28	112.5
Nut Shape Index	11	64.0	2.52	24	114
Height	11	106.5	2.73	36	122
Distal Angle	11	110.0	3.13	44	126
'Pawnee' 2024 Dataset QTLs					
Rectangularity	3	158.0	2.87	82	268
Distal Blockiness	9	56.4	2.66	0	294
Rectangularity	9	56.4	4.10	0	124
Ovoid	10	64.0	3.50	50	74
Circularity	11	62.0	4.11	30	72
Nut Shape Index	11	62.0	3.88	28	72
Height	11	106.5	2.60	28	125.6
Distal Angle	11	108.0	3.13	32	128
Proximal Blockiness	12	93.4	2.75	20	424.3
Proximal Angle	12	105.8	2.83	49.2	384

Table 1.4: QTLs detected in 'Elliott for the combined dataset (top), 2023 dataset (middle) and 2024 dataset (bottom) when a genome-wide QTL analysis was conducted using BLUE values. Peak positions (cM) and corresponding LOD values within the QTL region are reported. Interval start and end were calculated with a 95% Bayesian credible interval. QTLs detected within all three datasets are listed in bold.

Trait	LG	QTL peak (cM)	LOD	Interval start (cM)	Interval end (cM)
'Elliott' Combined Dataset QTLs					
Proximal Blockiness	4	11.0	2.55	0	300.1
Proximal Blockiness	7	212.0	2.60	72	267.8
Proximal Angle	7	214.6	2.85	82	267.8
Circularity	7	245.8	2.93	142.6	267.8
Nut Shape Index	7	245.8	2.65	142	267.8
Distal Angle	8	0	3.51	0	64
Circularity	8	0	3.05	0	78.1
Nut Shape Index	8	2.0	3.13	0	78.1
Width	8	78.1	3.37	2	82
'Elliott' 2023 Dataset QTLs					
Width	3	290.9	2.63	8	290.9
Proximal Angle	7	214.6	3.32	82	267.8
Circularity	7	245.8	3.76	212	267.8
Height	7	245.8	2.84	214	267.8
Nut Shape Index	7	245.8	3.64	210	267.8
Distal Angle	8	0	3.77	0	62
Circularity	8	2.0	3.23	0	62.7
Nut Shape Index	8	2.0	3.04	0	64
Width	8	78.1	2.74	0	87.9
'Elliott' 2024 Dataset QTLs					
Ovoid	4	36.8	2.57	0	234
Distal Angle	8	0	3.12	0	66
Circularity	8	0	3.08	0	80
Nut Shape Index	8	2.0	3.15	0	80
Proximal Angle	8	25.8	2.70	0	80
Width	8	78.1	3.04	0	82
Proximal Blockiness	12	80.2	3.10	40	187.7
Ovoid	12	80.0	2.60	10	178

Table 1.5: Genome, position, top hit accession number, and description of candidate genes found within regions containing stable QTLs.

Genome	Gene ID	Chr.	Start (bp)	End (bp)	Description	Top Hit Accession
Pawnee	CiPaw.11G055700.1	11	10871613	10874465	Cytochrome P450-related	A0A8T1NVJ4
Pawnee	CiPaw.11G056100.1	11	10957529	10959817	UDP-arabinopyranose mutase	A0A2I4G506
Pawnee	CiPaw.11G077700.1	11	23021779	23023865	Expansin-like B1	A0A2I4E5N6
Pawnee	CiPaw.11G097900.1	11	31069946	31079935	JMJ zinc-finger	A0A2I4GAF6
Elliott	CiEll.08G023700.1	8	2165322	2169085	YUCCA2-related	A0A8T1Q4B3
Elliott	CiEll.08G022400.1	8	2083836	2084309	Auxin responsive SAUR-like	A0A8T1PP82
Elliott	CiEll.08G083700.1	8	10106203	10110299	ADP-ribosylation factor 1 (ARF1)	I1NBF7
Elliott	CiEll.08G084300.1	8	10226128	10237759	Agenet domain-containing/ DUF724	A0A922EBC7

Literature Cited

Agustin-Salazar, Sarai, Pierfrancesco Cerruti, Luis Ángel Medina-Juárez, et al. 2018. "Lignin and Holocellulose from Pecan Nutshell as Reinforcing Fillers in Poly (Lactic Acid) Biocomposites." *International Journal of Biological Macromolecules* 115 (August): 727–36. https://doi.org/10.1016/j.ijbiomac.2018.04.120.

Altschul, Stephen, Thomas Madden, Alejandro Schäffer, et al. 1997. "Gapped BLAST and PSI-BLAST: A New Generation of Protein Database Search Programs." *Nucleic Acids Research* 25 (17): 3389–402. https://doi.org/10.1093/nar/25.17.3389.

Bhattarai, Gaurab, Vincent Bonhomme, and Patrick Conner. 2022. "Image-Based Morphometric Analysis Reveals Moderate to Highly Heritable Nut Shape Traits in Pecan." *Euphytica* 218 (7): 102. https://doi.org/10.1007/s10681-022-03049-1.

Bhattarai, Gaurab, Shanshan Cao, Nolan Bentley, et al. 2025. *High-Density Linkage Mapping and Identification of Quantitative Trait Loci Associated with Scab Resistance in Pecan*. Journal of the American Society for Horticultural Science. March 1. https://doi.org/10.21273/JASHS05460-24.

Brasil, Juliana Nogueira, Luiz Mors Cabral, Nubia B. Eloy, et al. 2015. "AIP1 Is a Novel Agenet/Tudor Domain Protein from Arabidopsis That Interacts with Regulators of DNA Replication, Transcription and Chromatin Remodeling." *BMC Plant Biology* 15 (1): 270. https://doi.org/10.1186/s12870-015-0641-z.

Brewer, Marin Talbot, Lixin Lang, Kikuo Fujimura, Nancy Dujmovic, Simon Gray, and Esther van der Knaap. 2006. "Development of a Controlled Vocabulary and Software Application to Analyze Fruit Shape Variation in Tomato and Other Plant Species." *Plant Physiology* 141 (1): 15–25. https://doi.org/10.1104/pp.106.077867.

Browman, Karl W, and Saunak Sen. 2009. *A Guide to QTL Mapping with R/Qtl*. 1st ed. Statistics for Biology and Health. Springer New York, NY. https://link.springer.com/book/10.1007/978-0-387-92125-9.

Cao, Ke, Pei Zhao, Gengrui Zhu, et al. 2016. "Expansin Genes Are Candidate Markers for the Control of Fruit Weight in Peach." *Euphytica* 210 (3): 441–49. https://doi.org/10.1007/s10681-016-1711-5.

Cao, Xi, Ke-Zhen Yang, Chuan Xia, Xue-Qin Zhang, Li-Qun Chen, and De Ye. 2010. "Characterization of DUF724 Gene Family in Arabidopsisthaliana." *Plant Molecular Biology* 72 (1): 61–73. https://doi.org/10.1007/s11103-009-9551-5.

Cao, Xu, Honglei Yang, Chunqiong Shang, Sang Ma, Li Liu, and Jialing Cheng. 2019. "The Roles of Auxin Biosynthesis YUCCA Gene Family in Plants." *International Journal of Molecular Sciences* 20 (24): 24. https://doi.org/10.3390/ijms20246343.

Carroll, Becky, and Michael Smith. 2017. “Establishing a Pecan Orchard.” Oklahoma State Extension, February 1. https://extension.okstate.edu/fact-sheets/establishing-a-pecan-orchard.html.

Chakrabarti, Manohar, Na Zhang, Christopher Sauvage, et al. 2013. “A Cytochrome P450 Regulates a Domestication Trait in Cultivated Tomato.” *Proceedings of the National Academy of Sciences of the United States of America* 110 (42): 17125–30. https://doi.org/10.1073/pnas.1307313110.

Conner, Patrick, and Katherine Stevenson. 2004. *Pathogenic Variation of Cladosporium Caryigenum Isolates and Corresponding Differential Resistance in Pecan*. HortScience. June 1. https://doi.org/10.21273/HORTSCI.39.3.553.

Cosgrove, Daniel. 2015. “Plant Expansins: Diversity and Interactions with Plant Cell Walls.” *Current Opinion in Plant Biology* 25 (June): 162–72. https://doi.org/10.1016/j.pbi.2015.05.014.

Didelot, Frederique, Laurent Brun, and Luciana Parisi. 2007. “Effects of Cultivar Mixtures on Scab Control in Apple Orchards.” *Plant Pathology* 56 (6): 1014–22. https://doi.org/10.1111/j.1365-3059.2007.01695.x.

Dou, Junling, Shengjie Zhao, Xuqiang Lu, et al. 2018. “Genetic Mapping Reveals a Candidate Gene (ClFS1) for Fruit Shape in Watermelon (Citrullus Lanatus L.).” *Theoretical and Applied Genetics* 131 (4): 947–58. https://doi.org/10.1007/s00122-018-3050-5.

Gonzalo, Maria Jose, Marin Talbot Brewer, Claire Anderson, David Sullivan, Simon Gray, and Esther Van Der Knaap. 2009. “Tomato Fruit Shape Analysis Using Morphometric and Morphology Attributes Implemented in Tomato Analyzer Software Program.” *Journal of the American Society for Horticultural Science* 134 (1): 77–87. https://doi.org/10.21273/jashs.134.1.77.

Gonzalo Pascual, Maria Jose, Marin Talbot Brewer, Claire Anderson, David Sullivan, Simon Gray, and Esther van der Knaap. 2009. “Tomato Fruit Shape Analysis Using Morphometric and Morphology Attributes Implemented in Tomato Analyzer Software Program.” *American Society for Horticultural Science* 134 (1): 77–87.

Grattapaglia, Dario, and R. Sederoff. 1994. “Genetic Linkage Maps of Eucalyptus Grandis and Eucalyptus Urophylla Using a Pseudo-Testcross: Mapping Strategy and RAPD Markers.” *Genetics* 137 (4): 1121–37. https://doi.org/10.1093/genetics/137.4.1121.

Honta, Hideyuki, Takuya Inamura, Teruko Konishi, Shinobu Satoh, and Hiroaki Iwai. 2018. “UDP-Arabinopyranose Mutase Gene Expressions Are Required for the Biosynthesis of the Arabinose Side Chain of Both Pectin and Arabinoxyloglucan, and Normal Leaf

Expansion in Nicotiana Tabacum." *Journal of Plant Research* 131 (2): 307–17. https://doi.org/10.1007/s10265-017-0985-6.

Jin, Wuyun, Wei Yan, Ming Ma, Agula Hasi, and Gen Che. 2023. "Genome-Wide Identification and Expression Analysis of the JMJ-C Gene Family in Melon (Cucumis Melo L.) Reveals Their Potential Role in Fruit Development." *BMC Genomics* 24 (1): 771. https://doi.org/10.1186/s12864-023-09868-3.

Keller, Beat, Michaela Jung, Simone Bühlmann-Schütz, et al. 2024. "The Genetic Basis of Apple Shape and Size Unraveled by Digital Phenotyping." *G3 Genes|Genomes|Genetics* 14 (5): jkae045. https://doi.org/10.1093/g3journal/jkae045.

Khokhar, Ehtisham, Dennis Lozada, Amol Nankar, et al. 2022. *High-Throughput Characterization of Fruit Phenotypic Diversity among New Mexican Chile Pepper (Capsicum Spp.) Using the Tomato Analyzer Software*. HortScience. December 1. https://doi.org/10.21273/HORTSCI16815-22.

Mangino, Giulio, Santiago Vilanova, Mariola Plazas, Jaime Prohens, and Pietro Gramazio. 2021. "Fruit Shape Morphometric Analysis and QTL Detection in a Set of Eggplant Introgression Lines." *Scientia Horticulturae* 282 (May): 110006. https://doi.org/10.1016/j.scienta.2021.110006.

Manichaikul, Ani, Josée Dupuis, Saunak Sen, and Karl Broman. 2006. "Poor Performance of Bootstrap Confidence Intervals for the Location of a Quantitative Trait Locus." *Genetics* 174 (1): 481–89. https://doi.org/10.1534/genetics.106.061549.

Min, Myung Ki, Mihue Jang, Myounghui Lee, et al. 2013. "Recruitment of Arf1-GDP to Golgi by Glo3p-Type ArfGAPs Is Crucial for Golgi Maintenance and Plant Growth." *Plant Physiology* 161 (2): 676–91. https://doi.org/10.1104/pp.112.209148.

Nankar, Amol, Ivanka Tringovska, Stanislava Grozeva, Velichka Todorova, and Dimitrina Kostova. 2020. "Application of High-Throughput Phenotyping Tool Tomato Analyzer to Characterize Balkan *Capsicum* Fruit Diversity." *Scientia Horticulturae* 260 (January): 108862. https://doi.org/10.1016/j.scienta.2019.108862.

Peng, Ze, Wenxiang Li, Xiaoqing Gan, et al. 2022. "Genome-Wide Analysis of SAUR Gene Family Identifies a Candidate Associated with Fruit Size in Loquat (Eriobotrya Japonica Lindl.)." *International Journal of Molecular Sciences* 23 (21): 21. https://doi.org/10.3390/ijms232113271.

Pérez de los Cobos, Felipe, Agustí Romero, Leontina Lipan, et al. 2024. "QTL Mapping of Almond Kernel Quality Traits in the F1 Progeny of 'Marcona' × 'Marinada.'" *Frontiers in Plant Science* 15 (November). https://doi.org/10.3389/fpls.2024.1504198.

Santerre, C. R. 1994. *Pecan Technology*. Springer. http://ebookcentral.proquest.com/lib/ugalib/detail.action?docID=6488987.

Souza, Wagner Rodrigo de, Rowan A.C. Mitchell, and Igor Cesarino. 2023. "Editorial: The Plant Cell Wall: Advances and Current Perspectives." *Frontiers in Plant Science* 14 (June): 1235749. https://doi.org/10.3389/fpls.2023.1235749.

Sparks, Darrell. 1992. *Pecan Cultivars: The Orchard's Foundation*. Pecan Production Innovations.

Stewart, Katherine, Thomas Passey, Carol Verheecke-Vaessen, et al. 2023. "Is It Feasible to Use Mixed Orchards to Manage Apple Scab?" *Fruit Research* 3 (1). https://doi.org/10.48130/FruRes-2023-0028.

Thompson, Tommy, and Patrick Conner. 2012. "Pecan." In *Fruit Breeding*, edited by Marisa Badenes and David Byrne. Springer US. https://doi.org/10.1007/978-1-4419-0763-9_20.

Thompson, Tommy, and Larry Grauke. 2003. "Pecan Nut and Kernel Traits Are Related to Shelling Efficiency." *HortScience: A Publication of the American Society for Horticultural Science* 38 (July). https://doi.org/10.21273/HORTSCI.38.4.586.

Wang, Yanping, Josh P Clevenger, Eudald Illa-Berenguer, Tea Meulia, Esther van der Knaap, and Liang Sun. 2019. "A Comparison of Sun, Ovate, Fs8.1 and Auxin Application on Tomato Fruit Shape and Gene Expression." *Plant and Cell Physiology* 60 (5): 1067–81. https://doi.org/10.1093/pcp/pcz024.

Wells, Lenny, and Patrick Conner. 2015. "Pecan Varieties for Georgia Orchards." University of Georgia Extenstion, February 24. https://extension.uga.edu/publications/detail.html?number=C898&title=pecan-varieties-for-georgia-orchards.

Wood, Bruce W. 2000. *Pollination Characteristics of Pecan Trees and Orchards*. HortTechnology. January 1. https://doi.org/10.21273/HORTTECH.10.1.120.

Wu, Song, Jie Yang, Youjun Huang, et al. 2010. "An Improved Approach for Mapping Quantitative Trait Loci in a Pseudo-Testcross: Revisiting a Poplar Mapping Study." *Bioinformatics and Biology Insights* 4 (February): 1–8. https://doi.org/10.4137/bbi.s4153.

Yu, Ting, Guo Ai, Qingmin Xie, et al. 2022. "Regulation of Tomato Fruit Elongation by Transcription Factor BZR1.7 through Promotion of SUN Gene Expression." *Horticulture Research* 9 (January): uhac121. https://doi.org/10.1093/hr/uhac121.

Zhang, Chuan, Liwen Cui, and Jinggui Fang. 2022. “Genome-Wide Association Study of the Candidate Genes for Grape Berry Shape-Related Traits.” *BMC Plant Biology* 22 (1): 42. https://doi.org/10.1186/s12870-022-03434-x.

CHAPTER 3

MUSCADINE: THE NATIVE GRAPE OF THE SOUTH

BACKGROUND AND INTRODUCTION

Muscadine Phylogeny

Muscadine grape, *Vitis rotundifolia,* is a fruit-bearing vine native to the southeastern United States. All grapes belong to the *Vitis* genus, which is divided into two subgenera: *Vitis* and *Muscadinia* (Guzmán-Ardiles et al. 2023). The *Vitis* subgenus includes the familiar European or "bunch" grapes (*Vitis vinifera)* popularly used for table fruit and wine. *Muscadinia,* on the other hand, represents a distinct lineage comprising only two recognized species. Historically, some taxonomists classified *Muscadinia and Vitis* as separate genera within the Vitaceae family, but phylogenic studies support their treatment as subgenera within the *Vitis* genus (Ma et al. 2018; Guzmán-Ardiles et al. 2023).

Muscadines differ markedly from bunch grapes in both morphology and physiology. Most notably, *Muscadinia* species possess 40 chromosomes, while *Vitis* species have 38. Muscadine clusters are smaller, with only four to ten berries, and the berries have noticeably thick, resilient skin. In contrast, bunch grapes produce much larger clusters with thin-skinned berries. Once ripe, muscadine berries will readily detach from the pedicel, while *V. vinifera* grapes remain firmly attached. Additional distinctions are evident in vine characteristics such as bark texture, wood density, and tendril branching (Conner and

Worthington 2022). These differences make the two subgenera easily distinguishable throughout the growing season.

The Native American Grape

Muscadine grapes are a native North American fruit crop with a distinct cultural history from other grapes. While grapes as a genus originated across the Northern Hemisphere, occupying diverse climatic conditions, *Muscadinia* is endemic to the southeastern United States (Guzmán-Ardiles et al. 2023). Its native range encompasses the coastal plain and piedmont regions, stretching from Louisiana to Georgia and from Florida northward to North Carolina. The range extends, to a lesser extent, into eastern Texas, Kentucky, and Virginia (Hickey et al. 2019; Conner and Worthington 2022).

Muscadines have long been part of the southeastern landscape, particularly in the Appalachian region, where indigenous peoples referred to the grape as "askuponong" (Core 1967). These groups consumed the berries fresh or dried and utilized the vines as rope. Its abundance and adaptability made muscadine an important cultural and ecological resource long before Europeans reached the area (Hickey et al. 2019).

Early colonists quickly took note of the fruit's large, dark-colored berries, nicknaming them "bullace" or "bullet grapes" for their resemblance to the eyes of cows. Before long, the settlers began cultivating and utilizing muscadine (Hickey et al. 2019; Vasanthaiah et al. 2011). The muscadine's adaptation to the region's harsh environment offered clear advantages over European grapes. While *Vitis vinifera* suffered with excessive humidity, variable precipitation patterns, and diseases, *Muscadinia* flourished in the climate and maintained resistance to phylloxera and Pierce's disease (Hickey et al. 2019). Muscadine's

natural resistance to these stresses made it the dominant grape for early American wine production, which dates back to the Spanish settlements in 16th century Florida (Vasanthaiah et al. 2011).

Cultivation and Early Industry

The use of muscadine grapes for wine production made them the first American grape to be widely cultivated. During colonial times, wild muscadine vines were selected for desirable characteristics such as berry size, fruity flavor, productivity, and persistence on the vine. Some selections were also made for superior winemaking potential (Hickey et al. 2019). Along the coastal states of Virginia and the Carolinas, one of the most famous cultivars, Scuppernong' was discovered in the mid-18th century. It quickly surpassed all other cultivars in popularity due to its exceptional winemaking qualities. As settlers continued to establish themselves across the South, muscadine cultivation expanded. Large vineyards were planted for winemaking, and the vines became common features of home gardens (Conner and Worthington 2022). These native vines, naturally adapted to local environmental conditions, flourished across the region.

Commercial vineyards of the time consisted primarily of dioecious plants, in which male vines were distributed throughout the vineyard or pollen was supplied from nearby wild vines (Hickey et al. 2019). Around 60% of muscadine production was devoted to wine, but by the 1920s the industry suffered a severe collapse due to the Great Depression and Prohibition. These events caused an abrupt decline in grape prices and widespread overproduction (Conner and Worthington 2022).

The muscadine industry did not begin to recover until the 1960s, when renewed interest in wine consumption and specialty crop production spurred expansion. Acreage increased rapidly through the 1980s as muscadine gained traction as an alternative to traditional agronomic crops (Olien 1990). Industry productivity improved with the introduction of pesticides and the release of new cultivars that provided a foundation for continued growth. These cultivar releases were the product of two formal breeding programs. One was initiated in 1908 through collaboration between North Carolina State University and the USDA, and another was established at the University of Georgia in 1909 (Hickey et al. 2019; Conner and Worthington 2022).

Muscadine Breeding

Since the establishment of these foundational breeding programs, significant progress has been made in muscadine improvement. Many of the traits emphasized today such as firmer, sweeter, and larger fruits on vigorous, productive vines have been favored since the earliest stages of cultivation, long before the development of formal breeding programs (Guzmán-Ardiles et al. 2023). The North Carolina and Georgia programs both began with a small number of parent vines from the wild selected for these desirable characteristics (Conner and Worthington 2022).

Breeding procedures have traditionally involved intercrossing superior selections and subsequently crossing outstanding progeny among themselves (Conner et al. 2023). Crosses can be made using stored or fresh pollen and may involve male or hermaphroditic pollen parents and female or hermaphroditic seed parents. However, most modern breeding programs make use of the female vines as the seed parents because emasculation

frequently damages hermaphroditic flowers resulting in drop. Similarly, male vines are seldom used as pollen parents in current crossed because berry characteristics are not evaluated. However, because the initial breeding material was derived from a limited number of parents, the genetic base of modern muscadine is relatively narrow (Conner et al. 2023). This constraint has led to reduced genetic variability and raised concerns about potential inbreeding depression, manifesting as decreased vine vigor. Consequently, new sources of genetic diversity are being sought.

Despite this limitation, the achievements of muscadine breeding have been substantial. Native muscadine are dioecious, and one of the earliest objectives of the North Carolina program was the development of cultivars with hermaphroditic flowers. These cultivars improved yields by eliminating the need for non-fruiting male pollinator vines, enhancing fruit set, and increasing cluster size (Hickey et al. 2019). At the beginning of the University of Georgia's program, breeding efforts focused on improving harvestability and developing cultivars with sweeter, larger berries. These early cultivars were commonly grown in local markets or home gardens and were primarily used for processed muscadine products (Conner and Worthington 2022; Conner et al. 2023). By the latter half of the 20th century, the North Carolina breeding program had refined its efforts toward wine cultivars, while the University of Georgia concentrated on fresh-market selections.

Modern breeding programs continue to target specific market needs. Cultivars intended for the fresh market are selected for large berry size, soluble solids content above 14%, firm flesh, dry stem scar, and tender skin. In contrast, processing cultivars are valued for high juice yield and may tolerate a wet stem scar. Wine cultivars are bred for attributes

such as high vigor and yield, color stability and elevated sugar and acid content, with berry size being of lesser importance (Conner and Worthington 2022). These tailored improvements have enabled multiple thriving markets for muscadine products and reinforced the crop's importance in Southern horticulture.

Production Markets

Today, muscadines are commercially and privately cultivated throughout their native region, and wild muscadine are still prevalent across the landscape as well. While acreage estimates are not surveyed regularly, Georgia and North Carolina have historically been the highest producing states, which appears to remain the case today (Fonsah and Awondo 2016; Hickey et al. 2019). The potential industrial uses of muscadine are diverse, but broadly, fruit is grown either for the fresh market or for processing into value-added products (Hickey et al. 2019).

The most basic form of muscadine consumption is simply eating the berries raw. As a fresh-market fruit, muscadine is praised for its distinctive aroma and sweet, bold flavor. The berries are characterized by pronounced "foxy" or "candy-like" aromatic notes that make them unique among grapes (Conner and Worthington 2022). In fact, consumers often cite the distinctive flavor as the most appealing aspect of eating fresh muscadines (Brown et al. 2016). Fresh muscadines are common features at farmers' markets and local food stores in production regions, and U-pick operations have also increased public access and familiarity (Olien and Hegwood 1990).

Beyond fresh consumption, many consumers enjoy a wide array of processed muscadine products. Value-added items include juice, vinegar, dried fruit, purées, sweet

spreads, and, most notably, wine (Morris and Brady 2007). As in the years of early cultivation, wine remains the dominant product and the primary driver of commercial muscadine production. Surveys indicate that more than half of regional consumers (56.6%) are familiar with muscadine wine, making it the most recognized and preferred muscadine product (Duarte and O'Neill 2012a). Muscadine wine is often associated with its pronounced sweetness, and additional sugar is commonly added during production to enhance this characteristic. Some consumers, however, find the flavor overly sweet or fruity. As wineries diversify offerings with varying levels of sweetness and dryness, consumer acceptance and market potential may continue to grow (Canziani et al. 2018; Duarte and O'Neill 2012a).

Another important processing avenue involves the production of sweet spreads, including jellies, jams, and preserves. These products are familiar to many consumers, and a survey found that 48.7% recognize muscadine jelly and 24.3% are familiar with muscadine jam (Duarte and O'Neill 2012a). Spreads are typically made from whole or crushed fruit, with differences in fruit-to-sugar ratios and pulp consistency distinguishing product types. Production challenges include the tough berry skins, which often fail to soften sufficiently during cooking. To achieve the desired texture, producers may pretreat skins with pectinase when fruit pieces are retained in jams or preserves (Morris and Brady 2007).

A smaller but emerging market for muscadine lies in the nutraceutical industry. Ongoing research into the health-promoting properties of muscadine grapes has created new opportunities for product development. Extracts made from pomace have been shown to inhibit carcinogenesis by suppressing proteins involved in metastasis (God et al. 2007).

Clinical studies using muscadine extracts in cancer patients suggest these products are safe and may improve overall well-being (Bitting et al. 2021). Black-fruited muscadine varieties and wines have been found to contain higher levels of resveratrol, a compound with antioxidant and anti-inflammatory properties, compared to European grape species (Ector et al. 1996). Additional studies have demonstrated that muscadine seed and skin extracts possess significant concentrations of anthocyanins, phenolics, and high oxygen radical absorbance capacity, underscoring their potential in nutraceutical applications (Striegler et al. 2005; Pastrana-Bonilla et al. 2003). As awareness of these health benefits grows, future expansion of the nutraceutical market appears promising.

Despite their versatility, muscadine grapes remain a niche crop, relatively unknown outside of their local growing region. This sentiment is not new. Over a century ago, Newman (1907) remarked that the value of muscadines was not "appreciated by the people of the South as much as it should be," which is a perspective that has echoed across generations. Although the muscadine market remains small and underdeveloped, the crop holds tremendous potential due to its remarkable disease resistance, adaptability to the southeastern U.S. climate, and status as a native, locally grown, and sustainable fruit crop (Duarte and O'Neill 2012b; Hickey et al. 2019).

Familiarity with muscadine-based products like jellies, jams, health products, and wine has enhanced consumer appreciation for the crop. Expanding exposure to these products could further stimulate interest and increase demand for both processed and fresh muscadines (Canziani et al. 2018; Hickey et al. 2019). To support the continued growth of the fresh-market industry, breeding programs must prioritize improvements to fruit

texture and storability, which remain two of the major limitations to market expansion (Conner and Worthington 2022).

Fruit Texture

As consumer familiarity and interest in fresh-market muscadine increases, texture has emerged as a key trait influencing both acceptance and marketability. Texture is one of the most important attributes in fresh fruit consumption, shaping enjoyment while eating as well as perceptions of freshness (Fillion and Kilcast 2002). Texture refers to the structural, mechanical, and surface properties of foods experienced through touch and pressure, perceived by the mouth or fingers (Tunick 2011). Studying texture, however, can be challenging since similar terms, like tough, firm, or leathery, are often used interchangeably, and perception can also be influenced by visual and auditory cues (Fillion and Kilcast 2002). To overcome this subjectivity, texture can be evaluated mechanically by measuring force and deformation to produce objective force–deformation curves (Conner 2013).

Texture has been well characterized in *V. vinifera* grapes, where mechanical and sensory attributes such as hardness, gumminess, chewiness, and crispness have been used to distinguish wine and table grape varieties (Río Segade et al. 2011; Rolle et al. 2012; Sato and Yamada 2003). Grapes are often described through sensory attributes including skin friability, skin thickness, and flesh firmness. For example, the pulp may be characterized as crisp, jelly-like, or tough, reflecting the way it fractures when force is applied. A crisp pulp breaks quickly and cleanly under low force, a jelly-like pulp deforms gradually, and a tough pulp resists deformation until higher force is applied. Berry texture is

also shaped by the strength and breakability of the skin, which should be firm enough to protect the berry but delicate enough to yield easily during eating (Conner 2013).

Consumers typically prefer grapes described as "crisp," with thinner skins that break easily and a firm, cohesive pulp. In consumer studies comparing *V. vinifera* and muscadine varieties, *V. vinifera* grapes received the highest ratings for both skin and pulp texture. Muscadine genotypes bred for processing scored lowest in pulp liking due to their softer texture that is advantageous in juicing. In contrast, muscadine genotypes with firmer flesh and thinner skins, which more closely resemble table grapes, received the highest rating of all muscadine genotypes evaluated (Brown et al. 2016).

Traditionally, muscadines are known for their thick, leathery skins and soft pulp that readily slips from the skin, a texture that many consumers find unfamiliar or undesirable. This has limited their popularity as a fresh fruit despite their strong regional following and suitability for processed products. However, substantial breeding progress has been made toward improving both skin and pulp texture, with modern selections increasingly aligning with consumer preferences for firmness and crispness (Conner and Worthington 2022). Texture differs widely among cultivars, ranging from thick-skinned berries with mushy pulp to *V. vinifera*–like fruit with thinner skins and firm, crisp pulp (Brown et al. 2016). Continued selection for such traits are essential for expanding the fresh-market appeal of muscadine.

Storage

While improving texture is key to increasing consumer acceptance of fresh-market muscadine, maintaining that quality after harvest presents another major challenge. Muscadine's short shelf life is another major limitation to market expansion. Even fruit with

ideal firmness at harvest can quickly lose desirable characteristics during storage. Fruit quality naturally deteriorates after harvest as metabolic processes continue after removal from the plant. This postharvest period, known as senescence, involves biological processes such as protein, lipid, and nucleic acid degradation, which in turn affect texture, taste, aroma, nutritional value, and visual quality (Pott et al. 2020). The rate and pattern of these changes differ depending on the fruit's ripening classification. Climacteric fruits, such as bananas or tomatoes, continue to ripen after harvest with increased ethylene production and respiration. In contrast, non-climacteric fruits like grapes do not undergo this ripening surge. Instead, ethylene production declines, and postharvest changes primarily reflect gradual tissue degradation, leading to fruit death rather than continued maturation (Himelrick 2003).

During storage, fruits lose moisture, soften, and become more susceptible to microbial decay. The length of storage life depends on both preharvest vineyard practices and postharvest handling techniques. Among the most effective strategies for prolonging shelf life are maintaining optimal temperature and humidity conditions, which can slow respiration and reduce water loss (Himelrick 2003). Even moderate dehydration can severely impact marketability since water losses of just 5–10% of initial fruit weight result in visible wilting, shriveling, browning, and flavor decline (Lufu et al. 2020). Moisture loss is also closely linked to a reduction in firmness, one of the primary indicators of texture quality (Paniagua Gonzalez et al. 2013).

In general, storing fruits at lower temperatures slows respiration and senescence, whereas higher temperatures accelerate both water loss and enzymatic activity. At elevated

temperatures, fruit cuticles become more permeable due to lipid reorientation, increasing water diffusion and promoting dehydration (Lufu et al. 2020). For muscadine grapes, the optimal storage temperature has been reported between –0.5 °C and 0 °C, although chilling injury can occur below 1.7 °C, complicating postharvest management (Shahkoomahally et al. 2021; Himelrick 2003). Thus, storage systems must carefully balance temperature reduction with the prevention of chilling injury.

Humidity also plays a critical role in extending shelf life. Because fruits are composed of 85–90% water, maintaining a relative humidity of 90–95% minimizes the diffusion of moisture through the berry skin (Lufu et al. 2020; Himelrick 2003). Despite meeting these temperature and humidity recommendations, muscadines still have a notoriously short shelf life of only two to three weeks, restricting their availability to a narrow harvest window (Barchenger et al. 2015).

Efforts to improve storability in table grapes include fumigation with sulfur dioxide (SO_2), which is not suitable for muscadine because it leads to off-flavors in the fruit. However, alternative controlled-atmosphere methods show promise. Elevated CO_2 concentrations, for instance, have been found to extend muscadine shelf life and reduce decay (Shahkoomahally et al. 2021). Continued research into such storage innovations is essential to supporting the expansion of the muscadine fresh market, but this storage solution is not supported by current industry infrastructure.

Because firmness is a key determinant of both consumer satisfaction and storability, understanding the relationship between textural parameters and storage performance is vital. Studies in blueberries, for example, have shown that fruit with greater stiffness and

pulp firmness retains desirable texture and appearance after extended storage (Mengist et al. 2024). Similar factors may govern muscadine storability, providing a valuable framework for breeding and postharvest research aimed at improving self-life. Integrating postharvest physiology research with breeding programs for firmness and reduced water loss may help muscadine reach quality standards expected in modern fresh-fruit markets.

RESEARCH PURPOSE AND OBJECTIVE

Muscadine grapes are a hallmark crop of the southeastern United States, valued for their distinctive flavor and adaptability to local conditions, yet they remain underutilized and largely unfamiliar outside their native region. Expansion of the fresh-market industry is limited by consumer preference for thinner skins and firmer pulp than typically found in muscadine, as well as by the fruit's short storage life, which restricts distribution beyond local markets. Growing interest in value-added products such as muscadine wine, jelly, and nutraceuticals underscores the potential for broader market development, but success will depend on improving postharvest quality and storability. Understanding how texture-related traits change during storage and how current breeding priorities influence these characteristics is essential for achieving this goal. By analyzing variation in skin and pulp texture across diverse muscadine germplasm, correlations can be identified between these parameters and overall berry quality after storage, revealing which harvest-time traits are most indicative of desirable post-storage texture and offering guidance for breeding selections that enhance storability and consumer appeal.

Literature Cited

Barchenger, Derek, John Clark, Renee Threlfall, Luke Howard, and Cindi Brownmiller. 2015. "Evaluation of Physicochemical and Storability Attributes of Muscadine Grapes (Vitis Rotundifolia Michx.)." *HortScience* 50 (1): 104–11. https://doi.org/10.21273/HORTSCI.50.1.104.

Bitting, Rhonda, Janet Tooze, Scott Isom, et al. 2021. "Phase I Study of Muscadine Grape Extract for Patients with Advanced Cancer." *American Journal of Clinical Oncology* 44 (6): 239–46. https://doi.org/10.1097/COC.0000000000000814.

Brown, Kelly, Charles Sims, Asli Odabasi, Linda Bartoshuk, Patrick Conner, and Dennis Gray. 2016. "Consumer Acceptability of Fresh-Market Muscadine Grapes." *Journal of Food Science* 81 (11): S2808–16. https://doi.org/10.1111/1750-3841.13522.

Canziani, Bonnie, Erick Byrd, and James Boles. 2018. "Consumer Drivers of Muscadine Wine Purchase Decisions." *Beverages* 4 (4): 98. https://doi.org/10.3390/beverages4040098.

Conner, Patrick. 2013. "Instrumental Textural Analysis of Muscadine Grape Germplasm." *HortScience* 48 (9): 1130–34. https://doi.org/10.21273/HORTSCI.48.9.1130.

Conner, Patrick, Gaurab Bhattarai, Haley Williams, and Eric Stafne. 2023. *Pedigree Analysis of Modern Muscadine Cultivars Reveals a Narrow Genetic Base*. Journal of the American Society for Horticultural Science. January 1. https://doi.org/10.21273/JASHS05278-22.

Conner, Patrick, and Margaret Worthington. 2022. "Muscadine Grape Breeding." In *Plant Breeding Reviews*. John Wiley & Sons, Ltd. https://doi.org/10.1002/9781119874157.ch2.

Core, Earl 1967. "Ethnobotany of the Southern Appalachian Aborigines." *Economic Botany* 21 (3): 199–214. https://doi.org/10.1007/BF02860370.

Duarte, Abel Alonso, and Martin A. O'Neill. 2012a. "Consumption of Muscadine Grape By-products: An Exploration among Southern US Consumers." *British Food Journal* 114 (3): 400–415. https://doi.org/10.1108/00070701211213492.

Duarte, Abel Alonso, and Martin A. O'Neill. 2012b. "Muscadine Grapes, Food Heritage and Consumer Images: Implications for the Development of a Tourism Product in Southern USA." *Tourism Planning & Development* 9 (3): 213–29. https://doi.org/10.1080/21568316.2012.672451.

Ector, B. J., J. B. Magee, C. P. Hegwood, and M. J. Coign. 1996. "Resveratrol Concentration in Muscadine Berries, Juice, Pomace, Purees, Seeds, and Wines." *American Journal of Enology and Viticulture* 47 (1): 57. https://doi.org/10.5344/ajev.1996.47.1.57.

Fillion, Laurence, and David Kilcast. 2002. “Consumer Perception of Crispness and Crunchiness in Fruits and Vegetables.” *Food Quality and Preference* 13 (1): 23–29. https://doi.org/10.1016/S0950-3293(01)00053-2.

Fonsah, Esendugue, and Sebastian Awondo, eds. 2016. “Cost Estimates and Investment Analysis for Muscadine Grapes Production in Georgia.” *Journal of Food Distribution Research*, ahead of print. https://doi.org/10.22004/ag.econ.232281.

God, Jason M., Patricia Tate, and Lyndon L. Larcom. 2007. “Anticancer Effects of Four Varieties of Muscadine Grape.” *Journal of Medicinal Food* 10 (1): 54–59. https://doi.org/10.1089/jmf.2006.699.

Guzmán-Ardiles, Ruth Elena, Camila Pegoraro, Luciano Carlos da Maia, and Antônio Costa de Oliveira. 2023. “Genetic Changes in the Genus Vitis and the Domestication of Vine.” *Frontiers in Plant Science* 13 (February): 1019311. https://doi.org/10.3389/fpls.2022.1019311.

Hickey, Cain, Erick Smith, Shanshan Cao, and Patrick Conner. 2019. “Muscadine (Vitis Rotundifolia Michx., Syn. Muscandinia Rotundifolia (Michx.) Small): The Resilient, Native Grape of the Southeastern U.S.” *Agriculture* 9 (6): 6. https://doi.org/10.3390/agriculture9060131.

Himelrick, David G. 2003. “Handling, Storage and Postharvest Physiology of Muscadine Grapes: A Review.” *Small Fruits Review* 2 (4): 45–62. https://doi.org/10.1300/J301v02n04_06.

Lufu, Robert, Alemayehu Ambaw, and Umezuruike Linus Opara. 2020. “Water Loss of Fresh Fruit: Influencing Pre-Harvest, Harvest and Postharvest Factors.” *Scientia Horticulturae* 272 (October): 109519. https://doi.org/10.1016/j.scienta.2020.109519.

Ma, Zhi-Yao, Jun Wen, Stefanie M. Ickert-Bond, Ze-Long Nie, Long-Qing Chen, and Xiu-Qun Liu. 2018. “Phylogenomics, Biogeography, and Adaptive Radiation of Grapes.” Molecular Phylogenetics and Evolution 129 (December): 258–67. https://doi.org/10.1016/j.ympev.2018.08.021.

Mengist, Molla, Marti Pottorff, Ted Mackey, et al. 2024. “Assessing Predictability of Post-Storage Texture and Appearance Characteristics in Blueberry at Breeding Population Level.” *Postharvest Biology and Technology* 214 (August): 112964. https://doi.org/10.1016/j.postharvbio.2024.112964.

Morris, Justin, and Pamela Brady. 2007. “The Muscadine Experience: Adding Value to Enhance Profits.” *AAES Research Reports and Research Bulletins*, July 1. https://scholarworks.uark.edu/aaesrb/17.

Olien, William. 1990. “The Muscadine Grape: Botany, Viticulture, History, and Current Industry.” *HortScience* 25 (7).

Olien, William, and Patrick Hegwood. 1990. “Muscadine—A Classic Southeastern Fruit.” *HortScience* 25 (7): 726–831. https://doi.org/10.21273/HORTSCI.25.7.726.

Paniagua Gonzalez, Andres, Andrew East, Jason Hindmarsh, and Julian Heyes. 2013. “Moisture Loss Is the Major Cause of Firmness Change during Postharvest Storage of Blueberry.” *Postharvest Biology and Technology* 79 (May): 13–19. https://doi.org/10.1016/j.postharvbio.2012.12.016.

Pastrana-Bonilla, Eduardo, Casimir C. Akoh, Subramani Sellappan, and Gerard Krewer. 2003. “Phenolic Content and Antioxidant Capacity of Muscadine Grapes.” *Journal of Agricultural and Food Chemistry* 51 (18): 5497–503. https://doi.org/10.1021/jf030113c.

Pott, Delphine M., José G. Vallarino, and Sonia Osorio. 2020. “Metabolite Changes during Postharvest Storage: Effects on Fruit Quality Traits.” *Metabolites* 10 (5): 5. https://doi.org/10.3390/metabo10050187.

Río Segade, Susana, Ignacio Orriols, Simone Giacosa, and Luca Rolle. 2011. “Instrumental Texture Analysis Parameters as Winegrapes Varietal Markers and Ripeness Predictors.” *International Journal of Food Properties* 14 (6): 1318–29. https://doi.org/10.1080/10942911003650320.

Rolle, Luca, René Siret, Susana Río Segade, Chantal Maury, Vincenzo Gerbi, and Frédérique Jourjon. 2012. “Instrumental Texture Analysis Parameters as Markers of Table-Grape and Winegrape Quality: A Review.” Article. *American Journal of Enology and Viticulture* 63 (1): 11–28. https://doi.org/10.5344/ajev.2011.11059.

Sato, Akihiko, and Masahiko Yamada. 2003. *Berry Texture of Table, Wine, and Dual-Purpose Grape Cultivars Quantified*. HortScience. July 1. https://doi.org/10.21273/HORTSCI.38.4.578.

Shahkoomahally, Shirin, Ali Sarkhosh, Logan M. Richmond-Cosie, and Jeffrey K. Brecht. 2021. “Physiological Responses and Quality Attributes of Muscadine Grape (Vitis Rotundifolia Michx. to CO2-Enriched Atmosphere Storage.” *Postharvest Biology and Technology* 173 (March): 111428. https://doi.org/10.1016/j.postharvbio.2020.111428.

Striegler, R. K., J. R. Morris, P. M. Carter, J. R. Clark, R. T. Threlfall, and L. R. Howard. 2005. *Yield, Quality, and Nutraceutical Potential of Selected Muscadine Cultivars Grown in Southwestern Arkansas*. HortTechnology. January 1. https://doi.org/10.21273/HORTTECH.15.2.0276.

Tunick, Michael H. 2011. “Food Texture Analysis in the 21st Century.” *Journal of Agricultural and Food Chemistry* 59 (5): 1477–80. https://doi.org/10.1021/jf1021994.

Vasanthaiah, Hemanth, Devarajan Thangadurai, Sheikh Basha, Digambar Biradar, Devaiah Kambiranda, and Clifford Louime. 2011. “Muscadiniana.” In *Wild Crop Relatives: Genomic and Breeding Resources: Temperate Fruits*, edited by Chittaranjan Kole. Springer. https://doi.org/10.1007/978-3-642-16057-8_4.

CHAPTER 4

EVALUATING TEXTURE AND STORABILITY IN MUSCADINE GRAPE (*VITIS ROTUNDIFOLIA)*

Anne Marie Gahagan, Patrick J. Conner, and Angelos Deltsidis. To be submitted to *The Journal of the American Society for Horticultural Science*.

Abstract

Muscadine (*Vitis rotundifolia*) is a grape species native to the southeastern United States, valued regionally but limited in broader markets due to its short shelf life and textural differences from table grapes (*V. vinifera*). Although breeding has improved muscadine texture, its relatively soft pulp and thick skins remain barriers to consumer acceptance. In this study, 29 muscadine genotypes from the University of Georgia's breeding program were evaluated for textural properties, color, chemical composition, and storability after two and four weeks of cold storage (4 °C, 95% RH) across two years. Extensive phenotypic variation was observed among genotypes. Comparisons with *V. vinifera* confirmed that while some muscadine genotypes exhibit flesh firmness comparable to or exceeding *V. vinifera*, their skin remains approximately twice as thick and generally tougher, as indicated by berry penetration work measurements. During storage, berry firmness (BF), flesh maximum force (FMF), and color lightness all declined, underscoring the continuing challenge of maintaining storability. However, correlations among traits revealed that breeding targets for firmer flesh and thinner skins do not negatively impact postharvest stability. Genotypes with higher BF and FMF at harvest maintained superior texture during storage, suggesting that selecting for greater firmness at harvest is a viable strategy to enhance storability and support the market expansion of fresh muscadines.

Introduction

Despite a century of cultivation, *Vitis rotundifolia* (muscadine grape) remains underrecognized as a fresh-fruit commodity. Even within its native range in the southeastern United States, consumer familiarity is largely confined to processed products such as wine and jelly rather than fresh berries (Duarte and O'Neill 2012b). One regional survey reported that while over half of respondents were familiar with muscadine wine (56.6%) and nearly half with jelly (48.7%), only 16.4% recognized muscadines as a fresh fruit (Duarte and O'Neill 2012a). Interest in muscadine-derived nutraceuticals, including resveratrol and other antioxidant and anticarcinogenic compounds, has increased demand for muscadine products, but this interest has not yet translated into broad acceptance of the fresh berries (Striegler et al. 2005; God et al. 2007; Ector et al. 1996). Misalignment between the fruit's sensory attributes and mainstream consumer expectations, combined with the crop's limited postharvest longevity, continues to constrain expansion of the fresh market compared to other muscadine products.

Among quality traits like appearance, flavor, and aroma, texture is one of the most influential factors shaping consumer preferences for fresh fruits (Rolle et al. 2012). Texture is a multidimensional construct encompassing mechanical and structural properties sensed by the mouth and fingers, and it strongly influences judgements of quality (Conner 2013; Tunick 2011). For grapes, this preference corresponds to berries that are firm yet easy to chew, and berries deviating from these traits exhibit lower acceptability and reduced consumption (Sato and Yamada 2003). In general, these preferences are better aligned with

the texture of *Vitis vinifera* table grapes, which typically have crisp pulp and thin skin, making them easy and enjoyable to chew. Alternatively, muscadine grapes have softer pulp with thick, leathery skin, which feels tough while chewing. Sensory-panel studies indicate that, although consumers appreciate the flavor and aroma of muscadine grapes, cultivars with thick skins and soft flesh receive lower acceptance scores than firmer genotypes or *V. vinifera* grapes (Brown et al. 2016). Crisp fruit also conveys freshness and superior quality (Fillion and Kilcast 2002). In contrast, the naturally soft pulp of muscadine grapes may lessen this perception, leading retailers unfamiliar with the crop to view it as lower quality and hesitate to sell it, which further restricts its market distribution.

Instrumental texture analysis enables objective and comparable quantification of the mechanical properties that underlie these sensory perceptions. Force–deformation curves generated by universal testing machines describe the response of berry tissue to applied force, allowing reproducible comparisons of texture characteristics. Parameters such as flesh firmness, skin friability, and skin thickness are particularly informative in distinguishing muscadine texture profiles (Conner 2013). However, analysis of such traits tends to be inconsistent across studies. For example, “firmness” has been variously defined as the maximum force (N) required to penetrate the skin tissue (Walker et al. 2001), the force (N) required to achieve a 20% deformation of initial berry height (Carreño et al. 2014), the distance (mm) of deformation upon subjecting the berry to a constant force (Rolle et al. 2012), or the resistance to compression ($g \cdot mm^{-1}$) by a load cell (Shahkoomahally et al. 2021). Measurements may be taken at the berry equator or apex (Felts et al. 2018), further

complicating standardization. The lack of a unified protocol and shared terminology has limited progress in breeding and characterization of muscadine texture traits, necessitating a large-scale genotype texture analysis under standardized protocols.

Beyond consumer texture preference, muscadine is also highly perishable, which constrains its market reach and availability. As a non-climacteric fruit, muscadine does not undergo additional ripening after harvest; postharvest changes primarily reflect senescence, leading toward fruit death, rather than maturation (Shahkoomahally et al. 2021; Himelrick 2003). During senescence, the fruit undergoes respiration resulting in moisture loss, microbial decay, and progressive softening (Himelrick 2003). Color degradation is also a key indicator of senescence, as pigment oxidation and biochemical changes alter berry color during storage (Valverde et al. 2005). Therefore, postharvest water loss, textural degradation, and color change are key factors influencing the storability of muscadine.

Temperature and relative humidity are among the most important environmental factors governing these postharvest changes. Temperature directly affects fruit physiology and the rate of metabolic processes such as respiration and transpiration. Elevated storage temperatures increase the kinetic energy available for water molecules to evaporate from the fruit surface, accelerating moisture loss. Moreover, higher temperatures cause lipids in the cuticle to reorient and become more permeable, allowing greater vapor diffusion and water loss through the skin (Lufu et al. 2020). These effects contribute to faster softening, shriveling, and the decline in overall fruit quality during storage.

Humidity likewise plays a decisive role in determining storage longevity. Most fruits and vegetables consist of approximately 85–90% water by weight and continue to lose water vapor postharvest through transpiration (Himelrick 2003). Excessive water loss results in fruit that becomes wilted, shriveled, tough, mushy, and lacking in flavor. To minimize transpiration, the ambient water content should be maintained as close as possible to that of the product itself. Thus, postharvest water loss can be greatly reduced by manipulating the relative humidity of the storage environment (Lufu et al. 2020). High relative humidity slows transpiration and helps preserve firmness and turgor, extending shelf life. Achieving an optimal balance between temperature and humidity helps maintain the marketable quality of fresh muscadine berries during storage.

Even under refrigeration, muscadine berries often experience rapid textural decline which shortens the marketable period and limits distribution potential (Shahkoomahally et al. 2021). Recommended cold storage conditions (1–5 °C) typically extend shelf life to two or three weeks, with high humidity environments sometimes allowing fruit to reach the upper limit of this range (Takeda et al. 1983; Barchenger et al. 2015). The effects of storage conditions are further modulated by fruit surface and maturity characteristics. Attributes such as cuticle thickness, lenticel density, and overall surface-area-to-volume ratio influence water loss and decay susceptibility (Lufu et al. 2020). While more mature fruits tend to be softer upon harvest and more prone to decay during storage, they also possess more developed epidermal tissues and generally lose moisture more slowly than immature fruit (Walker et al. 2001; Sastry 1985). Collectively, these findings suggest that harvesting

mature, but not overripe fruit, is essential to achieving both high initial quality and maximum storage potential.

In light of these challenges, systematic evaluation of texture-related traits and postharvest stability across muscadine germplasm is needed. Current breeding efforts have focused on improving textural quality by selecting berries with thinner skin and firmer pulp, but the effect of these selections on storability has not been evaluated. A clearer understanding of the relationships between genotype, texture, and storage performance under standardized procedures and terminology will support breeding efforts to improve marketability and consumer acceptance of fresh muscadine grapes.

Methods

Plant Materials

Fruits were harvested from 29 muscadine genotypes from the University of Georgia's germplasm collection. The genotypes were selected to represent a broad range of important texture attributes and included both bronze and black berries. Vines from which berries were harvested were grown on land managed by the University of Georgia across two sites in Tift County, GA (31°30'34.88"N, 83°38'55.26"W or 31°28'40.6"N 83°31'40.6"W). Vines were trained to a single wire trellis with two cordons per vine. Drip irrigations was used, and diseases and insects were controlled according to commercial guidelines (Poling et al. 2003). For comparison purposes only, each year a sample of green *V. vinifera* table grapes was purchased from a local supermarket and processed similarly to the muscadine

samples by cutting the berry pedicel right above the attachment point to the berry and packing in the clamshells similarly to the muscadine samples.

Sample Collection and Storage Conditions

Muscadine berries were harvested during August and September of 2024 and 2025 according to the harvest window of the genotype. Due to the asynchronous ripening of muscadine grape berries, and the large diversity of berry firmness and color traits, fruit maturity was assessed using a sodium chloride (NaCl) density gradient prior to harvesting the vines (Lanier and Morris 1979). As vines approached harvest, a preliminary subsample of berries was floated in an 8% NaCl brine solution. Berries that floated were considered underripe, while those that sank were rinsed and transferred to a 9% NaCl solution. Berries that then floated in the 9% solution were classified as optimally ripe (Conner 2013). When the majority of the berries were determined to be optimally ripe, the vine was harvested. Ripe berries, as determined by density gradient performance, were examined for visual and tactile traits such as coloration near the pedicel and softness to guide final berry selection during harvest.

After harvest, berries were transported to the laboratory in an air-conditioned vehicle and allowed to equilibrate to room temperature for around one hour as berries with obvious deformity, injury, or insect damage were discarded. For each genotype, berries were evenly distributed into twelve ventilated plastic clamshell containers (1 lb. strawberry). The clamshells were designated so that four replicates were reserved for each storage duration of 0, 2, and 4 weeks. Clamshells assigned to 2 weeks or 4 weeks were weighed and placed

in cold storage at 4 °C and 95% relative humidity. Temperature and humidity were continuously monitored throughout storage.

Prior to analysis at time points post-storage, berries were equilibrated to room temperature for approximately three hours. Each analysis used four replicates of ten berries randomly selected from each of four clamshells. Measurement protocols and terminology followed by Conner (2013) to promote standardization and ensure comparability with previous characterizations (Table 2.1).

Berry Firmness and Diameter

Berry firmness (BF) and berry diameter (BD) were recorded to measure the size of the berries and firmness of the whole berry, mimicking the sensation of squeezing a fruit between finger and thumb. These were measured using the FirmTech II Fruit Firmness Tester (BioWorks Inc., USA). The instrument was calibrated daily with a 250 g weight on the load cell and either a 31.58 mm or 18.64 mm size reference, depending on berry size for each genotype. Instrument control and data acquisition were managed through FirmTech software (BioWorks Inc., USA). Berries were positioned within the turntable indentations with the stem scar oriented to the right, ensuring that measurements were taken along the equatorial plane. As the turntable rotated, firmness ($g \cdot /mm^{-1}$) was calculated as the slope of the line between the minimum and maximum force thresholds, determined by linear regression of the compression data collected by the type 2 flat metal probe (~1 cm diameter). The instrument simultaneously recorded berry diameter as the height from the base of the turntable indentation to the top of the berry.

Whole Berry Penetration Tests

The objective of the whole berry penetration test was to quantify the force and distance required to puncture an intact berry and produce measurements for berry deformation at first peak (BDFP) and berry maximum force (BMF). Measurements were performed using a TA.XT2i texture analyzer (Stable Micro Systems, UK) equipped with an HDP/90 platform and a 25 kg load cell. The analyzer was calibrated using an unloaded cell (zero force) followed by a 5 kg standard weight.

Berries were positioned on their equatorial plane with the stem scar facing to the right and stabilized within a 1 cm conical depression on a metal stage. A 2 mm cylindrical probe compressed the berry at a constant speed of 1 $mm \cdot s^{-1}$ until the skin was punctured. The distance from initial contact to maximum force represents BDFP. Maximum force corresponded to skin rupture and the subsequent release of resistance, representing the value for BMF. These two values were used to approximate a triangular area to calculate berry penetration work (BPW) as (BDFP × BMF)/2, since berry penetration work was defined as the area under the force–deformation curve from initial contact to the point of maximum force (Sato and Yamada 2003; Conner 2013).

Flesh Maximum Force

Flesh maximum force (FMF) was measured to provide an assessment of flesh firmness, irrespective of the skin. FMF was determined using the same TA.XT2i texture analyzer with parameters based on those used for the whole berry penetration tests. A ~1 cm diameter section of skin was removed with a razor blade to expose a flat surface of flesh.

Berries were placed on their equatorial plane with the exposed surface facing the probe and stabilized within the metal stage indentation. The analyzer was fitted with a 5 mm cylindrical probe, set to travel at 0.5 $mm \cdot s^{-1}$. After first contact, the probe descended into the flesh an additional 3 mm, and the maximum force recorded during this interval was reported as FMF.

Skin Thickness

Skin thickness (ST) was measured using the TA.XT2i texture analyzer equipped with a 2 mm cylindrical probe. A small section of skin was excised, and adhering flesh was gently removed. The sample was positioned skin-side up beneath the probe. The probe advanced at 0.1 $mm \cdot s^{-1}$ until a force of 100 N was reached, effectively displacing the skin and contacting the metal plate below. The distance traveled from initial contact to maximum force was recorded as ST.

Compositional Analysis

Berry composition was analyzed from juice samples collected from berries preserved at −4 °C. At each time point, ten berries from each replicate were frozen for later analysis. Samples were placed in a water bath of cold tap water (~12-18 °C) until thawed (~3-4 hours). Juice was extracted by manually pressing thawed berries with a stainless-steel juicer and filtering the liquid through fine-mesh cloth bags. The extracted juice was used to measure total soluble solids (TSS), pH, and titratable acidity (TA).

Total soluble solids were measured by pipetting juice onto an Atago Pocket Refractometer (ATAGO Co., LTD, Japan). The instrument was cleaned between samples and standardized using deionized water. Juice pH was determined with the Accumet Basic AB15

benchtop pH meter (Fisher Scientific Inc., USA), which was cleaned between samples and calibrated using pH 10, pH 7, and pH 4 buffer standards. Titratable acidity (TA) was quantified using an automated titration system (Metrohm Inc., USA) equipped with a 20-sample turntable. The system was standardized daily with pH 10, pH 7, and pH 4 solutions. For each sample, 6 g of juice were diluted with deionized water to a total volume of 15 mL. The diluted juice was transferred to plastic tubes compatible with the titrator's turntable. The juice was automatically titrated to pH 8.2 with 0.1 M potassium hydroxide (KOH). TA was expressed as a percentage of tartaric acid equivalents.

Post-Storage Assessments

To evaluate weight loss (WL), the initial mass (g) of each replicate was recorded prior to storage, along with the mass of the empty clamshell container. After storage at both 2 weeks and 4 weeks, each replicate was reweighed. The clamshell weight was subtracted from initial and final measurements, and WL was calculated as a percentage in Excel as:

$$WL = [(\text{initial weight} - \text{final weight})/\text{initial weight}] \times 100$$

After storage, berries were examined for visible signs of decay. Berries that were shriveled, split, or rotten were removed prior to subsequent analyses but remained included in weight measurements. The number of decayed berries and sound berries was recorded for each replicate, and percent marketability (PM) was calculated as:

$$PM = (\text{sound berries}/\text{total berries}) \times 100$$

Loss of firmness (LF) and loss of flesh max force (LFMF) were calculated to estimate softening of berries during storage through the change in BF and FMF. Values were

expressed as the percentage decrease from initial firmness to firmness after four weeks of storage:

$$LF = [(BF0 - BF4)/BF0] \times 100$$

$$LFMF = [(FMF0 - FMF4)/FMF0] \times 100$$

**Numbers following abbreviations correspond to time in storage*

Berry Color

Berry color was characterized by lightness (L*), hue angle (h°), and chroma (C*), using an Aeros Spectrophotometer (HunterLab, USA), a dual-beam, non-contact reflectance colorimeter. The instrument was standardized daily following the manufacturer's protocol, which utilized a calibrated white tile, black glass standard, and a green diagnostic tile for performance verification. A small clear glass bowl filled with berries was placed on the rotating platform beneath the sensor. The instrument's auto-height function adjusted the sample-to-sensor distance for optimal reflectance. Color measurements were recorded over a 10 s duration, collecting seven readings per second across two full rotations of the platform.

Statistical Analysis

For each genotype, a complete replication consisted of twelve clamshell containers, with four clamshells assigned to each storage time point. While complete replications were obtained for all 30 (29 muscadine + 1 *V. vinifera* grape) genotypes in 2024, insufficient fruit was available for 'Fry' and 'Ga. 6-1-269' the following year (2025). Additional genotypes were

excluded from analysis in 2025 because the vines were no longer viable (Ga. 18-5-106, Ga. 14-2-3, and Ga. 17-2-67), totaling 25 (24 muscadine +1 *V. vinifera* grape) genotypes in 2025.

All data analyses were conducted in R (version 4.4.2; R Core Team, 2024). To evaluate temporal variation, each trait was first analyzed by one-way ANOVA with year as the fixed factor. Traits showed significant year effects ($p < 0.05$) and were subsequently summarized separately for 2024 and 2025. Within each year, mean and standard deviation values were calculated for each genotype × storage-time combination across all measured traits. Relationships between all muscadine traits were examined using the *rcorr*() function from the Hmisc package (Harrell et al. 2025) with the Pearson method to compute correlation coefficients and corresponding significance values. Correlations were computed on trait means, calculated so that each genotype was represented by a single value per trait at each time point, with *V. vinifera* grape samples excluded. The purpose was to examine relationships among all measured attributes at harvest and after storage.

To evaluate whether each texture attribute changed across storage times, analyses were conducted using the full dataset including all replicates for each muscadine genotype. For each trait, an analysis of variance (ANOVA) was performed with storage time as a fixed factor to test for overall differences. Following significant ANOVA results, Tukey's Honest Significant Difference (HSD) tests were applied to determine pairwise differences between storage times, and significance groupings were assigned using letter codes to indicate which storage times differed (Lenth et al. 2025). This approach allowed a comprehensive assessment of temporal changes in each texture trait.

Results and Discussion

Textural Attributes

A wide array of muscadine germplasm from the University of Georgia muscadine breeding program was measured for several traits influential to textural perception including berry firmness (BF), berry deformation at first peak (BDFP), berry maximum force (BMF), berry penetration work (BPW), and flesh maximum force (FMF). This germplasm includes both genotypes with a more traditional berry texture of soft flesh and tough skins ('Delicious', 'Late Fry', Paulk', 'Triumph') and genotypes possessing firmer flesh and/or crisp skin (Ga. 10-1-329, Ga. 18-5-106, 'Lane', 'Ruby Crisp'). The genotypic and phenotypic variation for these traits in the germplasm pool provides a strong foundation for examining textural differences in muscadine and their effect on post-harvest storage quality.

The majority of genotypes were measured in 2024 and 2025, although a few genotypes were not evaluated in 2025 due to poor vine health or the removal of the vine from the vineyard. While overall trends remained consistent between years, individual trait values often differed within the same genotype over years, and years were analyzed separately. Texture attributes are complex traits influenced by preharvest, harvest, and postharvest factors (Lufu et al. 2020). Despite consistent vineyard management and harvest practices, environmental variation likely contributed to year-to-year differences. Berry ripeness has been shown to substantially affect textural attributes and storage potential, and density sorting has been employed to separate all berries by maturity prior to textural analysis to standardize ripeness (Walker et al. 2001; Conner 2013a; Crespan et al. 2021). Walker et al.

(2001) analyzed differences in storability compared to their maturity level, and Conner (2013) and Crespan et al. (2021) analyzed berries within a mid-grade maturity range. In the present study, density tests were not feasible for sorting the large number of samples employed and were instead used primarily to gauge overall maturity of each genotype prior to harvest. This may have resulted in some textural differences between years due to berry ripeness. However, because harvest practices here more closely resemble commercial muscadine production, these findings provide insight into storability under typical industry conditions.

Traditional muscadine texture is composed of a soft pulp enclosed by a thick, tough skin. Because of the skin toughness, consumers will often bite the end of the berry, squeeze out and eat the pulp and surrounding juice, and discard the skin. Unfortunately, much of the beneficial nutraceutical content resided in the discarded skins. Breeders are therefore striving to produce berries with thinner, crisper skins and firmer pulps so that the entire berry is more likely to be eaten (Conner 2013a; Conner and Worthington 2022). Increasing berry firmness would also be beneficial in helping to avoid rejection of the fruit by grocers who sometimes perceive soft muscadine berries as being overripe.

Berry firmness (BF) as measured by the FirmTech 2 machine approximates the firmness perceived by squeezing a berry between the fingers and is a good overall measure of berry condition. BF in this germplasm had a 3-fold difference and ranged from 173 to 524 $g \cdot mm^{-1}$ at harvest (Tables 2.2, 2.3). *V. vinifera* samples exhibited BF values of 316 and 414 $g \cdot mm^{-1}$ at harvest in 2024 and 2025 respectively. While most muscadine samples were less

firm than *V. vinifera*, several genotypes exhibited similar or greater firmness. Because BF is a key selection trait in the breeding program and strongly influences both consumer and retailer impressions, its behavior during storage is of particular interest. Firmness decreased across all genotypes in both years after four weeks of storage (Figs. 2.1, 2.2), but the decline was proportional to initial firmness. Genotypes that were firmer at harvest tended to remain firmer after storage. The consistent differences observed between genotypes underscore the strong genetic basis of BF and its potential for continued improvement through breeding.

BDFP, BMF, and BPW together provide an integrated measure of the texture experienced when biting into a grape (Conner 2013a). At harvest, BDFP ranged from 3.22 to 8.82 mm, BMF from 5.45 to 15.5 N (Tables 2.2, 2.3). BPW showed an approximate 5-fold difference, ranging from 12.3 to 60.9 mJ at harvest. This wide variation underscores the substantial textural diversity within muscadine germplasm. In comparison, *V. vinifera* samples generally exhibited lower BDFP, BMF, and especially BPW values than *V. rotundifolia*. On average, the BPW of *V. rotundifolia* was 4.6–6.2 times higher than that of *V. vinifera*, highlighting the tougher skins and softer pulp characteristic of muscadines.

Although muscadines are known for their soft pulps, firmer-fleshed germplasm is available (Conner 2013a), and recent cultivar releases have emphasized this trait (Conner 2013b; 2020). FMF at harvest exhibited a sevenfold range, from 0.79 to 5.6 N, among muscadine genotypes (Tables 2.2, 2.3). In 2024, the firmest *V. rotundifolia* genotype exceeded the *V. vinifera* samples in FMF, but in 2025, the *V. vinifera* sample had firmer flesh

than any *V. rotundifolia* sample. The development of flesh firmness similar to *V. vinifera* is in contrast to skin attributes which remain distinct between the two species. Muscadine ST varied from 1-2 mm and was generally about twice as thick as *V. vinifera* skin (Tables 2.2, 2.3). However, given the frequent rainfall in the production region of *V. rotundifolia* and the dry climate in most *V. vinifera* table grape production regions, the development of similar skin attributes may not be desirable, as it could increase fruit cracking and fungal rot.

While not directly related to texture, berry size is another key distinguishing feature between muscadine and table grapes. Compared to *V. vinifera*, muscadines generally produce larger berries, as reflected in their greater berry diameter (BD). This trait varied widely among the germplasm evaluated. In 2024, BD ranged from 21.42 to 32.59 mm, and in 2025 from 22.83 to 33.46 mm, compared to approximately 21 mm for *V. vinifera* (Tables 2.2, 2.3). 'Supreme' produced the largest berries, followed closely by 'Ga. 12-5-138' and 'Ga. 8-1-313,' whereas 'Delicious' and 'Triumph' had the smallest.

The traits BF, BMF, and FMF all decreased during storage (Tables 2.2, 2.3), reflecting the gradual softening consequential to postharvest senescence (Lufu et al. 2020; Himelrick 2003). The largest declines occurred between week 0 and week 2, followed by smaller changes thereafter, consistent with reports by Walker et al. (2001). This pattern suggests reliable measurement and uniform handling among berries within each year. However, some traits behaved differently between years. BPW, which integrates BDFP and BMF, showed distinct trends in 2024 and 2025. In 2025, BPW remained stable, likely because

BDFP increased while BMF declined. However, in 2024, BDFP was largely unchanged during storage, causing BPW to decrease in parallel with the loss of BMF.

Physiochemical attributes

Berry color was measured using an Aeros spectrophotometer which measures the reflectance from a group of berries on a rotating plate. This type of color measurement more closely resembles the overall perception a consumer receives when viewing a package of berries than does individual measures on the berry surface. Barchenger et al. (2015) reported LCH values of 42.2, 14.5, and 87.3 for 'Fry' and 27.0, 5.6, and 301.1 for 'Supreme' across all time points. Aeros spectrophotometer LCH values for 'Fry' were 33.0, 20.7, 83.9 and for 'Supreme' were 14.5, 2.1, and 28.3. These values seem roughly comparable considering *h*° of 360 borders 0 and sun exposure on black berries can greatly decrease L*.

Black genotypes had L* values ranging from about 2.4 to 23.4 at harvest (Table 2.4) while bronze genotypes varied from 26.8 to 42.6 (Table 2.5). 'RubyCrisp', which is notable for its red coloration (Conner 2020) with an L* value of 18.5 to 21.0 at harvest was more similar to the black genotypes. As expected, C* was quite low in the black genotypes, averaging 4.1 and 3.8 at harvest in 2024 and 2025 respectively, while in bronze genotypes it averaged 19.0 and 18.4 respectively. Interestingly, *h*° in the black genotypes increased from 25.2 in 2024 to 46.8 in 2025. However, *h*° becomes unstable and less meaningful when L* and C* are low as in these black-colored genotypes (Fairchild 2013). In the bronze genotypes *h*° was more consistent and averaged 83.6 and 79.0 in 2024 and 2025 respectively.

In both black and bronze genotypes L* decreased with storage time in 2024, but L* increased slightly with storage in black genotypes in 2025 and did not vary in bronze genotypes in 2025. C* did not vary with storage in any samples and *h*° only declined slightly in 2024 in the bronze genotypes. Mirroring our results in 2024, Barchenger (2015) reported a 25% reduction in L* among black genotypes and a 20% reduction in L* bronze genotypes after three weeks of storage. While some darkening of berries occurred with storage, this change was not a major cause of loss of marketability.

In general, the physiochemical attributes of titratable acidity (TA), pH, and total soluble solids (TSS) are not considered strong indicators of postharvest storability because they typically show limited change during storage (Barchenger et al. 2015; Takeda et al. 1983). Across both years, muscadine fruit had slightly lower pH and TSS than *V. vinifera*. TA in muscadine was generally higher than in *V. vinifera*, with the exception of week 4 in 2025, when muscadine TA was marginally lower. Measurement of pH declined over time, with a more pronounced decrease observed in 2025. TSS decreased modestly during storage in 2024, which is consistent with trends reported by Walker et al. (2001), but TSS did not change significantly in 2025.

As noted by Barchenger et al. (2015), TA often varies unpredictably between years, and this was reflected in the cultivars examined here. For instance, TA values for 'Delicious' were 0.21% in 2024 and 0.38% in 2025, while 'Supreme' measured 0.18% and 0.31% in those same years. Similarly, Walker et al. (2001) reported a harvest TA of 0.57% for 'Triumph,' compared with 0.19% and 0.37% in 2024 and 2025 in this study. Inconsistencies

between studies as well as between years support the conclusion that TA is not a reliable metric for assessing postharvest storability, especially given that TA remained stable across storage periods in both years. In contrast, the observed decline in pH and slight decrease in TSS may signal subtle changes in flavor during storage. Because flavor is a key determinant of consumer acceptance, these shifts may represent an additional challenge to muscadine storability.

Correlations Among Textural Traits

Correlations among textural traits help reveal which harvest-time traits are most indicative of desirable post-storage texture and offer guidance for breeding selections that enhance storability and consumer appeal (Figure 2.3). Increasing berry firmness (BF) is one of the most important goals in the breeding program as soft berries can be rejected by the retailer. BF was positively correlated with FMF and negatively correlated with BDFP across all storage time points. BF was previously reported to be positively associated with FMF in ripe berries (Conner 2013a). Strong positive correlations between FMF at harvest and BF through all postharvest storage time points indicate that selecting for increased flesh firmness is a viable strategy to increase BF after storage. As expected, FMF and BDFP were negatively correlated throughout storage. These relationships were reported earlier for fresh fruit (Conner 2013a), and indicate that flesh firmness contributes substantially to overall berry firmness and that berries with softer flesh require greater deformation before puncture. Sato and Yamada (2003) found that the difficulty of chewing fruit was closely associated with deformation. Together, these findings suggest that berries with lower FMF

resemble the undesirable “jelly-like” texture rather than the preferred crisp texture (Conner 2013a). The decrease in FMF and concurrent increase in BDFP during storage indicate that berries become more difficult to chew and develop a less desirable texture over time.

Muscadine berries are known for their relatively thick and tough skin, traits that adapt them well to remaining viable during the frequent rainfall encountered during the harvest season, but which are not preferred by consumers (Brown et al. 2016; Hickey et al. 2019). ST was positively correlated with BF at all storage points, indicating that thicker skins contribute to overall firmness. However, ST was not correlated with BDFP or BPW, and only slightly correlated with BMF, revealing that thicker skins can still masticate relatively easily. Interestingly, ST was correlated with FMF at weeks 2 and 4. Because the skin is not directly involved in the FMF measurement, this association suggests that skin thickness and firmness-related traits may be genetically linked. Supporting this, Crespan et al. (2021) identified a major QTL in wine grapes associated with multiple berry firmness traits as well as skin thickness. While breeding for thinner skins may improve consumer acceptance, it should not be prioritized over improved flesh firmness if these traits are genetically linked.

Berry diameter (BD) was positively correlated with berry firmness (BF) and skin thickness (ST) (Fig. 2.3). Larger berries are generally expected to lose moisture more slowly due to their lower surface-area-to-volume ratio (Lufu et al. 2020). However, no significant correlations were detected between BD and weight loss (WL) or percent marketability (PM). Likewise, BD was not associated with loss of berry firmness (LF) or loss of flesh maximum force (LFMF), indicating that berry size does not directly influence softening during storage.

The correlation between BD and BF may reflect artificial selection on both traits within the UGA muscadine breeding program, where large, firm berries are prioritized, and several recent selections exhibit both characteristics. The association between BD and ST is less clear, but it may result from indirect selection pressure since larger berries with thinner skins could be more susceptible to cracking or damage and are thus not selected in the breeding process. This relationship underscores a potential tradeoff in breeding objectives. While consumers prefer large berries with thin skins, larger berries tend to develop thicker skins. Achieving both desirable size and texture may therefore require careful genetic selection to decouple these correlated traits within muscadine germplasm. A potential solution may be to select thicker skins which fracture easily and have reduced bitter or sour flavor so that consumers do not object to their presence.

Storability and Postharvest Changes

Storability was evaluated through percent marketable (PM), weight loss (WL), and the loss of key texture traits over time. As noted previously, attributes such as berry firmness (BF), berry maximum force (BMF), and flesh maximum force (FMF) all declined during storage, indicating progressive textural degradation and quality loss. Moisture loss is a major driver of postharvest softening and overall quality decline (Lufu et al. 2020; Paniagua Gonzalez et al. 2013). Most WL occurred between harvest and week 2, coinciding with the sharpest decreases in firmness-related traits. Weight loss was slightly greater in 2025 than in 2024, reaching maximum values of 5.1% and 3.1%, respectively. These losses remain at or below the 5–10% threshold typically associated with unmarketability (Lufu et al. 2020).

The relatively limited WL observed here likely reflects the maintenance of appropriate storage conditions (4 °C and 95% relative humidity), which minimize transpiration. Although previous studies have reported strong associations between weight loss and fruit softening (Paniagua Gonzalez et al. 2013; Valverde et al. 2005; Shahkoomahally et al. 2021), correlations between WL and other traits in this study were weak or non-significant. Nevertheless, the general trend indicated that WL increased as PM decreased, consistent with findings by Barchenger et al. (2015).

Percent marketable fruit declined steadily during storage. While water loss can contribute to unmarketability through wilting or shriveling (Himelrick 2003), this was not the primary cause here. Instead, loss of marketability was largely due to decay or advanced softening, consistent with observations by Walker et al. (2001). After four weeks of storage, PM averaged 78.45% in 2024 and 66.43% in 2025, comparable to decay rates of 19.2% at two weeks and 25.7% at four weeks reported by Walker et al. (2001). Although correlations involving PM were generally low, PM was slightly positively correlated with BMF at week 2 and BPW at weeks 2 and 4. This suggests that genotypes maintaining higher marketability during storage retained greater skin integrity which is why the forced needed to puncture the berry was greater.

Loss of firmness (LF) and loss of flesh maximum force (LFMF) were calculated as additional indicators of storability. While LFMF showed only weak or non-significant correlations, LF was negatively associated with BDFP, BMF, and BPW. Because LF represents the total decrease in firmness across the storage period, its correlation with

BDFP, BMF, and BPW at week 0 suggests that genotypes with tougher skins may retain more firmness in storage. Firm fruit with a tender skin will have a lower BDFP (Conner 2013a). However, since LF was not correlated with FMF, it seems that tougher skins are associated with firmness retention in storage. The development of new genotypes with more friable skins is a major goal of the breeding program and these selections will need to be monitored for storability.

Conclusions

The muscadine germplasm pool at UGA exhibits broad variation in textural, physiochemical, and storability traits, reflecting both natural diversity and ongoing breeding progress. Skins remain substantially thicker and tougher than those of *V. vinifera*, though several genotypes now show firmness levels comparable to table grapes. Firmness-related traits such as berry firmness (BF), berry maximum force (BMF), and flesh maximum force (FMF) declined during storage, particularly within the first two weeks, yet firmer berries at harvest generally retained texture, supporting firmness at harvest as a reliable predictor of storability. Correlations between berry diameter, firmness, and skin thickness indicate linked selection pressures that favor large, thick-skinned fruit, potentially at odds with consumer preferences for thinner skins. Future improvement will rely on balancing firmness, skin integrity, and sensory appeal to enhance both marketability and shelf life.

Tables and Figures

Table 2.1: Protocols used for characterization of muscadine grape germplasm including the name of the test, abbreviations, units, and parameters for the TA.XT2i texture analyzer (if applicable).

Test	Abbr.	Probe Type	Test Speed ($mm \cdot s^{-1}$)	Probe trigger point (N)	Probe end point	Unit
Berry deformation at first peak	BDFP	2-mm cylinder	1	0.07	12 mm	mm
Berry maximal force	BMF	2-mm cylinder	1	0.07	12 mm	N
Flesh maximal force	FMF	5-mm cylinder	0.5	0.07	3 mm	N
Skin thickness	ST	5-mm cylinder	0.1	0.07	100 N	mm
Berry firmness	BF					g·mm-1
Berry diameter	BD					mm
Total soluble solids	TSS					%
Titratable acidity	TA					%
Lightness	L*					
Chroma	*C**					
Hue angle	*h*°					

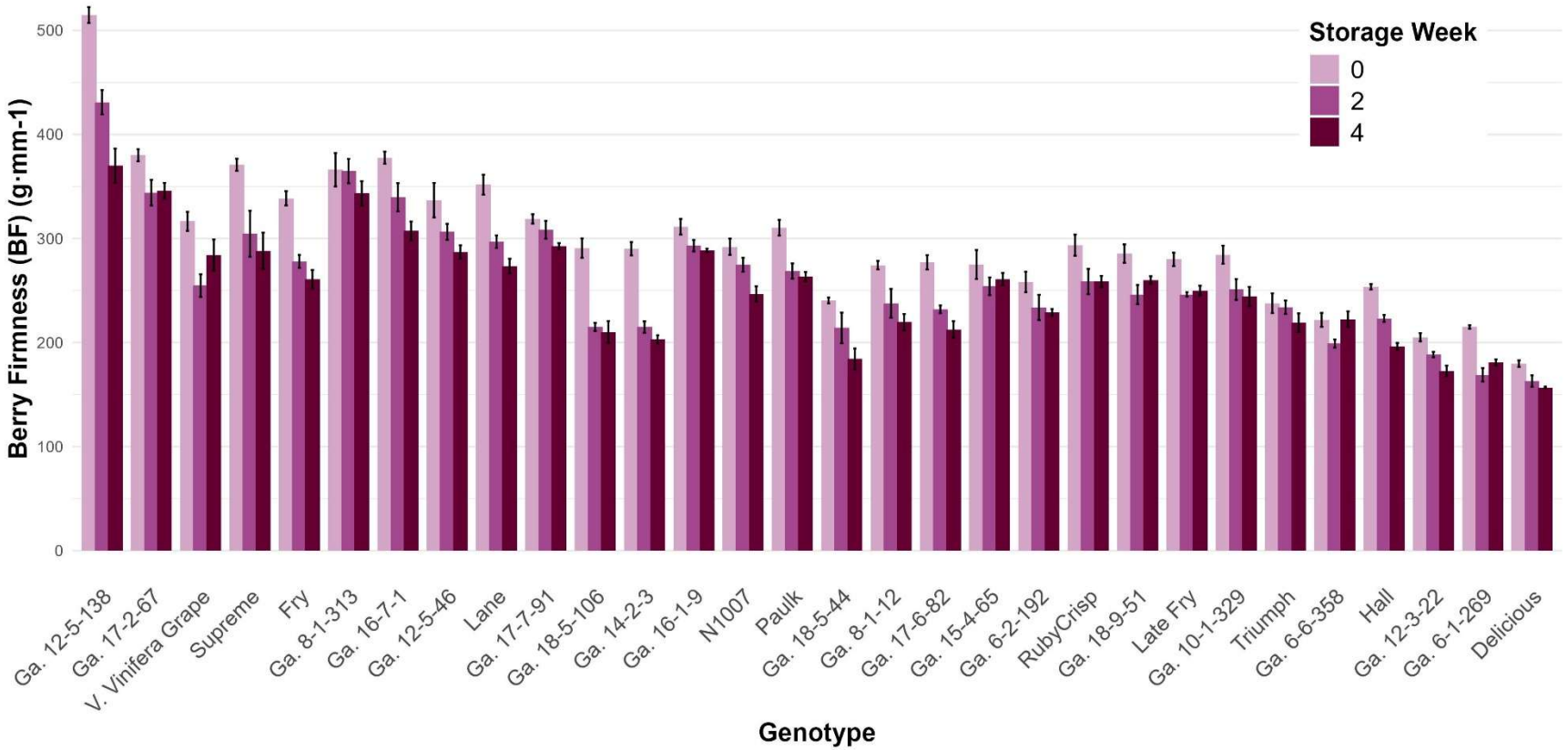

Figure 2.10: Berry firmness (BF) of muscadine genotypes averaged for 2024 showing the loss of firmness after 2 and 4 weeks of cold storage.

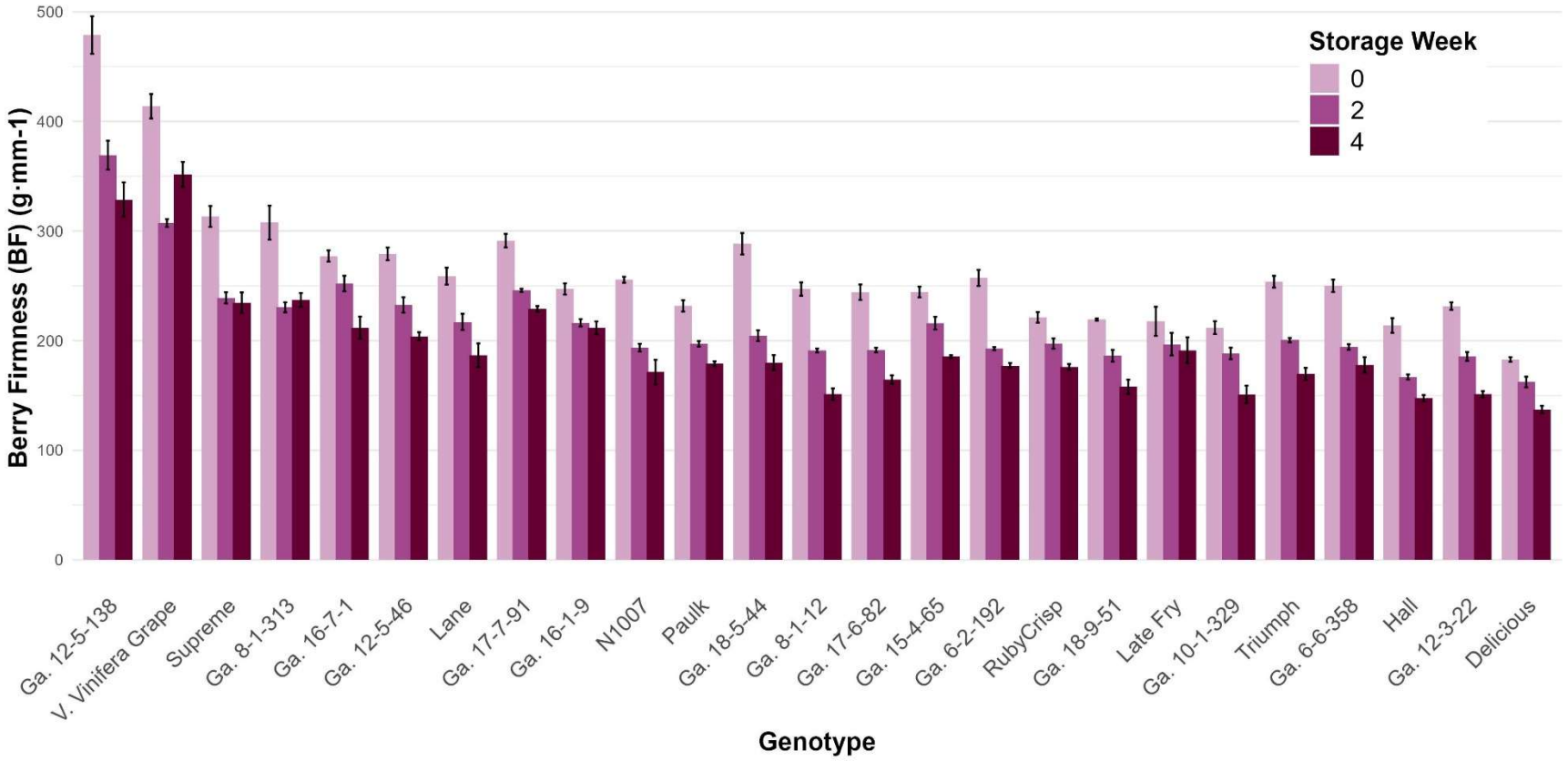

Figure 11: Berry firmness (BF) of muscadine genotypes averaged for 2025 showing the loss of firmness after 2 and 4 weeks of cold storage.

Table 2.2: Textural and storage attributes of fresh-market muscadine genotypes across 0, 2, and 4 weeks of storage in 2024.

Genotype	Week	Berry diameter (mm)	Berry Firmness ($g \cdot mm^{-1}$)	Berry deformation at first peak (mm)	Berry maximum force (N)	Berry penetration work (mJ)	Flesh maximum force (N)	Skin thickness (mm)	Percent marketable	Weight loss (%)
Delicious	0	22.59 ± 0.96	179.73 ± 6.30	7.44 ± 0.41	7.58 ± 0.20	28.26 ± 1.93	0.94 ± 0.06	1.05 ± 0.05	100.00 ± 0.00	0.00 ± 0.00
	2	23.32 ± 0.45	163.08 ± 10.86	7.60 ± 0.55	6.69 ± 0.28	25.35 ± 2.74	0.94 ± 0.04	1.17 ± 0.03	88.47 ± 2.61	1.00 ± 0.03
	4	22.92 ± 0.13	156.83 ± 1.72	7.74 ± 0.38	6.84 ± 0.29	26.50 ± 1.98	0.82 ± 0.09	1.17 ± 0.06	63.15 ± 6.15	0.10 ± 0.04
Fry	0	26.41 ± 0.45	338.58 ± 13.65	5.04 ± 0.35	10.37 ± 0.19	26.36 ± 2.00	2.41 ± 0.17	1.87 ± 0.06	100.00 ± 0.00	0.00 ± 0.00
	2	26.24 ± 0.39	277.98 ± 12.54	5.25 ± 0.26	9.78 ± 0.43	25.87 ± 2.00	2.28 ± 0.16	1.74 ± 0.06	100.00 ± 0.00	1.13 ± 0.15
	4	26.04 ± 0.31	260.78 ± 17.88	5.16 ± 0.11	9.43 ± 0.43	24.60 ± 1.47	1.76 ± 0.15	1.83 ± 0.05	87.97 ± 3.36	0.22 ± 0.20
Ga. 10-1-329	0	27.73 ± 0.43	284.38 ± 17.41	5.21 ± 0.19	9.04 ± 0.63	23.52 ± 2.17	2.54 ± 0.35	1.77 ± 0.13	100.00 ± 0.00	0.00 ± 0.00
	2	27.30 ± 0.55	251.01 ± 20.18	5.24 ± 0.34	6.52 ± 0.16	17.13 ± 1.16	2.79 ± 0.61	1.72 ± 0.09	98.92 ± 1.24	-0.06 ± 0.16
	4	27.00 ± 0.39	244.27 ± 18.35	4.64 ± 0.24	5.31 ± 0.71	12.44 ± 2.01	2.16 ± 0.15	1.62 ± 0.09	78.73 ± 1.34	0.48 ± 0.13
Ga. 12-3-22	0	26.29 ± 0.29	205.11 ± 7.90	7.42 ± 0.19	10.71 ± 0.87	39.82 ± 4.17	1.36 ± 0.18	1.33 ± 0.07	100.00 ± 0.00	0.00 ± 0.00
	2	26.62 ± 0.74	188.46 ± 5.27	6.98 ± 0.45	7.92 ± 0.41	27.90 ± 3.14	1.31 ± 0.09	1.50 ± 0.08	99.53 ± 0.94	0.82 ± 0.31
	4	25.69 ± 0.25	172.77 ± 10.07	6.37 ± 0.27	6.04 ± 0.43	19.54 ± 2.14	1.35 ± 0.07	1.38 ± 0.02	83.79 ± 5.81	0.48 ± 0.22
Ga. 12-5-138	0	30.54 ± 0.80	514.74 ± 15.21	3.47 ± 0.22	11.45 ± 0.51	20.06 ± 1.85	4.77 ± 0.60	1.87 ± 0.04	100.00 ± 0.00	0.00 ± 0.00
	2	30.23 ± 1.00	430.91 ± 23.27	3.77 ± 0.29	9.49 ± 0.52	18.05 ± 2.12	4.31 ± 0.45	1.76 ± 0.06	100.00 ± 0.00	0.66 ± 0.12
	4	28.62 ± 0.36	369.92 ± 32.88	3.76 ± 0.54	8.61 ± 0.77	16.53 ± 3.51	3.47 ± 0.34	1.90 ± 0.08	91.15 ± 3.47	-0.14 ± 0.16
Ga. 12-5-46	0	30.24 ± 0.93	336.83 ± 33.25	5.58 ± 0.24	12.77 ± 0.68	35.78 ± 3.18	3.94 ± 0.51	1.74 ± 0.05	100.00 ± 0.00	0.00 ± 0.00
	2	30.64 ± 0.58	306.39 ± 15.35	6.30 ± 0.21	11.06 ± 0.45	34.91 ± 1.28	2.59 ± 0.13	1.60 ± 0.03	99.31 ± 1.39	0.61 ± 0.16
	4	29.70 ± 0.18	286.84 ± 13.13	5.62 ± 0.27	9.40 ± 0.52	26.87 ± 2.75	2.52 ± 0.16	1.60 ± 0.06	91.39 ± 5.41	0.24 ± 0.19
Ga. 14-2-3	0	25.67 ± 0.44	290.19 ± 12.83	5.06 ± 0.25	6.49 ± 0.40	16.53 ± 1.59	2.71 ± 0.17	1.57 ± 0.08	100.00 ± 0.00	0.00 ± 0.00
	2	25.52 ± 0.89	214.85 ± 11.01	4.79 ± 0.29	4.77 ± 0.59	11.58 ± 1.78	2.10 ± 0.08	1.42 ± 0.10	91.17 ± 1.37	1.16 ± 0.67
	4	25.32 ± 0.91	203.09 ± 7.91	5.02 ± 0.24	4.71 ± 0.16	11.93 ± 0.70	1.58 ± 0.18	1.42 ± 0.06	19.77 ± 3.73	0.06 ± 0.90
Ga. 15-4-65	0	25.73 ± 0.20	275.03 ± 27.82	7.27 ± 0.40	14.17 ± 0.88	51.93 ± 6.10	1.89 ± 0.11	1.40 ± 0.09	100.00 ± 0.00	0.00 ± 0.00
	2	25.68 ± 0.47	254.02 ± 16.91	7.78 ± 0.70	12.46 ± 1.03	48.67 ± 7.23	2.25 ± 0.18	1.38 ± 0.03	99.53 ± 0.94	0.48 ± 0.20
	4	25.72 ± 0.68	261.00 ± 11.76	6.91 ± 0.21	11.71 ± 0.64	40.62 ± 3.40	2.02 ± 0.17	1.44 ± 0.07	79.27 ± 2.41	-0.18 ± 0.70
Ga. 16-1-9	0	27.87 ± 0.21	311.28 ± 15.10	4.51 ± 0.05	8.63 ± 0.37	19.55 ± 0.85	3.31 ± 0.25	1.76 ± 0.08	100.00 ± 0.00	0.00 ± 0.00
	2	27.51 ± 0.27	293.08 ± 11.07	4.76 ± 0.38	7.68 ± 0.31	18.30 ± 2.18	3.63 ± 0.44	1.92 ± 0.07	100.00 ± 0.00	0.35 ± 0.11
	4	27.60 ± 0.66	288.60 ± 3.20	4.58 ± 0.31	7.40 ± 0.52	17.08 ± 2.22	3.16 ± 0.30	1.71 ± 0.10	86.06 ± 4.70	0.60 ± 0.17

Ga. 16-7-1	0	25.62 ± 0.19	377.65 ± 11.67	5.93 ± 0.19	14.99 ± 0.40	44.37 ± 1.94	3.07 ± 0.38	1.74 ± 0.06	100.00 ± 0.00	0.00 ± 0.00
	2	25.04 ± 0.85	339.55 ± 27.23	5.13 ± 0.30	12.56 ± 0.30	32.40 ± 2.41	3.51 ± 0.37	1.56 ± 0.07	98.80 ± 1.52	0.00 ± 0.64
	4	25.55 ± 0.48	307.29 ± 17.99	5.48 ± 0.29	11.16 ± 0.43	30.63 ± 2.53	2.68 ± 0.08	1.50 ± 0.06	88.29 ± 3.21	0.54 ± 0.08
Ga. 17-2-67	0	26.22 ± 0.29	379.95 ± 11.55	5.77 ± 0.64	15.12 ± 0.40	44.04 ± 5.77	3.90 ± 0.21	1.67 ± 0.05	100.00 ± 0.00	0.00 ± 0.00
	2	26.06 ± 0.54	344.06 ± 24.66	5.90 ± 0.06	13.82 ± 0.13	40.71 ± 0.72	2.92 ± 0.28	1.55 ± 0.04	99.50 ± 1.00	0.88 ± 0.20
	4	26.45 ± 0.46	345.85 ± 15.24	5.72 ± 0.26	13.92 ± 0.63	39.99 ± 3.22	3.02 ± 0.26	1.57 ± 0.08	66.13 ± 1.92	0.41 ± 0.11
Ga. 17-6-82	0	28.73 ± 0.27	277.08 ± 13.67	5.98 ± 0.38	9.08 ± 0.52	27.44 ± 3.27	1.95 ± 0.09	1.76 ± 0.02	100.00 ± 0.00	0.00 ± 0.00
	2	28.59 ± 0.26	231.92 ± 7.51	5.86 ± 0.13	7.12 ± 0.41	20.92 ± 1.47	1.91 ± 0.15	1.54 ± 0.11	99.38 ± 1.25	0.71 ± 0.54
	4	28.31 ± 0.87	212.53 ± 16.01	5.79 ± 0.25	6.79 ± 0.27	19.77 ± 1.58	1.77 ± 0.16	1.62 ± 0.07	58.61 ± 4.33	0.63 ± 0.18
Ga. 17-7-91	0	25.66 ± 0.39	318.80 ± 8.92	5.66 ± 0.39	12.67 ± 0.65	35.98 ± 3.79	2.53 ± 0.23	1.42 ± 0.06	100.00 ± 0.00	0.00 ± 0.00
	2	26.06 ± 0.51	308.37 ± 17.20	5.41 ± 0.23	11.50 ± 0.48	31.35 ± 1.68	2.75 ± 0.07	1.33 ± 0.10	96.85 ± 1.82	1.03 ± 0.51
	4	26.17 ± 0.32	292.62 ± 5.99	5.91 ± 0.32	11.96 ± 0.17	35.66 ± 1.89	2.41 ± 0.20	1.34 ± 0.04	60.72 ± 2.11	0.62 ± 0.18
Ga. 18-5-106	0	28.52 ± 0.60	290.79 ± 18.64	4.56 ± 0.36	6.15 ± 0.57	13.96 ± 1.48	1.84 ± 0.23	1.15 ± 0.07	100.00 ± 0.00	0.00 ± 0.00
	2	27.18 ± 0.17	214.98 ± 7.84	5.06 ± 0.39	4.74 ± 0.11	11.97 ± 0.82	1.78 ± 0.23	1.17 ± 0.06	98.58 ± 0.95	0.72 ± 0.16
	4	27.29 ± 0.26	210.14 ± 20.84	4.70 ± 0.15	4.71 ± 0.29	11.15 ± 0.88	1.50 ± 0.06	1.23 ± 0.06	58.01 ± 6.73	-0.24 ± 0.07
Ga. 18-5-44	0	26.69 ± 0.38	240.49 ± 5.57	4.72 ± 0.28	6.83 ± 0.20	16.10 ± 1.40	1.87 ± 0.21	0.94 ± 0.04	100.00 ± 0.00	0.00 ± 0.00
	2	25.91 ± 0.26	214.03 ± 29.34	5.32 ± 0.52	5.70 ± 0.36	14.98 ± 1.42	1.65 ± 0.23	1.06 ± 0.04	97.73 ± 0.87	1.43 ± 0.15
	4	25.90 ± 0.36	184.23 ± 20.07	5.04 ± 0.48	5.20 ± 0.37	13.41 ± 1.97	1.81 ± 0.23	0.98 ± 0.08	84.36 ± 2.71	1.79 ± 0.98
Ga. 18-9-51	0	28.14 ± 0.61	285.44 ± 17.73	5.83 ± 0.41	7.49 ± 0.23	21.95 ± 1.17	2.40 ± 0.26	1.71 ± 0.07	100.00 ± 0.00	0.00 ± 0.00
	2	28.55 ± 0.38	246.16 ± 18.44	5.85 ± 0.50	6.43 ± 0.17	18.89 ± 1.50	2.40 ± 0.28	1.58 ± 0.08	93.61 ± 5.10	0.81 ± 0.13
	4	29.14 ± 0.14	260.12 ± 7.38	4.99 ± 0.14	6.49 ± 0.22	16.25 ± 0.77	2.30 ± 0.23	1.60 ± 0.07	59.91 ± 4.43	-0.06 ± 0.21
Ga. 6-1-269	0	29.11 ± 0.22	214.92 ± 3.38	7.96 ± 0.26	9.19 ± 0.37	36.83 ± 2.73	1.41 ± 0.10	1.39 ± 0.08	100.00 ± 0.00	0.00 ± 0.00
	2	28.41 ± 0.66	168.97 ± 12.97	8.06 ± 0.36	6.62 ± 0.16	26.69 ± 1.76	1.36 ± 0.17	1.56 ± 0.10	100.00 ± 0.00	4.26 ± 0.18
	4	28.98 ± 0.83	180.85 ± 5.97	7.14 ± 0.43	6.76 ± 0.39	24.32 ± 2.65	1.41 ± 0.03	1.51 ± 0.05	80.16 ± 5.60	-0.31 ± 0.19
Ga. 6-2-192	0	26.44 ± 0.25	258.21 ± 19.65	5.45 ± 0.21	10.05 ± 0.52	27.41 ± 2.35	1.99 ± 0.20	1.77 ± 0.15	100.00 ± 0.00	0.00 ± 0.00
	2	25.91 ± 0.26	233.70 ± 24.20	5.97 ± 0.43	10.06 ± 0.30	30.02 ± 2.84	2.21 ± 0.15	1.70 ± 0.11	98.49 ± 1.89	1.05 ± 0.28
	4	26.86 ± 0.47	229.07 ± 6.39	5.82 ± 0.31	8.31 ± 0.14	24.23 ± 1.11	2.10 ± 0.14	1.60 ± 0.08	96.46 ± 1.03	1.03 ± 0.43
Ga. 6-6-358	0	28.56 ± 0.64	221.82 ± 13.47	8.14 ± 0.25	13.27 ± 0.38	54.01 ± 1.21	1.34 ± 0.15	1.56 ± 0.03	100.00 ± 0.00	0.00 ± 0.00
	2	28.33 ± 0.54	199.00 ± 7.69	9.16 ± 0.95	11.16 ± 0.56	50.86 ± 5.49	1.37 ± 0.08	1.51 ± 0.07	99.34 ± 1.32	0.09 ± 0.07
	4	28.78 ± 0.37	222.31 ± 15.15	8.21 ± 0.48	10.89 ± 0.18	44.70 ± 2.42	1.23 ± 0.08	1.50 ± 0.04	70.66 ± 4.82	-0.06 ± 0.27
Ga. 8-1-12	0	28.80 ± 0.63	274.34 ± 8.05	5.84 ± 0.26	9.25 ± 0.50	27.26 ± 2.04	2.44 ± 0.25	1.32 ± 0.05	100.00 ± 0.00	0.00 ± 0.00
	2	27.91 ± 0.65	237.71 ± 27.64	5.65 ± 0.36	8.14 ± 0.50	23.38 ± 2.58	2.41 ± 0.17	1.56 ± 0.05	100.00 ± 0.00	-0.36 ± 0.13
	4	28.50 ± 0.63	219.56 ± 15.80	6.17 ± 0.48	7.38 ± 0.08	23.01 ± 2.07	2.20 ± 0.20	1.41 ± 0.05	95.21 ± 2.80	0.89 ± 0.30

Ga. 8-1-313	0	31.21 ± 0.47	366.01 ± 32.03	5.53 ± 0.45	13.31 ± 0.41	37.24 ± 3.50	3.19 ± 0.41	1.92 ± 0.06	100.00 ± 0.00	0.00 ± 0.00
	2	30.41 ± 0.57	364.77 ± 23.28	5.58 ± 0.73	11.47 ± 0.78	31.54 ± 4.69	3.98 ± 1.01	2.06 ± 0.04	96.60 ± 2.59	-0.27 ± 0.25
	4	30.74 ± 1.17	343.35 ± 23.26	5.80 ± 0.59	12.46 ± 0.20	36.33 ± 4.07	3.14 ± 0.28	1.98 ± 0.05	60.85 ± 7.76	0.07 ± 0.19
Hall	0	26.45 ± 0.43	253.60 ± 5.20	6.92 ± 0.27	12.06 ± 0.20	42.00 ± 1.97	1.33 ± 0.17	1.61 ± 0.09	100.00 ± 0.00	0.00 ± 0.00
	2	25.91 ± 0.26	223.18 ± 6.88	6.81 ± 0.40	9.77 ± 1.07	33.58 ± 5.32	1.52 ± 0.10	1.45 ± 0.05	100.00 ± 0.00	1.07 ± 0.03
	4	25.69 ± 0.49	196.31 ± 6.69	7.36 ± 0.55	9.07 ± 0.64	33.46 ± 4.43	1.43 ± 0.10	1.49 ± 0.07	100.00 ± 0.00	1.27 ± 0.37
Lane	0	26.76 ± 0.52	351.72 ± 19.06	4.55 ± 0.32	10.98 ± 0.38	24.98 ± 1.36	3.38 ± 0.38	1.65 ± 0.27	100.00 ± 0.00	0.00 ± 0.00
	2	26.09 ± 0.36	296.93 ± 12.02	4.87 ± 0.63	9.90 ± 0.61	24.07 ± 3.04	3.49 ± 0.12	1.51 ± 0.05	98.84 ± 1.34	1.31 ± 0.18
	4	26.32 ± 0.37	273.49 ± 14.05	4.63 ± 0.27	9.13 ± 0.27	21.22 ± 1.46	3.42 ± 0.31	1.56 ± 0.07	100.00 ± 0.00	1.24 ± 0.33
Late Fry	0	26.98 ± 0.47	279.96 ± 12.96	7.26 ± 0.21	13.23 ± 0.58	48.11 ± 3.43	2.39 ± 0.15	1.77 ± 0.05	100.00 ± 0.00	0.00 ± 0.00
	2	27.38 ± 0.38	246.25 ± 4.13	6.79 ± 0.32	11.19 ± 0.24	37.43 ± 1.56	2.12 ± 0.10	1.76 ± 0.09	99.02 ± 1.96	1.10 ± 0.05
	4	27.51 ± 0.43	249.93 ± 9.46	7.20 ± 0.29	10.55 ± 0.17	38.04 ± 1.27	1.67 ± 0.07	1.75 ± 0.02	69.82 ± 1.28	0.74 ± 0.16
N1007	0	27.83 ± 0.27	292.06 ± 15.64	6.02 ± 0.34	10.41 ± 0.42	31.43 ± 0.85	2.47 ± 0.38	1.50 ± 0.06	100.00 ± 0.00	0.00 ± 0.00
	2	28.45 ± 0.65	274.74 ± 13.48	5.89 ± 0.26	9.71 ± 0.64	28.45 ± 2.67	2.51 ± 0.16	1.62 ± 0.02	100.00 ± 0.00	0.49 ± 0.41
	4	28.04 ± 0.45	246.61 ± 14.86	6.00 ± 0.31	8.28 ± 0.27	25.13 ± 0.52	2.40 ± 0.19	1.69 ± 0.05	97.88 ± 1.70	1.27 ± 0.27
Paulk	0	29.23 ± 0.14	310.38 ± 15.03	6.28 ± 0.22	13.01 ± 0.71	40.95 ± 3.13	2.51 ± 0.19	1.78 ± 0.07	100.00 ± 0.00	0.00 ± 0.00
	2	28.57 ± 0.44	268.72 ± 14.74	6.70 ± 0.09	12.53 ± 0.55	42.17 ± 2.46	2.04 ± 0.15	1.62 ± 0.04	98.78 ± 2.44	0.70 ± 0.12
	4	28.87 ± 0.42	263.42 ± 8.76	6.34 ± 0.29	11.67 ± 0.18	37.20 ± 2.27	1.86 ± 0.12	1.68 ± 0.11	84.93 ± 5.36	-0.59 ± 0.82
RubyCrisp	0	27.78 ± 0.10	293.60 ± 20.23	4.90 ± 0.28	9.20 ± 0.42	22.47 ± 2.34	2.84 ± 0.22	1.35 ± 0.08	100.00 ± 0.00	0.00 ± 0.00
	2	26.90 ± 0.32	258.60 ± 24.32	4.23 ± 0.28	6.85 ± 0.57	14.47 ± 1.61	3.17 ± 0.26	1.33 ± 0.11	99.09 ± 1.05	-0.03 ± 0.21
	4	26.99 ± 0.48	258.57 ± 10.99	4.69 ± 0.21	7.01 ± 0.31	16.53 ± 0.29	2.28 ± 0.25	1.30 ± 0.09	70.22 ± 6.67	0.78 ± 0.13
Supreme	0	31.98 ± 0.52	370.79 ± 11.69	5.96 ± 0.39	12.04 ± 0.65	35.71 ± 2.85	2.58 ± 0.36	1.98 ± 0.15	100.00 ± 0.00	0.00 ± 0.00
	2	31.54 ± 0.36	304.56 ± 44.17	6.08 ± 0.35	9.72 ± 0.81	29.54 ± 1.72	2.97 ± 0.46	2.06 ± 0.04	100.00 ± 0.00	2.13 ± 2.01
	4	30.96 ± 0.59	288.20 ± 34.76	5.70 ± 0.15	8.13 ± 0.73	23.50 ± 2.01	2.28 ± 0.21	1.94 ± 0.04	92.75 ± 1.87	0.64 ± 0.13
Triumph	0	24.35 ± 0.61	237.81 ± 18.95	7.02 ± 0.24	11.75 ± 0.40	41.48 ± 2.20	2.86 ± 0.49	1.10 ± 0.09	100.00 ± 0.00	0.00 ± 0.00
	2	23.98 ± 0.18	233.99 ± 12.79	7.02 ± 0.32	10.69 ± 0.39	37.58 ± 2.96	2.74 ± 0.28	1.18 ± 0.06	100.00 ± 0.00	0.26 ± 0.10
	4	24.36 ± 0.29	219.04 ± 17.81	7.68 ± 0.40	10.47 ± 0.82	40.37 ± 4.99	2.94 ± 0.25	1.17 ± 0.07	98.88 ± 0.75	1.26 ± 0.60
V. Vinifera grape	0	21.47 ± 0.71	316.43 ± 18.37	3.01 ± 0.32	4.62 ± 0.23	7.03 ± 1.12	4.38 ± 0.33	0.57 ± 0.03	100.00 ± 0.00	0.00 ± 0.00
	2	20.86 ± 0.46	254.73 ± 21.74	3.54 ± 0.37	4.76 ± 0.33	8.49 ± 1.50	3.23 ± 0.42	0.58 ± 0.02	99.57 ± 0.86	0.64 ± 0.24
	4	20.99 ± 0.61	284.00 ± 29.93	3.29 ± 0.16	4.35 ± 0.31	7.22 ± 0.78	3.26 ± 0.25	0.58 ± 0.01	89.80 ± 1.96	-0.83 ± 0.41

V.	0	21.42	173.018	3.22	5.45	12.26	0.89	0.9	100	0
rotundifolia	2	22.74	150.83	3.52	3.89	9.54	0.9	1.03	85.53	0
minimum[z]	4	22.76	154.9	3.42	4.43	9.98	0.76	0.92	15.69	0
V.	0	32.59	524.46	8.48	15.5	60.91	5.64	2.09	100	0
rotundifolia	2	31.96	464.33	10.39	13.97	58.44	5.18	2.11	100	4.43
maximum[z]	4	32.16	411.6	8.83	14.6	47.66	3.8	2.04	100	3.1
V.	0	27.52 a	297.63 a	5.91 a	10.73 a	32.26 a	2.49 a	1.57 a	100 a	0 c
rotundifolia	2	27.25 a	261.72 b	5.99 a	9.17 b	27.89 b	2.45 a	1.55 a	98.33 a	0.81 a
average[z,y]	4	27.24 a	249.92 b	5.87 a	8.61 b	25.9 b	2.16 b	1.54 a	78.45 b	0.47 b

[z]Minimum, maximum, and averages are comprehensive of all values excluding the *V. vinifera* grape sample.

[y]Mean values within a column followed by the same letter are not significantly different (Tukey's Honest Significant Difference (HSD) test $P<0.05$)

Table 2.3: Textural and storage attributes of fresh-market muscadine genotypes across 0, 2, and 4 weeks of storage in 2025.

Genotype	Week	Berry diameter (mm)	Berry Firmness ($g \cdot mm^{-1}$)	Berry deformation at first peak (mm)	Berry maximum force (N)	Berry penetration work (mJ)	Flesh maximum force (N)	Skin thickness (mm)	Percent marketable	Weight loss (%)
Delicious	0	23.31 ± 0.26	182.86 ± 4.22	6.51 ± 0.21	6.91 ± 0.55	22.60 ± 2.45	0.83 ± 0.04	1.11 ± 0.04	100.00 ± 0.00	0.00 ± 0.00
	2	24.22 ± 0.41	162.27 ± 9.79	7.80 ± 0.25	6.76 ± 0.46	26.33 ± 1.15	0.75 ± 0.02	1.14 ± 0.02	79.09 ± 1.42	1.70 ± 0.07
	4	23.11 ± 0.29	137.16 ± 6.67	7.21 ± 0.13	5.60 ± 0.20	20.35 ± 0.87	0.76 ± 0.04	1.13 ± 0.05	65.53 ± 2.32	1.54 ± 0.09
Ga. 10-1-329	0	26.79 ± 0.61	211.85 ± 11.77	6.41 ± 0.21	7.42 ± 0.59	23.94 ± 2.59	1.64 ± 0.11	1.73 ± 0.05	100.00 ± 0.00	0.00 ± 0.00
	2	26.94 ± 0.41	188.36 ± 10.53	6.50 ± 0.13	5.55 ± 0.50	18.05 ± 1.83	1.48 ± 0.10	1.61 ± 0.08	79.51 ± 4.89	2.05 ± 0.02
	4	26.33 ± 0.63	150.86 ± 16.04	6.63 ± 0.44	4.36 ± 0.27	14.43 ± 0.77	1.22 ± 0.15	1.62 ± 0.11	48.02 ± 7.56	1.60 ± 0.19
Ga. 12-3-22	0	26.90 ± 0.29	231.49 ± 6.86	6.26 ± 0.20	8.32 ± 0.19	26.14 ± 0.88	1.17 ± 0.08	1.23 ± 0.03	100.00 ± 0.00	0.00 ± 0.00
	2	26.24 ± 0.47	185.62 ± 7.96	6.98 ± 0.28	7.60 ± 0.27	26.71 ± 1.59	1.10 ± 0.05	1.29 ± 0.06	96.36 ± 1.38	1.50 ± 0.09
	4	25.36 ± 0.35	151.02 ± 5.93	6.88 ± 0.14	5.67 ± 0.75	19.56 ± 2.95	1.03 ± 0.09	1.24 ± 0.10	71.85 ± 6.79	2.08 ± 0.14
Ga. 12-5-138	0	32.39 ± 0.90	478.88 ± 34.32	3.56 ± 0.20	9.55 ± 0.82	17.29 ± 2.38	2.98 ± 0.36	1.79 ± 0.04	100.00 ± 0.00	0.00 ± 0.00
	2	32.86 ± 0.39	369.27 ± 26.41	4.49 ± 0.36	9.31 ± 0.78	21.25 ± 3.65	3.09 ± 0.20	1.85 ± 0.02	86.63 ± 3.22	1.98 ± 0.05
	4	32.58 ± 0.76	328.74 ± 31.41	4.95 ± 0.22	9.06 ± 0.17	22.74 ± 1.01	2.95 ± 0.44	1.80 ± 0.03	57.65 ± 5.27	2.05 ± 0.20
Ga. 12-5-46	0	29.55 ± 0.80	279.16 ± 11.67	5.63 ± 0.25	10.00 ± 0.57	28.01 ± 2.32	2.62 ± 0.25	1.44 ± 0.07	100.00 ± 0.00	0.00 ± 0.00
	2	29.34 ± 0.03	232.52 ± 13.99	6.23 ± 0.37	9.28 ± 0.82	29.03 ± 4.20	2.13 ± 0.21	1.48 ± 0.03	86.50 ± 4.18	1.56 ± 0.12
	4	29.30 ± 0.36	203.95 ± 7.36	7.23 ± 0.66	8.97 ± 0.51	32.37 ± 2.37	1.86 ± 0.29	1.47 ± 0.07	71.55 ± 3.92	1.18 ± 0.08
Ga. 15-4-65	0	26.34 ± 0.73	244.37 ± 9.78	7.27 ± 0.25	12.91 ± 0.43	47.17 ± 3.37	1.88 ± 0.13	1.41 ± 0.05	100.00 ± 0.00	0.00 ± 0.00
	2	25.88 ± 0.28	215.95 ± 11.55	7.88 ± 0.61	10.67 ± 0.79	42.22 ± 6.36	1.72 ± 0.16	1.37 ± 0.02	84.13 ± 6.26	2.03 ± 0.04
	4	26.33 ± 0.26	185.39 ± 2.72	8.01 ± 0.35	10.86 ± 0.65	43.71 ± 3.22	1.42 ± 0.17	1.31 ± 0.08	78.19 ± 4.04	1.36 ± 0.17
Ga. 16-1-9	0	28.54 ± 0.36	247.17 ± 10.29	5.55 ± 0.28	7.16 ± 0.30	20.01 ± 1.68	2.15 ± 0.01	1.69 ± 0.05	100.00 ± 0.00	0.00 ± 0.00
	2	27.95 ± 0.49	216.31 ± 6.82	5.90 ± 0.26	7.02 ± 0.21	20.90 ± 0.71	2.21 ± 0.06	1.56 ± 0.06	92.05 ± 2.92	2.08 ± 0.09
	4	28.33 ± 0.24	211.59 ± 11.71	5.88 ± 0.35	6.70 ± 0.14	19.74 ± 1.28	1.91 ± 0.22	1.62 ± 0.02	84.47 ± 4.46	2.09 ± 0.15
Ga. 16-7-1	0	25.67 ± 0.35	277.27 ± 10.31	6.67 ± 0.04	12.50 ± 0.39	41.72 ± 1.53	1.79 ± 0.14	1.40 ± 0.07	100.00 ± 0.00	0.00 ± 0.00
	2	25.79 ± 0.13	252.11 ± 14.19	7.17 ± 0.24	11.58 ± 0.32	41.44 ± 1.78	1.90 ± 0.02	1.36 ± 0.05	88.17 ± 1.18	1.36 ± 0.44
	4	26.09 ± 0.51	211.95 ± 19.91	7.12 ± 0.20	10.12 ± 0.63	36.07 ± 2.07	1.60 ± 0.21	1.42 ± 0.06	77.84 ± 3.63	1.35 ± 0.17
Ga. 17-6-82	0	29.02 ± 0.67	244.23 ± 14.04	6.14 ± 0.29	7.95 ± 0.37	24.54 ± 1.88	1.62 ± 0.12	1.50 ± 0.06	100.00 ± 0.00	0.00 ± 0.00
	2	28.23 ± 0.67	191.35 ± 4.24	6.53 ± 0.24	6.13 ± 0.75	20.31 ± 3.28	1.36 ± 0.05	1.44 ± 0.12	75.72 ± 5.10	2.59 ± 0.19
	4	27.97 ± 0.22	164.44 ± 7.91	6.34 ± 0.36	5.07 ± 0.24	16.23 ± 1.40	1.21 ± 0.09	1.63 ± 0.11	38.14 ± 5.50	2.47 ± 0.34

Ga. 17-7-91	0	27.19 ± 0.34	291.31 ± 12.38	5.93 ± 0.44	10.97 ± 0.87	32.74 ± 4.51	1.88 ± 0.11	1.42 ± 0.01	100.00 ± 0.00	0.00 ± 0.00
	2	27.19 ± 0.18	245.90 ± 2.88	6.16 ± 0.17	9.84 ± 0.36	30.40 ± 1.62	1.74 ± 0.05	1.40 ± 0.04	89.98 ± 1.80	1.43 ± 0.08
	4	27.35 ± 0.43	228.97 ± 5.15	6.58 ± 0.29	10.13 ± 0.45	33.55 ± 3.08	1.72 ± 0.16	1.50 ± 0.02	71.75 ± 5.77	1.12 ± 0.09
Ga. 18-5-44	0	27.51 ± 0.38	288.39 ± 19.65	4.54 ± 0.18	6.74 ± 0.24	15.46 ± 0.92	1.73 ± 0.09	1.18 ± 0.03	100.00 ± 0.00	0.00 ± 0.00
	2	27.35 ± 0.37	204.50 ± 9.85	5.27 ± 0.19	5.32 ± 0.35	14.31 ± 1.29	1.72 ± 0.10	1.09 ± 0.03	88.04 ± 1.46	2.99 ± 0.21
	4	27.12 ± 0.45	180.08 ± 13.58	6.22 ± 0.28	5.43 ± 0.22	17.12 ± 1.30	1.29 ± 0.09	1.09 ± 0.02	57.65 ± 7.97	4.09 ± 0.18
Ga. 18-9-51	0	29.13 ± 0.45	219.16 ± 2.03	6.80 ± 0.26	7.67 ± 0.38	26.19 ± 1.27	1.74 ± 0.02	1.71 ± 0.05	100.00 ± 0.00	0.00 ± 0.00
	2	28.19 ± 0.87	186.21 ± 10.66	7.36 ± 0.18	6.20 ± 0.39	22.92 ± 1.73	1.56 ± 0.09	1.70 ± 0.04	85.01 ± 4.14	1.93 ± 0.10
	4	29.17 ± 0.33	157.89 ± 12.99	7.30 ± 0.56	5.47 ± 0.21	20.37 ± 2.27	1.32 ± 0.07	1.69 ± 0.10	64.98 ± 6.67	1.50 ± 0.16
Ga. 6-2-192	0	27.19 ± 0.21	257.28 ± 14.67	5.99 ± 0.31	8.00 ± 0.12	23.86 ± 1.19	1.45 ± 0.11	1.71 ± 0.04	100.00 ± 0.00	0.00 ± 0.00
	2	26.86 ± 0.45	192.74 ± 2.79	6.16 ± 0.32	6.70 ± 0.35	20.72 ± 1.91	1.34 ± 0.08	1.53 ± 0.05	90.58 ± 1.08	3.21 ± 1.10
	4	26.59 ± 0.25	177.28 ± 4.61	7.04 ± 0.15	6.75 ± 0.33	23.96 ± 1.43	1.25 ± 0.09	1.50 ± 0.07	71.66 ± 7.53	4.14 ± 0.08
Ga. 6-6-358	0	30.09 ± 0.44	250.05 ± 11.28	7.09 ± 0.29	11.16 ± 0.72	39.80 ± 3.16	1.33 ± 0.04	1.64 ± 0.05	100.00 ± 0.00	0.00 ± 0.00
	2	30.08 ± 0.29	194.22 ± 5.10	8.15 ± 0.36	9.96 ± 0.22	40.64 ± 2.41	1.22 ± 0.05	1.59 ± 0.03	81.77 ± 7.76	2.03 ± 0.06
	4	29.58 ± 0.22	177.92 ± 14.11	8.79 ± 0.27	9.12 ± 0.37	40.03 ± 2.58	1.10 ± 0.05	1.55 ± 0.08	70.19 ± 3.82	2.30 ± 0.11
Ga. 8-1-12	0	26.99 ± 0.55	247.11 ± 12.24	6.17 ± 0.51	7.65 ± 0.40	23.83 ± 2.87	1.82 ± 0.11	1.37 ± 0.08	100.00 ± 0.00	0.00 ± 0.00
	2	27.09 ± 0.51	190.96 ± 3.68	6.86 ± 0.38	6.37 ± 0.27	22.06 ± 2.01	1.62 ± 0.20	1.39 ± 0.05	96.44 ± 1.26	2.82 ± 0.15
	4	26.28 ± 0.64	151.14 ± 10.52	7.10 ± 0.27	5.67 ± 0.16	20.35 ± 1.32	1.43 ± 0.11	1.38 ± 0.03	77.03 ± 2.22	4.51 ± 0.22
Ga. 8-1-313	0	31.12 ± 0.44	307.73 ± 31.09	6.70 ± 0.15	11.41 ± 0.85	38.53 ± 3.41	2.30 ± 0.18	1.98 ± 0.06	100.00 ± 0.00	0.00 ± 0.00
	2	30.67 ± 0.53	230.42 ± 9.05	6.85 ± 0.29	10.33 ± 0.78	35.38 ± 4.07	2.13 ± 0.17	1.89 ± 0.10	79.82 ± 2.62	2.88 ± 0.19
	4	30.87 ± 0.14	237.14 ± 12.73	7.14 ± 0.43	10.12 ± 0.30	36.30 ± 1.91	1.99 ± 0.11	1.94 ± 0.01	72.31 ± 4.58	2.74 ± 0.15
Hall	0	26.58 ± 0.63	213.87 ± 13.46	7.31 ± 0.11	9.59 ± 0.45	35.10 ± 1.56	0.99 ± 0.04	1.41 ± 0.07	100.00 ± 0.00	0.00 ± 0.00
	2	26.04 ± 0.20	166.85 ± 4.68	7.88 ± 0.35	7.55 ± 0.79	30.07 ± 4.43	0.89 ± 0.03	1.44 ± 0.10	87.61 ± 0.90	2.97 ± 0.08
	4	25.39 ± 0.13	147.50 ± 5.81	8.17 ± 0.17	7.03 ± 0.33	28.91 ± 1.15	0.87 ± 0.04	1.43 ± 0.06	74.57 ± 2.64	4.89 ± 0.24
Lane	0	26.39 ± 0.70	258.86 ± 15.57	4.85 ± 0.20	7.26 ± 0.23	17.76 ± 1.20	2.10 ± 0.11	1.27 ± 0.08	100.00 ± 0.00	0.00 ± 0.00
	2	26.93 ± 0.50	217.12 ± 14.69	5.80 ± 0.27	7.99 ± 0.47	23.30 ± 1.96	1.92 ± 0.25	1.36 ± 0.06	87.01 ± 1.87	3.23 ± 0.15
	4	26.22 ± 0.61	186.70 ± 21.72	6.00 ± 0.28	7.83 ± 0.30	23.65 ± 1.61	1.80 ± 0.25	1.28 ± 0.04	60.42 ± 8.44	4.30 ± 0.18
Late Fry	0	28.40 ± 0.44	217.69 ± 26.53	8.08 ± 0.60	11.69 ± 0.51	47.57 ± 4.96	1.31 ± 0.18	1.81 ± 0.03	100.00 ± 0.00	0.00 ± 0.00
	2	28.45 ± 0.48	196.76 ± 20.76	8.86 ± 0.70	10.95 ± 0.56	48.53 ± 2.20	1.39 ± 0.14	1.76 ± 0.04	69.97 ± 13.02	1.10 ± 0.40
	4	28.10 ± 0.46	191.09 ± 23.87	8.93 ± 0.68	10.08 ± 0.53	45.15 ± 3.27	1.29 ± 0.18	1.86 ± 0.07	69.31 ± 8.79	0.71 ± 0.21
N1007	0	28.00 ± 0.94	255.50 ± 5.50	6.56 ± 0.33	8.70 ± 0.46	28.46 ± 2.52	1.55 ± 0.07	1.54 ± 0.03	100.00 ± 0.00	0.00 ± 0.00
	2	27.68 ± 0.17	193.48 ± 7.09	7.16 ± 0.13	7.38 ± 0.48	26.58 ± 2.30	1.42 ± 0.13	1.48 ± 0.04	76.84 ± 3.55	2.07 ± 0.08
	4	27.71 ± 0.08	171.32 ± 22.44	7.28 ± 0.46	7.15 ± 0.39	25.90 ± 1.44	1.28 ± 0.26	1.48 ± 0.02	56.19 ± 8.72	1.65 ± 0.85

Paulk	0	29.14 ± 0.41	231.70 ± 10.25	7.29 ± 0.07	10.66 ± 0.43	38.93 ± 1.63	1.44 ± 0.10	1.53 ± 0.08	100.00 ± 0.00	0.00 ± 0.00
	2	28.96 ± 0.38	197.03 ± 5.13	7.85 ± 0.28	9.73 ± 0.68	38.24 ± 3.79	1.37 ± 0.06	1.58 ± 0.04	76.67 ± 7.14	1.59 ± 0.17
	4	29.34 ± 0.11	178.93 ± 4.26	8.36 ± 0.36	9.50 ± 0.34	39.60 ± 1.54	1.17 ± 0.09	1.61 ± 0.12	71.72 ± 12.54	1.15 ± 0.16
RubyCrisp	0	28.82 ± 0.91	221.21 ± 9.71	6.24 ± 0.35	8.16 ± 0.43	25.78 ± 2.30	1.35 ± 0.14	1.22 ± 0.07	100.00 ± 0.00	0.00 ± 0.00
	2	27.95 ± 0.59	197.36 ± 9.37	5.89 ± 0.31	6.30 ± 0.44	18.59 ± 1.76	1.56 ± 0.12	1.18 ± 0.05	76.33 ± 5.31	0.14 ± 0.08
	4	27.75 ± 0.58	175.95 ± 5.47	5.82 ± 0.25	5.64 ± 0.34	16.54 ± 1.55	1.44 ± 0.09	1.27 ± 0.05	50.07 ± 8.24	0.30 ± 0.19
Supreme	0	31.32 ± 0.42	313.36 ± 19.01	5.12 ± 0.27	8.75 ± 0.35	22.90 ± 1.25	1.64 ± 0.21	1.63 ± 0.04	100.00 ± 0.00	0.00 ± 0.00
	2	30.74 ± 0.36	239.05 ± 10.16	6.13 ± 0.28	9.02 ± 0.56	27.88 ± 2.07	1.77 ± 0.13	1.66 ± 0.02	95.09 ± 2.86	1.76 ± 0.02
	4	30.53 ± 0.20	234.61 ± 18.69	6.16 ± 0.36	8.40 ± 0.44	25.99 ± 1.73	1.57 ± 0.07	1.68 ± 0.07	71.45 ± 8.09	2.52 ± 0.09
Triumph	0	24.08 ± 0.40	253.77 ± 10.78	6.65 ± 0.05	9.90 ± 0.46	33.16 ± 1.99	2.52 ± 0.19	1.07 ± 0.06	100.00 ± 0.00	0.00 ± 0.00
	2	24.10 ± 0.51	200.45 ± 3.99	7.66 ± 0.26	8.77 ± 0.55	34.01 ± 2.99	1.70 ± 0.08	1.12 ± 0.05	88.74 ± 6.36	2.89 ± 0.14
	4	23.70 ± 0.29	169.70 ± 11.13	8.28 ± 0.38	7.34 ± 0.24	30.64 ± 2.05	1.28 ± 0.09	1.10 ± 0.08	61.75 ± 5.36	4.29 ± 0.19
V. Vinifera grape	0	20.75 ± 0.51	413.89 ± 22.51	2.34 ± 0.11	4.05 ± 0.11	4.71 ± 0.28	5.49 ± 0.66	0.56 ± 0.02	100.00 ± 0.00	0.00 ± 0.00
	2	22.34 ± 0.77	307.35 ± 7.15	2.84 ± 0.19	3.80 ± 0.28	5.48 ± 0.72	3.79 ± 0.32	0.66 ± 0.24	94.23 ± 1.94	2.50 ± 0.11
	4	22.41 ± 0.30	351.75 ± 22.75	2.57 ± 0.06	4.16 ± 0.15	5.38 ± 0.32	3.95 ± 0.44	0.49 ± 0.01	88.67 ± 3.86	1.24 ± 0.23
V. rotundifolia minimum[z]	0	23.13	176.95	3.28	6.34	13.93	0.79	1.01	100	0
	2	23.4	152.33	4.15	4.93	13.21	0.73	1.05	50	0.047
	4	22.83	131.25	4.76	4.03	13.79	0.72	1.03	7.69	0.12
V. rotundifolia maximum[z]	0	33.46	513.82	8.82	13.5	54.63	3.3	2.03	100	0
	2	33.28	401.59	9.45	11.87	50.8	3.33	1.95	98.11	4.31
	4	33.38	359.77	9.86	11.77	48.46	3.38	1.96	90.24	5.11
V. rotundifolia average[z,y]	0	27.94 a	259.24 a	6.22 b	9.21 a	29.23 a	1.74 a	1.49 a	100 a	0 b
	2	27.74 a	211.12 b	6.81 a	8.18 b	28.33 a	1.63 a	1.47 a	84.92 b	2.08 a
	4	27.55 a	187.974 c	7.06 a	7.59 b	27.22 a	1.45 b	1.48 a	66.43 c	2.33 a

[z]Minimum, maximum, and averages are comprehensive of all values excluding the *V. vinifera* grape sample.

[y]Mean values within a column followed by the same letter are not significantly different (Tukey's Honest Significant Difference (HSD) test $P<0.05$)

Table 2.4: Colorimetric parameters of black fresh-market muscadine genotypes across 0, 2, and 4 weeks of storage in 2024 and 2025.

		2024			2025		
Genotype	Week	L*	C*	h°	L*	C*	h°
Delicious	0	16.71 ± 4.11	1.92 ± 0.58	35.58 ± 13.58	12.95 ± 2.40	2.47 ± 0.23	30.84 ± 17.82
	2	11.77 ± 0.60	4.58 ± 0.45	23.60 ± 4.24	12.09 ± 1.14	3.41 ± 0.66	15.69 ± 6.03
	4	11.05 ± 3.75	3.16 ± 1.18	24.66 ± 6.20	13.81 ± 1.26	2.60 ± 0.76	19.96 ± 4.40
Ga. 10-1-329	0	11.80 ± 2.07	3.22 ± 0.37	22.06 ± 6.84	11.74 ± 1.92	4.28 ± 1.24	18.87 ± 2.17
	2	14.49 ± 1.49	5.40 ± 2.57	17.95 ± 2.32	15.61 ± 2.37	3.27 ± 0.65	7.24 ± 1.77
	4	14.67 ± 2.14	7.08 ± 2.13	17.08 ± 2.18	15.05 ± 1.88	4.96 ± 1.60	14.47 ± 4.44
Ga. 12-3-22	0	17.39 ± 1.91	3.87 ± 1.83	18.53 ± 7.13	14.78 ± 2.19	4.58 ± 2.04	8.94 ± 5.11
	2	13.91 ± 1.87	6.76 ± 0.77	17.59 ± 3.32	14.09 ± 0.21	4.80 ± 1.25	10.58 ± 5.59
	4	15.63 ± 1.76	5.87 ± 1.55	13.46 ± 3.03	14.82 ± 1.57	4.18 ± 0.87	11.77 ± 1.34
Ga. 12-5-138	0	18.65 ± 4.16	1.48 ± 0.31	19.77 ± 16.76	14.23 ± 3.65	3.19 ± 1.05	115.19 ± 163.19
	2	15.34 ± 0.68	2.16 ± 0.43	21.58 ± 13.63	17.83 ± 6.06	1.62 ± 0.84	36.30 ± 30.45
	4	15.43 ± 1.82	2.59 ± 0.36	18.62 ± 8.94	14.62 ± 3.32	3.23 ± 0.65	22.02 ± 11.67
Ga. 12-5-46	0	15.00 ± 3.31	2.60 ± 1.19	20.66 ± 11.50	13.17 ± 2.55	2.61 ± 1.25	26.02 ± 7.53
	2	14.51 ± 2.82	2.19 ± 0.75	18.85 ± 7.19	15.14 ± 2.07	2.71 ± 0.63	5.73 ± 3.24
	4	14.75 ± 1.96	1.55 ± 0.19	19.54 ± 12.36	15.31 ± 1.68	1.88 ± 0.25	7.11 ± 7.08
Ga. 14-2-3	0	17.24 ± 1.49	9.46 ± 2.20	16.05 ± 2.58	13.69 ± 1.47	5.01 ± 3.14	19.12 ± 4.11
	2	15.30 ± 1.89	7.97 ± 2.10	17.41 ± 2.37	11.22 ± 2.58	3.88 ± 1.84	18.61 ± 6.32
	4	16.08 ± 3.63	9.44 ± 2.21	18.93 ± 2.63	14.28 ± 1.70	3.83 ± 0.55	19.11 ± 1.94
Ga. 15-4-65	0	15.48 ± 2.47	3.49 ± 1.63	20.10 ± 6.31	12.13 ± 6.11	1.23 ± 0.24	101.33 ± 162.98
	2	15.09 ± 2.30	4.07 ± 0.81	18.16 ± 4.19	15.22 ± 3.64	1.82 ± 0.38	101.27 ± 172.69
	4	14.24 ± 2.86	4.61 ± 1.24	16.46 ± 3.17	11.61 ± 3.03	2.34 ± 0.28	22.84 ± 5.19
Ga. 16-1-9	0	12.06 ± 3.13	1.86 ± 0.60	26.03 ± 15.06	12.95 ± 2.40	2.47 ± 0.23	30.84 ± 17.82
	2	13.82 ± 2.88	3.06 ± 1.67	14.86 ± 12.06	12.09 ± 1.14	3.41 ± 0.66	15.69 ± 6.03
	4	15.49 ± 2.75	2.16 ± 0.67	12.23 ± 2.95	13.81 ± 1.26	2.60 ± 0.76	19.96 ± 4.40

Ga. 16-7-1	0	13.79 ± 1.74	2.16 ± 0.13	14.11 ± 11.01	15.46 ± 2.68	2.01 ± 0.17	187.61 ± 191.53
	2	13.49 ± 1.44	2.48 ± 0.97	23.30 ± 9.41	12.21 ± 3.69	2.06 ± 0.57	100.18 ± 169.25
	4	9.16 ± 4.22	1.86 ± 0.14	18.45 ± 13.68	11.59 ± 3.91	1.66 ± 0.35	10.46 ± 11.12
Ga. 17-6-82	0	15.07 ± 3.45	6.62 ± 1.15	17.34 ± 3.58	14.58 ± 2.31	7.35 ± 1.73	19.98 ± 2.01
	2	14.51 ± 1.24	9.20 ± 1.38	18.33 ± 2.68	19.56 ± 2.53	9.83 ± 5.37	24.63 ± 5.84
	4	15.03 ± 3.76	12.62 ± 5.38	17.87 ± 1.73	18.04 ± 3.23	11.98 ± 5.41	17.33 ± 2.02
Ga. 18-5-106	0	17.67 ± 0.74	1.55 ± 0.54	10.72 ± 14.01			
	2	13.52 ± 0.87	2.39 ± 0.57	15.93 ± 6.78			
	4	10.86 ± 3.42	3.72 ± 0.89	29.90 ± 6.98			
Ga. 18-5-44	0	17.11 ± 3.56	1.35 ± 0.40	66.91 ± 27.61	14.34 ± 3.32	1.83 ± 0.30	38.61 ± 15.86
	2	17.14 ± 3.59	1.31 ± 0.22	43.56 ± 21.48	13.03 ± 3.68	1.28 ± 0.33	33.69 ± 10.84
	4	10.96 ± 4.74	2.14 ± 0.54	49.02 ± 20.61	16.39 ± 1.13	1.61 ± 0.38	38.16 ± 6.43
Ga. 18-9-51	0	15.60 ± 1.50	2.29 ± 0.60	22.76 ± 7.84	12.51 ± 2.82	2.12 ± 0.46	10.64 ± 5.87
	2	12.91 ± 4.39	2.49 ± 0.48	15.29 ± 5.90	13.76 ± 0.81	3.51 ± 0.70	12.88 ± 7.14
	4	14.05 ± 2.91	2.92 ± 0.44	20.87 ± 4.17	17.16 ± 1.23	2.40 ± 0.66	93.00 ± 177.05
Ga. 6-2-192	0	17.59 ± 3.82	3.74 ± 1.89	29.38 ± 22.58	18.12 ± 1.96	3.21 ± 1.22	13.59 ± 9.39
	2	18.14 ± 2.98	3.75 ± 0.96	17.35 ± 6.03	14.80 ± 2.01	2.67 ± 0.11	10.76 ± 5.40
	4	12.91 ± 1.59	5.36 ± 0.85	20.20 ± 1.60	14.67 ± 1.42	2.77 ± 0.18	16.06 ± 3.54
Ga. 8-1-313	0	14.72 ± 2.17	1.71 ± 0.24	36.61 ± 7.78	14.02 ± 4.35	2.55 ± 2.00	23.38 ± 17.60
	2	14.12 ± 2.49	2.16 ± 0.72	36.54 ± 9.11	19.64 ± 1.35	1.69 ± 0.14	22.92 ± 12.63
	4	15.21 ± 1.04	1.66 ± 0.29	24.48 ± 5.12	16.64 ± 3.05	3.96 ± 3.92	18.61 ± 6.45
Lane	0	18.10 ± 3.28	2.10 ± 0.71	21.91 ± 19.06	10.20 ± 2.76	1.95 ± 0.64	38.55 ± 2.53
	2	18.20 ± 3.34	2.37 ± 0.82	37.58 ± 12.95	15.48 ± 1.44	1.77 ± 0.39	18.09 ± 9.89
	4	13.14 ± 1.03	2.34 ± 0.81	18.90 ± 2.25	12.29 ± 2.67	1.93 ± 0.68	25.09 ± 7.23
Paulk	0	18.76 ± 2.77	8.98 ± 2.09	10.45 ± 5.19	15.73 ± 2.70	2.58 ± 0.71	93.58 ± 174.21
	2	15.70 ± 1.59	5.92 ± 1.33	18.71 ± 5.45	15.37 ± 1.56	3.58 ± 0.72	9.76 ± 7.00
	4	10.87 ± 1.69	7.17 ± 1.37	14.38 ± 4.67	16.21 ± 2.15	4.25 ± 1.38	12.93 ± 5.82
RubyCrisp	0	21.00 ± 2.03	17.69 ± 2.33	18.77 ± 4.85	18.48 ± 0.69	16.38 ± 2.04	23.66 ± 5.99
	2	18.66 ± 1.09	16.62 ± 1.16	16.51 ± 1.57	19.16 ± 2.64	16.53 ± 1.53	19.41 ± 1.71
	4	21.14 ± 1.97	18.10 ± 2.91	20.58 ± 4.93	18.95 ± 1.86	15.12 ± 2.09	19.51 ± 3.76

Supreme	0	18.12 ± 3.52	1.42 ± 0.76	51.21 ± 18.07	7.47 ± 4.94	1.91 ± 0.89	25.20 ± 8.62
	2	17.26 ± 5.54	1.83 ± 0.40	44.77 ± 19.47	14.65 ± 0.57	2.44 ± 0.48	16.36 ± 5.71
	4	13.75 ± 1.09	1.94 ± 0.45	22.96 ± 9.72	16.01 ± 3.23	2.78 ± 0.82	9.37 ± 2.63
V. Vinifera Grape	0	47.56 ± 1.37	28.14 ± 0.33	101.14 ± 0.40	47.83 ± 1.80	29.73 ± 1.25	98.43 ± 1.51
	2	45.52 ± 0.86	28.03 ± 2.05	98.38 ± 1.29	47.51 ± 1.69	29.26 ± 1.03	95.96 ± 0.50
	4	42.85 ± 2.98	26.10 ± 2.17	96.68 ± 0.80	46.19 ± 1.25	29.96 ± 0.48	95.97 ± 0.21
V. rotundifolia minimum[z]	0	7.41	0.73	0.21	2.42	0.89	1.02
	2	7.14	1.17	0.56	7.52	0.7	1.3
	4	4	1.27	0.8	7	1.01	0.91
V. rotundifolia maximum[z]	0	23.44	20.96	108	20.32	18.8	359.9
	2	23.91	17.61	72.41	25.7	18.78	359.88
	4	22.5	20.98	68.12	21.6	19.29	358.54
V. rotundifolia average[z,y]	0	16.41 b	4.08 a	25.21 a	13.74 b	3.84 a	46.77 a
	2	15.15 ab	4.57 a	23.05 a	15.23 a	3.93 a	27.3 a
	4	13.92 a	5.07 a	20.98 a	15.14 a	4.20 a	22.22 a

[z]Minimum, maximum, and averages are comprehensive of all values excluding the *V. vinifera* grape sample.

[y]Mean values within a column followed by the same letter are not significantly different (Tukey's Honest Significant Difference (HSD) test $P<0.05$)

Table 2.5: Colorimetric parameters of bronze fresh-market muscadine genotypes across 0, 2, and 4 weeks of storage in 2024 and 2025.

		2024			2025		
Genotype	Week	L*	C*	h°	L*	C*	h°
Fry	0	38.33 ± 2.23	19.83 ± 3.40	86.00 ± 2.82			
	2	32.07 ± 0.77	21.25 ± 1.49	82.38 ± 3.33			
	4	28.63 ± 1.71	20.88 ± 1.84	83.15 ± 2.14			
Ga. 17-2-67	0	37.05 ± 1.81	19.07 ± 1.41	77.93 ± 4.14			
	2	35.81 ± 3.06	18.82 ± 0.88	73.54 ± 2.58			
	4	30.81 ± 4.19	19.88 ± 1.63	73.13 ± 4.77			
Ga. 17-7-91	0	34.93 ± 0.88	18.53 ± 0.93	84.33 ± 2.66	34.88 ± 1.64	18.22 ± 0.79	85.44 ± 1.91
	2	34.94 ± 2.70	19.50 ± 1.36	87.53 ± 0.61	32.96 ± 3.40	18.27 ± 1.23	83.89 ± 1.78
	4	28.15 ± 4.26	19.29 ± 1.11	84.37 ± 3.35	33.20 ± 1.10	18.18 ± 0.86	85.62 ± 1.60
Ga. 6-1-269	0	35.83 ± 1.77	19.45 ± 0.73	90.09 ± 2.37			
	2	33.02 ± 1.59	18.36 ± 2.35	87.45 ± 2.24			
	4	35.95 ± 1.50	18.36 ± 0.51	88.10 ± 2.14			
Ga. 6-6-358	0	38.59 ± 1.07	17.64 ± 2.02	85.47 ± 2.84	34.13 ± 3.04	15.84 ± 0.50	80.06 ± 2.65
	2	33.88 ± 2.17	17.82 ± 0.85	82.96 ± 4.41	36.91 ± 1.94	15.28 ± 2.02	80.12 ± 4.21
	4	35.74 ± 0.83	18.04 ± 1.06	81.48 ± 1.42	33.73 ± 2.33	15.79 ± 1.11	75.68 ± 4.44
Ga. 8-1-12	0	36.75 ± 2.96	21.79 ± 1.35	85.55 ± 4.51	35.80 ± 1.15	19.26 ± 2.29	77.40 ± 1.26
	2	36.19 ± 2.18	23.28 ± 1.31	76.44 ± 7.10	32.64 ± 1.49	20.48 ± 1.25	76.29 ± 3.25
	4	36.81 ± 2.51	20.59 ± 1.02	80.13 ± 3.11	34.91 ± 1.40	19.44 ± 0.62	76.44 ± 2.12
Hall	0	41.81 ± 0.83	19.80 ± 1.66	85.11 ± 2.87	37.39 ± 0.37	21.39 ± 1.14	80.87 ± 2.13
	2	39.43 ± 1.03	21.52 ± 1.24	82.67 ± 3.19	34.97 ± 0.78	21.70 ± 1.32	77.12 ± 3.54
	4	36.61 ± 0.63	22.81 ± 1.68	81.72 ± 2.24	35.35 ± 1.02	20.77 ± 1.15	76.61 ± 1.16
Late Fry	0	38.51 ± 1.82	19.92 ± 1.93	78.67 ± 2.90	33.83 ± 3.01	19.49 ± 0.48	77.08 ± 3.46
	2	34.99 ± 1.34	19.57 ± 0.58	76.01 ± 4.55	32.39 ± 3.26	18.89 ± 1.39	73.83 ± 3.34
	4	32.19 ± 1.37	21.99 ± 0.58	77.68 ± 4.09	35.15 ± 1.93	18.12 ± 0.55	76.66 ± 1.69

N1007	0	36.96 ± 2.65	16.17 ± 3.97	78.85 ± 3.49	31.24 ± 1.66	18.40 ± 0.35	73.62 ± 3.67
	2	36.01 ± 2.51	20.75 ± 1.46	76.37 ± 3.23	31.51 ± 1.43	17.35 ± 0.45	71.01 ± 3.09
	4	31.54 ± 1.32	18.59 ± 1.05	74.36 ± 1.58	31.91 ± 2.45	17.38 ± 1.82	72.22 ± 3.76
Triumph	0	30.64 ± 2.79	17.46 ± 0.70	83.47 ± 2.64	34.71 ± 3.32	16.09 ± 3.20	78.68 ± 2.29
	2	31.81 ± 1.86	15.51 ± 2.63	75.64 ± 7.82	25.69 ± 1.52	15.40 ± 0.73	74.90 ± 5.36
	4	31.32 ± 3.10	18.04 ± 1.65	79.84 ± 8.14	32.01 ± 0.25	16.28 ± 1.29	74.51 ± 3.97
V. Vinifera Grape	0	47.56 ± 1.37	28.14 ± 0.33	101.14 ± 0.40	47.83 ± 1.80	29.73 ± 1.25	98.43 ± 1.51
	2	45.52 ± 0.86	28.03 ± 2.05	98.38 ± 1.29	47.51 ± 1.69	29.26 ± 1.03	95.96 ± 0.50
	4	42.85 ± 2.98	26.10 ± 2.17	96.68 ± 0.80	46.19 ± 1.25	29.96 ± 0.48	95.97 ± 0.21
V. rotundifolia minimum[z]	0	26.82	10.75	73.08	29.46	11.32	69.66
	2	29.42	12.04	65.38	23.76	13.7	67.36
	4	22.42	15.7	68.4	29.64	14.3	68.28
V. rotundifolia maximum[z]	0	42.56	23.23	92.07	38.55	22.59	87.85
	2	40.71	25.2	90.79	39.4	23.23	85.81
	4	40.49	25.1	90.98	37.1	21.83	87.01
V. rotundifolia average[z,y]	0	36.94 c	18.97 a	83.55 b	34.57 b	18.38 a	79.02 a
	2	34.82 b	19.64 a	80.1 a	32.44 a	18.19 a	76.74 a
	4	32.78 a	19.85 a	80.4 a	33.75 ab	17.99 a	76.82 a

[z]Minimum, maximum, and averages are comprehensive of all values excluding the *V. vinifera* grape sample.

[y]Mean values within a column followed by the same letter are not significantly different (Tukey's Honest Significant Difference (HSD) test $P<0.05$)

Table 2.6: Juice composition characteristics of fresh-market muscadine genotypes across 0, 2, and 4 weeks of storage in 2024 and 2025.

Genotype	Week	pH	TSS (%)	TA (%)	pH	TSS (%)	TA (%)
Delicious	0	3.18 ± 0.14	14.60 ± 0.38	0.21 ± 0.02	3.44 ± 0.06	13.72 ± 0.49	0.38 ± 0.02
	2	3.07 ± 0.03	14.38 ± 0.17	0.24 ± 0.01	3.36 ± 0.03	13.88 ± 0.75	0.48 ± 0.06
	4	3.08 ± 0.06	13.35 ± 2.24	0.24 ± 0.03	3.22 ± 0.04	13.20 ± 0.22	0.50 ± 0.06
Fry	0	2.92 ± 0.04	17.75 ± 0.87	0.27 ± 0.02			
	2	2.85 ± 0.06	17.05 ± 1.25	0.30 ± 0.03			
	4	2.88 ± 0.06	16.95 ± 0.70	0.31 ± 0.02			
Ga. 10-1-329	0	3.57 ± 0.04	17.10 ± 0.55	0.18 ± 0.01	3.85 ± 0.09	15.85 ± 0.39	0.25 ± 0.05
	2	3.41 ± 0.05	15.72 ± 0.74	0.25 ± 0.10	3.75 ± 0.06	15.65 ± 0.24	0.23 ± 0.02
	4	3.28 ± 0.06	15.53 ± 0.59	0.33 ± 0.12	3.61 ± 0.06	14.38 ± 0.51	0.23 ± 0.01
Ga. 12-3-22	0	3.44 ± 0.10	15.65 ± 0.53	0.20 ± 0.03	3.87 ± 0.06	15.03 ± 0.54	0.29 ± 0.02
	2	3.29 ± 0.07	14.95 ± 0.70	0.20 ± 0.01	3.69 ± 0.01	15.00 ± 0.49	0.22 ± 0.04
	4	3.40 ± 0.08	15.50 ± 0.53	0.22 ± 0.01	3.58 ± 0.11	14.82 ± 0.41	0.22 ± 0.07
Ga. 12-5-138	0	3.58 ± 0.10	15.78 ± 2.62	0.18 ± 0.01	3.85 ± 0.08	13.85 ± 0.70	0.18 ± 0.03
	2	3.36 ± 0.13	16.50 ± 0.62	0.20 ± 0.02	3.74 ± 0.08	14.07 ± 0.81	0.19 ± 0.03
	4	3.27 ± 0.07	15.97 ± 0.61	0.21 ± 0.00	3.73 ± 0.10	13.50 ± 0.57	0.26 ± 0.05
Ga. 12-5-46	0	3.18 ± 0.05	12.45 ± 0.90	0.23 ± 0.01	3.45 ± 0.11	12.18 ± 0.21	0.40 ± 0.02
	2	3.12 ± 0.07	12.47 ± 0.36	0.22 ± 0.01	3.40 ± 0.04	11.40 ± 0.36	0.47 ± 0.00
	4	3.10 ± 0.05	12.05 ± 0.13	0.23 ± 0.01	3.37 ± 0.06	11.55 ± 0.31	0.43 ± 0.05
Ga. 14-2-3	0	3.78 ± 0.13	17.27 ± 1.56	0.46 ± 0.60			
	2	3.62 ± 0.06	16.35 ± 0.30	0.21 ± 0.13			
	4	3.50 ± 0.06	14.80 ± 0.41	0.24 ± 0.17			
Ga. 15-4-65	0	3.34 ± 0.07	15.15 ± 0.55	0.20 ± 0.01	3.69 ± 0.13	13.18 ± 0.28	0.21 ± 0.02
	2	3.31 ± 0.01	14.50 ± 2.14	0.19 ± 0.01	3.61 ± 0.06	13.10 ± 0.22	0.21 ± 0.02
	4	3.20 ± 0.04	13.25 ± 2.37	0.23 ± 0.01	3.60 ± 0.05	12.62 ± 0.64	0.23 ± 0.00

Ga. 16-1-9	0	3.61 ± 0.10	15.45 ± 0.29	0.18 ± 0.01	3.91 ± 0.03	15.18 ± 0.53	0.29 ± 0.05
	2	3.50 ± 0.09	15.23 ± 0.46	0.18 ± 0.01	3.91 ± 0.08	15.00 ± 0.37	0.37 ± 0.03
	4	3.38 ± 0.05	15.80 ± 0.64	0.22 ± 0.01	3.77 ± 0.02	14.50 ± 0.58	0.29 ± 0.04
Ga. 16-7-1	0	3.32 ± 0.12	14.65 ± 0.54	0.26 ± 0.02	3.49 ± 0.11	13.32 ± 0.49	0.46 ± 0.03
	2	3.15 ± 0.04	14.22 ± 1.14	0.26 ± 0.00	3.45 ± 0.08	13.85 ± 0.42	0.50 ± 0.02
	4	3.14 ± 0.05	13.75 ± 0.74	0.28 ± 0.03	3.41 ± 0.04	13.25 ± 0.26	0.54 ± 0.02
Ga. 17-2-67	0	3.64 ± 0.05	19.52 ± 0.61	0.20 ± 0.02			
	2	3.44 ± 0.09	18.08 ± 0.83	0.24 ± 0.01			
	4	3.43 ± 0.04	16.35 ± 1.67	0.26 ± 0.03			
Ga. 17-6-82	0	3.70 ± 0.11	15.60 ± 1.40	0.17 ± 0.02	4.05 ± 0.03	14.50 ± 0.39	0.33 ± 0.07
	2	3.52 ± 0.07	15.82 ± 0.68	0.19 ± 0.01	3.89 ± 0.12	14.50 ± 0.68	0.33 ± 0.05
	4	3.50 ± 0.03	13.95 ± 1.72	0.17 ± 0.01	3.76 ± 0.06	13.82 ± 0.87	0.40 ± 0.02
Ga. 17-7-91	0	3.76 ± 0.11	16.58 ± 1.12	0.24 ± 0.16	3.63 ± 0.02	13.38 ± 0.38	0.37 ± 0.03
	2	3.52 ± 0.13	16.23 ± 0.66	0.18 ± 0.02	3.59 ± 0.08	13.70 ± 0.28	0.40 ± 0.03
	4	3.44 ± 0.04	15.68 ± 0.49	0.20 ± 0.02	3.56 ± 0.03	13.35 ± 0.26	0.42 ± 0.01
Ga. 18-5-106	0	3.76 ± 0.05	13.28 ± 2.89	0.40 ± 0.52			
	2	3.55 ± 0.08	15.32 ± 0.75	0.17 ± 0.01			
	4	3.40 ± 0.08	14.32 ± 0.40	0.20 ± 0.02			
Ga. 18-5-44	0	3.76 ± 0.10	15.50 ± 0.63	0.22 ± 0.19	4.12 ± 0.06	14.35 ± 0.33	0.73 ± 0.98
	2	3.66 ± 0.02	15.12 ± 0.36	0.13 ± 0.01	4.09 ± 0.03	14.60 ± 0.47	0.25 ± 0.01
	4	3.56 ± 0.06	15.53 ± 0.54	0.38 ± 0.45	4.01 ± 0.04	14.72 ± 0.52	0.27 ± 0.02
Ga. 18-9-51	0	3.63 ± 0.07	16.42 ± 0.89	0.18 ± 0.03	3.53 ± 0.02	12.60 ± 0.43	0.42 ± 0.06
	2	3.50 ± 0.05	16.30 ± 0.42	0.18 ± 0.01	3.50 ± 0.05	12.12 ± 0.79	0.43 ± 0.04
	4	3.43 ± 0.06	15.43 ± 0.43	0.20 ± 0.01	3.45 ± 0.04	12.45 ± 0.42	0.46 ± 0.02
Ga. 6-1-269	0	3.15 ± 0.14	13.83 ± 0.66	0.23 ± 0.03			
	2	2.96 ± 0.11	13.12 ± 1.09	0.30 ± 0.12			
	4	2.96 ± 0.04	13.75 ± 0.30	0.28 ± 0.01			
Ga. 6-2-192	0	3.29 ± 0.05	16.00 ± 0.73	0.18 ± 0.02	3.95 ± 0.08	13.75 ± 0.38	0.27 ± 0.05
	2	3.30 ± 0.03	15.62 ± 0.62	0.20 ± 0.01	3.83 ± 0.08	14.03 ± 0.38	0.33 ± 0.02
	4	3.26 ± 0.06	15.43 ± 0.78	0.22 ± 0.01	3.76 ± 0.05	13.85 ± 0.93	0.34 ± 0.03

Ga. 6-6-358	0	3.23 ± 0.11	14.15 ± 0.42	0.19 ± 0.02	3.85 ± 0.06	13.00 ± 0.29	0.36 ± 0.06
	2	3.07 ± 0.06	13.45 ± 0.50	0.27 ± 0.12	3.76 ± 0.10	13.50 ± 0.57	0.24 ± 0.02
	4	3.00 ± 0.04	13.78 ± 0.43	0.25 ± 0.01	3.72 ± 0.06	12.68 ± 0.34	0.27 ± 0.04
Ga. 8-1-12	0	3.40 ± 0.04	16.15 ± 0.17	0.18 ± 0.03	3.71 ± 0.05	15.10 ± 0.59	0.34 ± 0.01
	2	3.30 ± 0.08	15.55 ± 0.84	0.27 ± 0.12	3.65 ± 0.07	15.40 ± 0.41	0.42 ± 0.04
	4	3.22 ± 0.03	15.57 ± 0.43	0.23 ± 0.01	3.67 ± 0.07	14.78 ± 0.48	0.37 ± 0.06
Ga. 8-1-313	0	3.54 ± 0.06	18.10 ± 0.12	0.20 ± 0.02	3.79 ± 0.03	15.75 ± 0.34	0.35 ± 0.05
	2	3.43 ± 0.09	18.52 ± 0.22	0.20 ± 0.02	3.78 ± 0.07	15.60 ± 0.32	0.34 ± 0.05
	4	3.30 ± 0.08	16.32 ± 1.85	0.25 ± 0.03	3.67 ± 0.07	14.90 ± 0.48	0.39 ± 0.06
Hall	0	3.08 ± 0.08	15.30 ± 1.85	0.23 ± 0.01	3.78 ± 0.03	14.65 ± 0.13	0.40 ± 0.02
	2	2.87 ± 0.07	13.82 ± 0.46	0.27 ± 0.01	3.76 ± 0.09	15.15 ± 0.17	1.28 ± 1.71
	4	2.99 ± 0.03	14.65 ± 0.44	0.26 ± 0.00	3.69 ± 0.03	14.93 ± 0.46	0.41 ± 0.04
Lane	0	3.24 ± 0.13	15.95 ± 1.43	0.21 ± 0.03	3.90 ± 0.02	15.05 ± 0.45	0.29 ± 0.02
	2	3.09 ± 0.06	15.38 ± 0.74	0.25 ± 0.02	3.84 ± 0.11	15.28 ± 0.73	0.35 ± 0.04
	4	3.11 ± 0.06	14.53 ± 1.56	0.25 ± 0.02	3.68 ± 0.10	15.32 ± 0.34	0.40 ± 0.09
Late Fry	0	3.24 ± 0.10	13.93 ± 0.61	0.21 ± 0.03	3.86 ± 0.11	13.57 ± 0.50	0.34 ± 0.06
	2	3.10 ± 0.07	14.75 ± 0.91	0.22 ± 0.02	3.67 ± 0.04	13.10 ± 0.20	0.41 ± 0.02
	4	2.98 ± 0.06	13.53 ± 0.73	0.25 ± 0.02	3.62 ± 0.06	12.68 ± 0.46	0.40 ± 0.05
N1007	0	3.27 ± 0.14	14.47 ± 0.39	0.28 ± 0.02	4.07 ± 0.04	14.72 ± 0.24	0.29 ± 0.01
	2	3.34 ± 0.06	15.47 ± 0.43	0.24 ± 0.01	3.87 ± 0.05	15.25 ± 0.24	0.33 ± 0.05
	4	3.37 ± 0.12	15.03 ± 2.32	0.30 ± 0.10	3.82 ± 0.02	15.18 ± 0.17	0.32 ± 0.03
Paulk	0	3.23 ± 0.07	13.18 ± 0.84	0.21 ± 0.01	3.45 ± 0.04	13.80 ± 0.49	0.42 ± 0.01
	2	2.94 ± 0.06	13.10 ± 0.56	0.23 ± 0.02	3.40 ± 0.04	13.78 ± 0.39	0.44 ± 0.05
	4	2.98 ± 0.05	12.60 ± 0.26	0.25 ± 0.03	3.38 ± 0.04	13.90 ± 0.76	0.47 ± 0.01
RubyCrisp	0	3.48 ± 0.11	15.65 ± 0.53	0.21 ± 0.06	4.03 ± 0.04	14.82 ± 0.28	0.20 ± 0.10
	2	3.38 ± 0.08	14.55 ± 2.55	0.18 ± 0.02	3.89 ± 0.04	14.45 ± 0.30	0.24 ± 0.09
	4	3.22 ± 0.02	14.97 ± 0.21	0.21 ± 0.01	3.72 ± 0.00	13.03 ± 0.43	0.28 ± 0.06
Supreme	0	3.73 ± 0.09	18.20 ± 0.41	0.18 ± 0.01	3.69 ± 0.07	14.62 ± 0.41	0.31 ± 0.02
	2	3.65 ± 0.04	18.55 ± 0.30	0.15 ± 0.01	3.63 ± 0.03	15.10 ± 0.42	0.38 ± 0.02
	4	3.62 ± 0.08	16.98 ± 1.33	0.18 ± 0.01	3.50 ± 0.04	14.18 ± 0.22	0.44 ± 0.02

Triumph	0	3.17 ± 0.05	14.95 ± 0.62	0.19 ± 0.00	3.56 ± 0.06	14.05 ± 0.26	0.37 ± 0.01
	2	3.05 ± 0.02	14.78 ± 0.67	0.20 ± 0.01	3.59 ± 0.07	14.70 ± 0.36	0.37 ± 0.05
	4	3.12 ± 0.02	15.38 ± 1.09	0.22 ± 0.01	3.50 ± 0.02	14.50 ± 0.00	0.38 ± 0.03
V. Vinifera Grape	0	3.96 ± 0.07	17.18 ± 0.59	0.18 ± 0.01	3.76 ± 0.05	17.85 ± 0.51	0.30 ± 0.01
	2	3.95 ± 0.07	17.95 ± 0.54	0.15 ± 0.01	3.88 ± 0.03	18.30 ± 1.10	0.37 ± 0.06
	4	3.90 ± 0.07	17.98 ± 0.54	0.15 ± 0.01	3.88 ± 0.03	18.82 ± 0.17	0.42 ± 0.09
V. rotundifolia minimum[z]	0	2.86	10	0.12	3.35	11.9	0.1
	2	2.79	10.9	0.13	3.33	11.1	0.13
	4	2.82	9.7	0.13	3.18	11.2	0.18
V. rotundifolia maximum[z]	0	3.91	20.3	1.35	4.16	16.3	2.2
	2	3.7	19.3	0.47	4.14	16.3	3.85
	4	3.7	18.5	1.06	4.07	15.6	0.56
V. rotundifolia average[z,y]	0	3.42 a	15.61 a	0.22 a	3.77 a	14.32 a	0.34 a
	2	3.29 b	15.34 ab	0.22 a	3.7 b	14.42 a	0.38 a
	4	3.25 b	14.85 b	0.24 a	3.63 c	14.04 a	0.37 a

[Z]Minimum, maximum, and averages are comprehensive of all values excluding the *V. vinifera* grape sample.

[Y]Mean values within a column followed by the same letter are not significantly different (Tukey's Honest Significant Difference (HSD) test $P<0.05$)

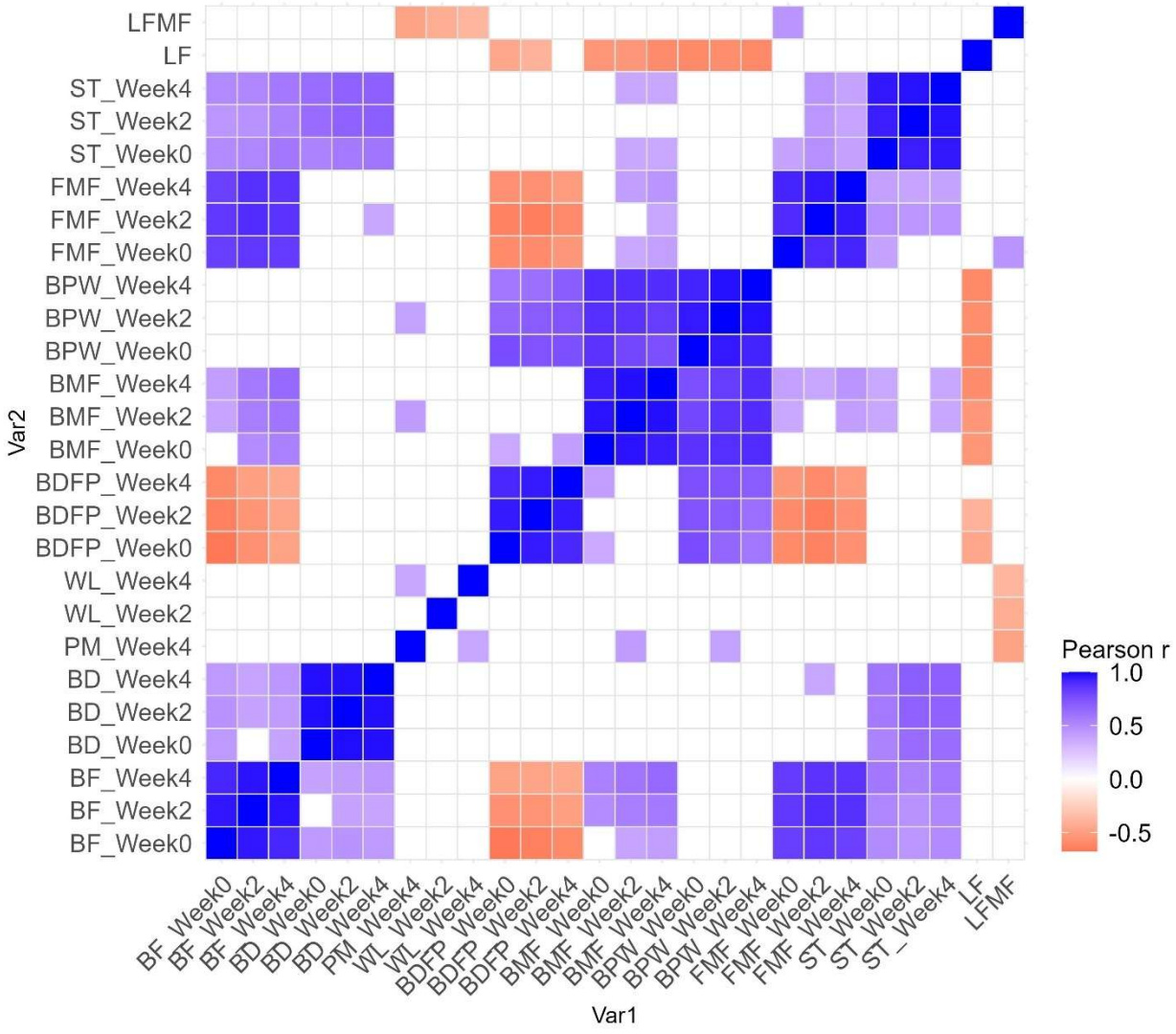

Figure 2.2: Pearson pairwise correlations between texture-related traits of muscadine grape across 0, 2, or 4 weeks of storage. Non-significant (P>0.5) correlations are represented by white tiles. (BF: berry firmness, BD: berry diameter, BDFP: berry deformation at first peak, BMF: berry maximum force, FMF: flesh maximum force, ST: skin thickness).

Literature Cited:

Barchenger, Derek W., John R. Clark, Renee T. Threlfall, Luke R. Howard, and Cindi R. Brownmiller. 2015. "Evaluation of Physicochemical and Storability Attributes of Muscadine Grapes (Vitis Rotundifolia Michx.)." *HortScience* 50 (1): 104–11. https://doi.org/10.21273/HORTSCI.50.1.104.

Brown, Kelly, Charles Sims, Asli Odabasi, Linda Bartoshuk, Patrick Conner, and Dennis Gray. 2016. "Consumer Acceptability of Fresh-Market Muscadine Grapes." *Journal of Food Science* 81 (11): S2808–16. https://doi.org/10.1111/1750-3841.13522.

Carreño, Iván, José Antonio Cabezas, Celia Martínez-Mora, et al. 2014. "Quantitative Genetic Analysis of Berry Firmness in Table Grape (Vitis Vinifera L.)." *Tree Genetics & Genomes* 11 (1): 818. https://doi.org/10.1007/s11295-014-0818-x.

Conner, Patrick. 2013a. "Instrumental Textural Analysis of Muscadine Grape Germplasm." *HortScience* 48 (9): 1130–34. https://doi.org/10.21273/HORTSCI.48.9.1130.

Conner, Patrick. 2013b. *'Lane': An Early-Season Self-Fertile Black Muscadine Grape*. HortScience. January 1. https://doi.org/10.21273/HORTSCI.48.1.128.

Conner, Patrick J. 2020. *'RubyCrisp' Muscadine Grape*. HortScience. June 1. https://doi.org/10.21273/HORTSCI14970-20.

Conner, Patrick, and Margaret Worthington. 2022. "Muscadine Grape Breeding." In *Plant Breeding Reviews*. John Wiley & Sons, Ltd. h https://doi.org/10.1002/9781119874157.ch2.

Crespan, Manna, Daniele Migliaro, Silvia Vezzulli, et al. 2021. "A Major QTL Is Associated with Berry Grape Texture Characteristics." *OENO One* 55 (1): 183–206. https://doi.org/10.20870/oeno-one.2021.55.1.3994.

Duarte, Abel Alonso, and Martin A. O'Neill. 2012a. "Consumption of Muscadine Grape By-products: An Exploration among Southern US Consumers." *British Food Journal* 114 (3): 400–415. https://doi.org/10.1108/00070701211213492.

Duarte, Abel Alonso, and Martin A. O'Neill. 2012b. "Muscadine Grapes, Food Heritage and Consumer Images: Implications for the Development of a Tourism Product in Southern USA." *Tourism Planning & Development* 9 (3): 213–29. https://doi.org/10.1080/21568316.2012.672451.

Ector, B. J., J. B. Magee, C. P. Hegwood, and M. J. Coign. 1996. "Resveratrol Concentration in Muscadine Berries, Juice, Pomace, Purees, Seeds, and Wines." *American Journal of Enology and Viticulture* 47 (1): 57. https://doi.org/10.5344/ajev.1996.47.1.57.

Fairchild, Mark. 2013. “Color Appearance Models.” In *Color Appearance Models*. John Wiley & Sons, Ltd. https://doi.org/10.1002/9781118653128.ch10.

Felts, Molly, Renee T. Threlfall, John R. Clark, and Margaret L. Worthington. 2018. “Physiochemical and Descriptive Sensory Analysis of Arkansas Muscadine Grapes.” *HortScience* 53 (11): 1570–78. https://doi.org/10.21273/HORTSCI13296-18.

Fillion, Laurence, and David Kilcast. 2002. “Consumer Perception of Crispness and Crunchiness in Fruits and Vegetables.” *Food Quality and Preference* 13 (1): 23–29. https://doi.org/10.1016/S0950-3293(01)00053-2.

God, Jason M., Patricia Tate, and Lyndon L. Larcom. 2007. “Anticancer Effects of Four Varieties of Muscadine Grape.” *Journal of Medicinal Food* 10 (1): 54–59. https://doi.org/10.1089/jmf.2006.699.

Harrell, Frank E. (Jr.), Cole Beck, and Charles Dupont. 2025. *Hmisc: Harrell Miscellaneous*. V. 5.2-4. Released October 5. https://cran.r-project.org/web/packages/Hmisc/index.html.

Hickey, Cain, Erick Smith, Shanshan Cao, and Patrick Conner. 2019. “Muscadine (Vitis Rotundifolia Michx., Syn. Muscandinia Rotundifolia (Michx.) Small): The Resilient, Native Grape of the Southeastern U.S.” *Agriculture* 9 (6): 6. https://doi.org/10.3390/agriculture9060131.

Himelrick, David. 2003. “Handling, Storage and Postharvest Physiology of Muscadine Grapes: A Review.” *Small Fruits Review* 2 (4): 45–62. https://doi.org/10.1300/J301v02n04_06.

Lanier, M., and J. Morris. 1979. “Evaluation of Density Separation for Defining Fruit Maturities and Maturation Rates of Once-over Harvested Muscadine Grapes1.” *Journal of the American Society for Horticultural Science* 104 (March): 249–52. https://doi.org/10.21273/JASHS.104.2.249.

Lenth, Russell, Julia Piaskowski, Balazs Banfai, et al. 2025. *Emmeans: Estimated Marginal Means, Aka Least-Squares Means*. V. R pacakge version 2.0.0. Released August 27. https://rvlenth.github.io/emmeans/.

Lufu, Robert, Alemayehu Ambaw, and Umezuruike Linus Opara. 2020. “Water Loss of Fresh Fruit: Influencing Pre-Harvest, Harvest and Postharvest Factors.” *Scientia Horticulturae* 272 (October): 109519. https://doi.org/10.1016/j.scienta.2020.109519.

Paniagua Gonzalez, Andres, Andrew East, Jason Hindmarsh, and Julian Heyes. 2013. "Moisture Loss Is the Major Cause of Firmness Change during Postharvest Storage of Blueberry." *Postharvest Biology and Technology* 79 (May): 13–19. https://doi.org/10.1016/j.postharvbio.2012.12.016.

Poling, E. B., C. M. Mainland, W. T. Bland, B. Cline, and K. A. Sorensen. 2003. *Muscadine Grape Production Guide for North Carolina*. AG-94. Raleigh, NC: NC State Extension. https://content.ces.ncsu.edu/muscadine-grape-production-guide

Rolle, Luca, René Siret, Susana Río Segade, Chantal Maury, Vincenzo Gerbi, and Frédérique Jourjon. 2012. "Instrumental Texture Analysis Parameters as Markers of Table-Grape and Winegrape Quality: A Review." Article. *American Journal of Enology and Viticulture* 63 (1): 11–28. https://doi.org/10.5344/ajev.2011.11059.

Sastry, S. K. 1985. "Moisture Losses from Perishable Commodities: Recent Research and Developments." *International Journal of Refrigeration* 8 (6): 343–46. https://doi.org/10.1016/0140-7007(85)90029-5.

Sato, Akihiko, and Masahiko Yamada. 2003. *Berry Texture of Table, Wine, and Dual-Purpose Grape Cultivars Quantified*. HortScience. July 1. https://doi.org/10.21273/HORTSCI.38.4.578.

Shahkoomahally, Shirin, Ali Sarkhosh, Logan M. Richmond-Cosie, and Jeffrey K. Brecht. 2021. "Physiological Responses and Quality Attributes of Muscadine Grape (Vitis Rotundifolia Michx. to CO2-Enriched Atmosphere Storage." *Postharvest Biology and Technology* 173 (March): 111428. https://doi.org/10.1016/j.postharvbio.2020.111428.

Striegler, R. K., J. R. Morris, P. M. Carter, J. R. Clark, R. T. Threlfall, and L. R. Howard. 2005. *Yield, Quality, and Nutraceutical Potential of Selected Muscadine Cultivars Grown in Southwestern Arkansas*. HortTechnology. January 1. https://doi.org/10.21273/HORTTECH.15.2.0276.

Takeda, Fumiomi, Mary S. Saunders, and James A. Saunders. 1983. "Physical and Chemical Changes in Muscadine Grapes During Postharvest Storage." Article. *American Journal of Enology and Viticulture* 34 (3): 180–85. https://doi.org/10.5344/ajev.1983.34.3.180.

Tunick, Michael H. 2011. "Food Texture Analysis in the 21st Century." *Journal of Agricultural and Food Chemistry* 59 (5): 1477–80. https://doi.org/10.1021/jf1021994.

Valverde, Juan Miguel, Fabián Guillén, Domingo Martínez-Romero, Salvador Castillo, María Serrano, and Daniel Valero. 2005. "Improvement of Table Grapes Quality and Safety

by the Combination of Modified Atmosphere Packaging (MAP) and Eugenol, Menthol, or Thymol." *Journal of Agricultural and Food Chemistry* 53 (19): 7458–64. https://doi.org/10.1021/jf050913i.

Walker, Teresa, Justin Morris, Renee Threlfall, Gary Main, Olusola Lamikanra, and Stephen Leong. 2001. *Density Separation, Storage, Shelf Life, and Sensory Evaluation of "Fry" Muscadine Grapes*. HortScience. August 1. https://doi.org/10.21273/HORTSCI.36.5.941.